DROWSINESS DETECTION WHILE DRIVING USING FRACTAL ANALYSIS AND WAVELET TRANSFORM

By

PRACHI PARIKH

A thesis submitted to the

Graduate School-New Brunswick

Rutgers, The State University of New Jersey

and

The Graduate School of Biomedical Sciences

University of Medicine and Dentistry of New Jersey

in partial fulfillment of the requirements

for the degree of

Master of Science

Graduate Program in Biomedical Engineering

written under the direction of

Dr. Evangelia Micheli-Tzanakou

and approved by

____

____

____

New Brunswick, New Jersey

October, 2007

ABSTRACT OF THE THESIS

Drowsiness Detection While Driving using Fractal analysis and Wavelet Transform

By Prachi Parikh

Thesis Director:
Dr. Evangelia Micheli-Tzanakou

The EEG signal plays a key role as a nondestructive testing method in the diagnosis and functional determination of the brain. EEG recordings represent changes in alertness, arousal, sleep and cognition. Boredom, fatigue and monotony of a task may induce drowsiness that leads to a decrease in alertness. This can have serious consequences in tasks involving constant vigilance and control such as driving. In the current study, EEG signals are recorded using a car simulator and analyzed using Fractal analysis and Wavelet Transform. It is observed that there is an increase in the alpha frequencies in the latter stages of driving indicating a state of drowsiness. The analysis techniques used provide results quickly, which is essential to provide instant feedback.

ACKNOWLEDGEMENTS

I would like to express my heartfelt gratitude to my thesis director, Dr. Tzanakou for her academic guidance. I am grateful to her for her support and encouragement in the completion of this thesis. I would also like to thank Dr. Shoane and Dr. Drzeweicki for being on the presentation committee.

I dedicate this thesis to my parents, Smita and Upendra Parikh. They have always supported me in all my endeavors and have shown tremendous love and patience. They have been my pillars of strength and this degree would not have been possible without their faith in my abilities.

Table Of Contents

LIST OF ILLUSTRATIONS

LIST OF TABLES

CHAPTER 1

INTRODUCTION

1.1 Drowsy Driving

According to the National Sleep Foundation's 2005 Sleep in America poll [1], 60% of adult drivers, about 168 million people, say they have driven a vehicle while feeling drowsy in the past year, and more than one-third, (37% or 103 million people), have actually fallen asleep at the wheel. 13% of the 103 million people say they have nodded off at the wheel at least once a month. Four percent of the drivers, approximately eleven million, admit they have had an accident or near accident because they dozed off or were too tired to drive.

The 2004 AAA Foundation for Traffic Safety Internet survey [2] reported that nine out of every ten North American police officers have stopped a driver who they believed was drunk, but turned out to be drowsy. The National Highway Traffic Safety Administration [3] estimates that up to 100,000 police-reported crashes annually involve drowsiness or fatigue as a principal causal factor. Several drowsy driving incidents have resulted in jail sentences for the driver. Multi-million dollar settlements have been awarded to families of crash victims as a result of lawsuits filed against individuals as well as businesses whose employees were involved in drowsy driving crashes.

Drowsiness causes impaired reaction time, judgment and vision [32]. This leads to decreased performance, vigilance and motivation. To summarize, drowsy driving crashes can result in high personal and economic costs.

1.2 The Electroencephalogram

The Electroencephalogram (EEG) is the electrical pattern record on the surface of the brain formed by the aggregate of synchronized neural activities from millions of neurons acting together. It can be roughly defined as the mean electrical activity of the brain in different sites of the head. The EEG is recorded from electrodes placed in standard positions on the scalp, and has typical amplitude of 2-100 microvolts (μV) and a frequency spectrum from 0.1 to 60 Hz. Figure 1.1 shows a sample EEG waveform [4].

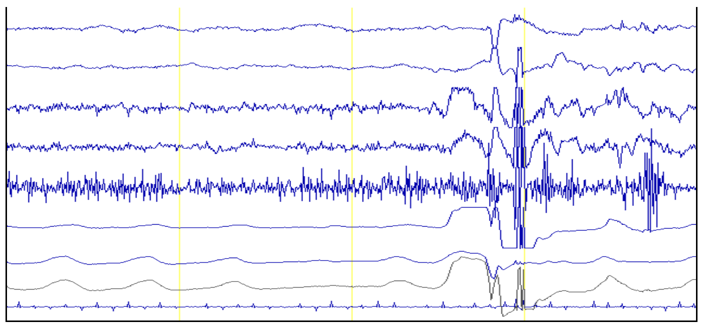

Fig. 1.1 Sample EEG [4]

Most of the activity occurs within the following frequency bands; delta (0.5 - 4 Hz), theta (4-8 Hz), alpha (8-13 Hz), beta (13-22 Hz) and gamma (30-40 Hz). The EEG activity in particular frequency bands is often correlated with particular cognitive states.

Delta is the frequency range up to 4 Hz and is often associated with the very young and certain encephalopathies and underlying lesions. It is seen in deep sleep.

Theta is the frequency range from 4 Hz to 8 Hz and is associated with drowsiness, childhood, adolescence and young adulthood. This EEG frequency can sometimes be produced by hyperventilation. Theta waves can be seen during hypnagogic states such as trances, hypnosis, deep daydreams, lucid dreaming and light sleep and the preconscious state just upon waking, and just before falling asleep.

Alpha (Berger's wave) is the frequency range from 8 Hz to 13 Hz. It is the characteristic of a relaxed, alert state of consciousness and is present by the age of two years. Alpha rhythms are best detected with the eyes closed. Alpha attenuates with drowsiness and open eyes, and is best seen over the occipital (visual) cortex.

Beta is the frequency range above 13 Hz and below 25 Hz. Low amplitude beta with multiple and varying frequencies is often associated with active, busy or anxious thinking and active concentration. Rhythmic beta with a dominant set of frequencies is associated with various pathologies and drug effects.

Gamma waves have a frequency range of between 30 and 40 Hz. Gamma rhythms appear to be involved in higher mental activity, including perception and consciousness.

1.3 EEG and Driving

The EEG signal plays a key role as a nondestructive testing method in the diagnosis and functional determination of the brain [5]. EEG recordings represent changes in alertness, arousal, sleep and cognition. Boredom, fatigue and monotony of a task may induce drowsiness that leads to a decrease in alertness. This can have serious consequences in tasks involving constant vigilance and control. Alertness is a physiological variable that can be measured. A single principal component of EEG variance has been shown to be linearly related to minute-scale changes in detection performance [6]. The EEG variations arise from simultaneous changes in brain mechanisms controlling central arousal and alertness. The one to one relationship between changes in performance and the EEG spectrum during drowsiness make it possible to have practical methods based on the EEG to estimate alertness in real time.

1.4 Various Studies of Alertness

Alertness is one of the most important functions in determining the performance of an individual. Studies have incorporated subjective and objective measures of alertness. Terán-Santos, et al conducted a case-control study of the relation between sleep apnea and the risk of traffic accidents [7]. The study considered 102 subjects who were drivers that had been involved in traffic accidents due to fatigue. These subjects completed questionnaires related to feelings of drowsiness based on the Epworth Sleepiness Scale [24]. Statistical analysis of the surveys and recordings from polysomnography determined the results of the study.

Experiments have been conducted by introducing an alertness maintenance device in a driving simulator [16]. Self-rating and eye-closures were examined and it was determined that the introduction of such a device helped decrease the bouts of drowsiness.

Jansen and Dawant [14] have designed a knowledge-based system that uses an object-oriented approach for EEG analysis. Specific waveforms and sleep stages are represented by frames with slots describing the properties (the morphological and spatio-temporal information) of the named object. Each frame has its own signal processing module. A detection module identifies the particular EEG feature and then initiates the corresponding signal processing module.

Image Processing of eye movements has also been used as an analysis technique to monitor awakening levels [9]. The subject was asked to drive a car for an hour on a test course during which the EEG and eye movements were recorded using a CCD camera attached to the driver’s cap. The onset of drowsiness has been related to the appearance of grouped alpha waves in the EEG [10]. It was observed that there was an increase in the eye movement with the appearance of grouped alpha waves.

The Fourier Transform (FT) [35] has been the traditional method of analysis of signals. It involves averaging all the spectra of the signals using the FT, calculating the percentage of total power, and evaluating the relative differences.

The spectral shape of brain activity has also been used to classify different stages of human alertness [11]. The C3 channel (the location in the left hemisphere on the midline nearest to the central part of the cerebral cortex) was sampled at 100 Hz. The relationship between the EEG power spectra was measured using the Welch method [34], and wakefulness was determined. The classification was made every 10 seconds. A trend appeared when the spectrum was extracted over this period and this was assumed to be a suitable time interval for an alarm signal to be given if the individual's alertness level was insufficient. It was observed that when the brain activity decreases, the EEG spectrum was dominant in the alpha band (8 to 13 Hz).

Levendowski, et al [8] recorded EEG and Electrooculogram (EOG) in a 12-hour overnight study on subjects that were awakened from partial sleep deprivation. They used a discriminant function analysis (DFA) model, known as B-Alert System, to classify one second EEG epochs. This classification was designed to provide real-time drowsiness detection.

Schier [12] used a driving simulator to record the EEG from P3, P4, F3, F4 electrodes. Hanning window was applied to data segments of 1.28 seconds to compute the power spectra. It was observed that there was greater alpha activity in the later stages of driving, confirming the hypothesis that with increasing driving time retaining a constant level of alertness is rare.

At times, alpha activity cannot be detected easily by visual inspection in the first stages of decreasing vigilance. Tietze [13] has suggested a rationale that defines signals with amplitude higher than a predefined limit as “alpha events”. Fourier filtering in combination with an overlap-add method was used to calculate the amplitude of the peaks and the critical amplitude was determined to be twice the value of the mean.

Kirk and Lacourse [20] found that just by examining the spectral pattern of the EEG it is not clear that all frequencies contribute equal information. They performed Principal Component Analysis (PCA) on the time series of the spectral patterns to extract the frequencies with the largest amount of information. PCA involves a mathematical procedure that transforms a number of correlated variables into a smaller number of uncorrelated variables called “principal components” [37]. The first principal component accounts for as much of the variability in the data as possible, and each succeeding component accounts for as much of the remaining variability as possible. Thus PCA is a way to identify the patterns in data and highlights the similarities and differences. This has been used with an adaptive neural network to take into account the non-stationary property of the EEG signal [36].

Santana-Diaz et al [17] recorded the lateral position, steering wheel angle and vehicle speed, among other sensors while 10 subjects drove on a closed circuit. Mean and variance analysis was carried out to investigate the existence of quantitative difference between fatigue and normal driver behaviors. Principal Component Analysis was then used to eliminate redundancy and correlate the initial and new values.

The research by Makeig and Jung [18] investigated the feasibility of estimating the fluctuations in an operator’s global level of alertness, using non-invasive multichannel EEG data in real-time. The subjects were asked to respond to visual and auditory targets. EEG data were recorded and the power spectrum time series was calculated. The change in response was compared to the EEG spectrum using a cluster analysis program based on the centroid method. The Xerion neural network simulator [33] was trained for error estimation. The authors observed that once the network was trained, the system could successfully measure the alertness level using spontaneous EEG signals.

The Backpropagation algorithm has also been used for the classification of features extracted from the EEG [19]. The analysis is based on the existence of characteristic waves in the signal. It also included contextual analysis that rejects ambiguity and involves coherence analysis.

Khalifa et al [21] have designed a portable device for alertness detection that uses the Fast Fourier Transform to analyze the signals. The EEG was acquired on magnetic cassettes using the Holter System. Further classification was done using Kohonen artificial neural networks [45]. There was a negative correlation between scores of vigilance and the percentage of the delta band in the EEG. There was a positive correlation between the percentage of the other bands and the score of vigilance.

The Fourier Transform has been used extensively in signal processing. However, it does not give any information on the time at which a frequency component occurs. Hence it is best suited for stationary periodic functions. The short-time Fourier Transform (STFT) has been developed to overcome the disadvantages of the Fourier Transform. A moving window is applied to the signal and the Fourier Transform is applied to the signal within the window as the window is moved. This decomposes the signal into a set of frequency bands at any given time. However the STFT also has its limitations, such as its time-frequency resolution capability, which is due to the uncertainty principle. Low frequencies can be hardly depicted with short windows, whereas short pulses can only poorly be localized in time with long windows. This could be a disadvantage since some real signals have long duration low frequencies and short duration high frequencies. These signals can be better described by a transform that has a high frequency and low time resolution at low frequencies and a low frequency and high time resolution at high frequencies.

The EEG is a non-stationary signal and for its analysis, it is essential to determine its behavior at any moment. Multiresolution analysis [46] decomposes a signal into a smoothed version of the original signal and a set of detailed information at different scales. This enables us to extract the regularity of a singularity that characterizes the signal's behavior at that point. In the Wavelet Transform [46], the wavelet defines the bandpass filter that determines the detailed information. Associated with the wavelet is a smoothing function, which defines the complementary low pass filter.

To summarize, the Wavelet Transform has 3 features: Multiresolution, constant relative bandwidth i.e. time-width of the wavelet is adaptive to the frequency, and the ability to indicate if the signal is localized in the time domain or the frequency domain.

Yamaguchi [23] did a comparative study of normal and epileptic EEG records using Fourier Transform and Continuous Wavelet Transform. Daubechies wavelet of order 8 was used. It was observed that the local low frequency components in each EEG record were clearly depicted by the Wavelet Transform but not with Fourier Transform.

Wavelet Analysis of EEG data in rats after drug exposure gave a good prediction of the Central Nervous System dysfunction [22]. The mother wavelet chosen was the Morlet since it has a Gaussian window that provides the best time-frequency localization in terms of the uncertainty principle. A thresholding technique was applied to the wavelet coefficients and an accumulator was setup to determine consecutive occurrences of a particular frequency.

Yoong and Shengxun [29] used the Discrete Wavelet Transform to analyze EEG and found that different frequencies could be represented on different scales. Thus the features of the wavelet transform in each scale can represent the state of the EEG signal.

Wavelet Transform has been mainly used to date to differentiate between normal and epileptic EEG signals [23, 27]. It has also been used to study the effects of certain drugs [22], detect a psychiatric disorder like Alzheimer's, and detect the G-LOC phenomena in pilots which is the loss of consciousness due to large acceleration forces [27]. Analysis has also been used to detect spikes during Sleep Stages.

Idogiwa et al [28] recorded EEG of two subjects in response to a visual task. Using Wavelet Analysis they concluded that alpha activity becomes a dominant feature of the EEG after some time while doing monotonous work like driving.

Alertness level detection has been examined using the analysis of EEG signals by wavelet transform, and classification using Artificial Neural Networks [26]. EEG signals were decomposed into the frequency sub-bands using wavelet transform. A set of statistical features - mean, average power and standard deviation were extracted from the sub-bands to represent the distribution of wavelet coefficients. These statistical features were used as an input to an ANN with three discrete outputs: alert, drowsy and asleep. The error back-propagation neural network was selected as a classifier to discriminate the alertness level of a subject.

Mendoza et al [15] have presented a methodology based on Statistics, Wavelets and Support Vector Machines to perform a Driver's Impairment analysis whose goal was to supervise and diagnose in real time the vigilance state of car drivers. Drivers drove twice a day, with attached electrodes to record their EEG and EOG activity. At the same time, signals coming from the onboard sensors were recorded, and the scene in the cockpit and the environment of the vehicle were filmed. The variables from these recordings were used to compute a group of synthetic variables using Wavelet Analysis. The Haar wavelet was the mother wavelet used in this case. The coefficients obtained were then used to calculate the probability density function (PDF). The PDF was used to determine the vigilance state of the driver.

Until now, quantitative computerized EEG signal analysis has been based mainly on linear theory [38]. In recent years, there have been a lot of developments in nonlinear dynamics and deterministic chaos theory. These new techniques aid the extraction of additional information from EEG. This may increase the sensitivity of electrophysiological methods used for the analysis of EEG.

Pereda, et al [39] compared the differences between the EEG in the two hemispheres of nine healthy human subjects during different stages of sleep. The features used for comparison were the harmonic power spectral density within the EEG main spectral bands [34], the fractal dimension [47] and the correlation dimension [48]. The fractal dimensions calculated were able to provide information about the interhemispheric differences in human EEG during slow wave sleep, where spectral analysis could not.

Bullmore [40] et al used fractal analysis to analyze EEG during epileptic seizures. The method achieves data reduction without undue loss of diagnostically important information in the primary signal.

Studies have been carried out wherein the fractal dimension of EEG signals at different levels of handgrip forces was measured [41]. The fractal dimensions were computed using the Katz algorithm [42], Sevcik’s method [44] and Higuchi’s algorithm [43].

Driver alertness monitoring has been designed to detect when the driver's ability has become impaired, whether from inattention, drowsiness, or intoxication [32]. A simple system may merely sound an alarm. More complex systems could include warnings of impending collisions or that the vehicle is straying from the roadway.

In some systems, an infrared camera detects eye motion and computes trends that track driver vigilance [16]. Other methods monitor driver performance using lane-marker cameras to detect a wandering vehicle [15].

Schier and Gorman have designed a portable device to record the changes in spontaneous EEG during a driving task [30]. Two channels of EEG are recorded, amplified and then transferred to a portable computer using a microcontroller.

A Drowsy-Driver Detection and Warning System prototype has been designed that measures PERCLOS, the proportion of time that a driver’s eyes are closed over a specified interval, and provides warning sounds accordingly [31].

Currently, in the United States road shoulder rumble strips are being promoted as an effective countermeasure for drowsy driving [3]. Rumble strips are raised or grooved patterns constructed on, or in travel lane and shoulder pavements. The texture of rumble strips is different from the road surface. Vehicle tires passing over them produce a sudden rumbling sound and cause the vehicle to vibrate. Road agencies use rumble strips to warn motorists of an upcoming change that may require them to act.

However, rumble strips have their own limitations. They may give drivers a false sense of security about driving while sleepy. The strips are useful as alerting devices, but they will not protect drivers who continue to drive while drowsy. Being awakened by driving over a rumble strip is a warning to change sleep and driving behaviors for safety. The strips are not a technological quick fix for sleepy drivers.

1.5 Statement of objective

Numerous attempts have been undertaken to quantify and interpret the EEG. The ability of human subjects to sustain their initial level of performance during visual monitoring tasks in a low-arousal environment is limited. In this thesis, a realistic, simulator (with a steering wheel and foot pedals) will be used in combination with a computerized driving software (Need for Speed). The EEGs of 10 participants are recorded while subjects are driving. Previous studies [13] have shown that event-related responses in the alpha range are best defined in the occipital locations. The EEG is recorded primarily from these locations. The EEG recordings are then analyzed using Wavelet Transform and Fractal analysis.

Chapter 2 describes the materials and gives an overview of the methods used in this study. Chapter 3 summarizes the results obtained using Fractal analysis, and Chapter 4 reviews the results obtained using Wavelet Transform. Chapter 5 provides the discussions and suggestion for further work. Appendix A is a copy of the subject consent form. Appendix B and C provide the results of all subjects using Fractal analysis and Wavelet Transform respectively.

CHAPTER 2

MATERIALS AND METHODS

2.1 Subjects

Nine male and 1 female volunteers with normal or corrected-to-normal vision and no known neurophysiological impairments participated in this study [49]. The subjects were asked to come at the end of their day’s work for the experiment. They were asked to try and remain relaxed throughout the recording. This would avoid any unwanted signals due to clenching of hands, teeth or any other stress. A written consent form [Appendix A] was given to each subject to read and sign before participating in the study. Two of the ten subjects did the experiment twice on different days at different times for variability purposes.

2.2 Equipment

A simulator environment was designed [50]. It consisted of Microsoft’s Sidewinder Force Feedback Racing Wheel that has foot pedals. This wheel is used in combination with computerized driving software (Need for Speed Hot Pursuit III, Electronic Arts 1998). The conditions while driving including the road turns and the surroundings make up the driving circuit. The driving course chosen for all subjects was identical. An LCD display placed at a distance of 90cm from the driver presented an 'in-car’ view. Fig.2.1 shows the screen as seen by the subject using the simulator.

2.3 Driving Task

Subjects completed four laps of the course and their EEG was recorded during all laps. After the course was over, it was replayed and subjects were asked to simply observe the laps with their hands on the steering wheel and having minimum movement. The replay task was executed in accordance with the intake versus rejection model of Ray and Cole [52]. According to this model, alpha activity should increase when changing from a largely intake task (driving) to a mixed intake/rejection task (watching the replay). The lap time was obtained from the software at the completion of the course.

Fig. 2.1 Simulator Screen

2.4 Subject Preparation

A lot of experiments involving driver vigilance and alertness monitoring recorded the EEG signal from all channels. Kirk and Lacourse sampled four channels of data for their study on vigilance monitoring [51]. They were the EEG signals from O1-O2, EOG, stimulus marker and subject's response.

The EEG was recorded from the sites F3 and Oz with respect to Cz, and C3 with respect to O1 using an electrode cap. The bipolar EEG signal was selected as the primary predictive data because of the presence of alpha waves in the visual cortex during drowsiness and sleep [51].

Channel locations were selected as likely to contain independent alertness information on the basis of previous studies [66]. The electrode cap was designed using the 10-20 International System of Electrode Placement (Figures 2.2 and 2.3).

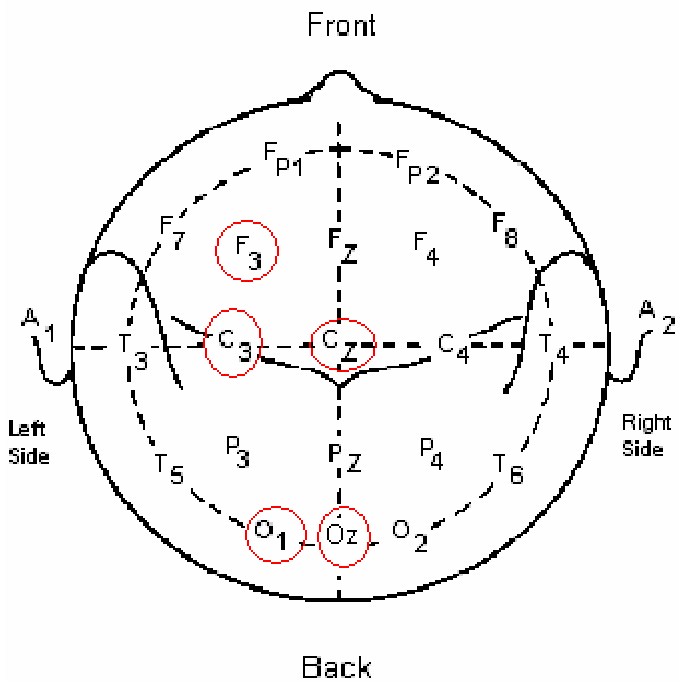

Fig. 2.2 10-20 The International System of Electrode Placement - Top View [17]

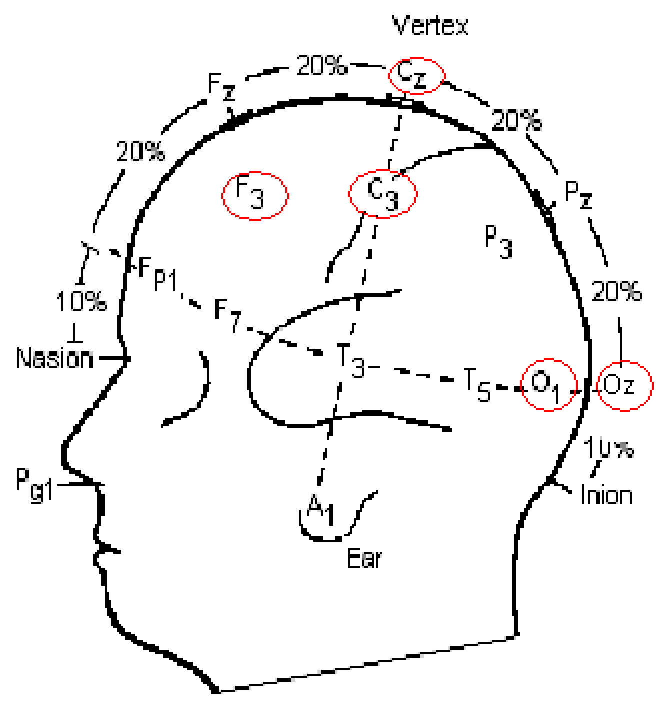

Fig. 2.3 10-20 The International System of Electrode Placement – Side View [65]

For accurate electrode mapping, it was ensured that the Cz electrode on the cap was exactly midway between the nasion and Inion, and also midway between the left and right earlobes. The scalp area was prepared by light abrasion and application of a conductive gel to reduce impedance. The final impedance was less than 3 kΩ for each electrode. The electrode cap was attached to the Grass Model 12 Neurodata Acquisition System containing 6 AC amplifiers set to an amplification of 100,000x, 0.3 Hz high pass and 300Hz low pass filters. The amplified and pre-filtered signals were sent from the Grass Model 12 to a Biopac Model MP100 data acquisition device. The Biopac was used to record the EEG signals at a sampling frequency of 312.5 Hz. Figure 2.4 below shows the schematic representation of the experimental setup.

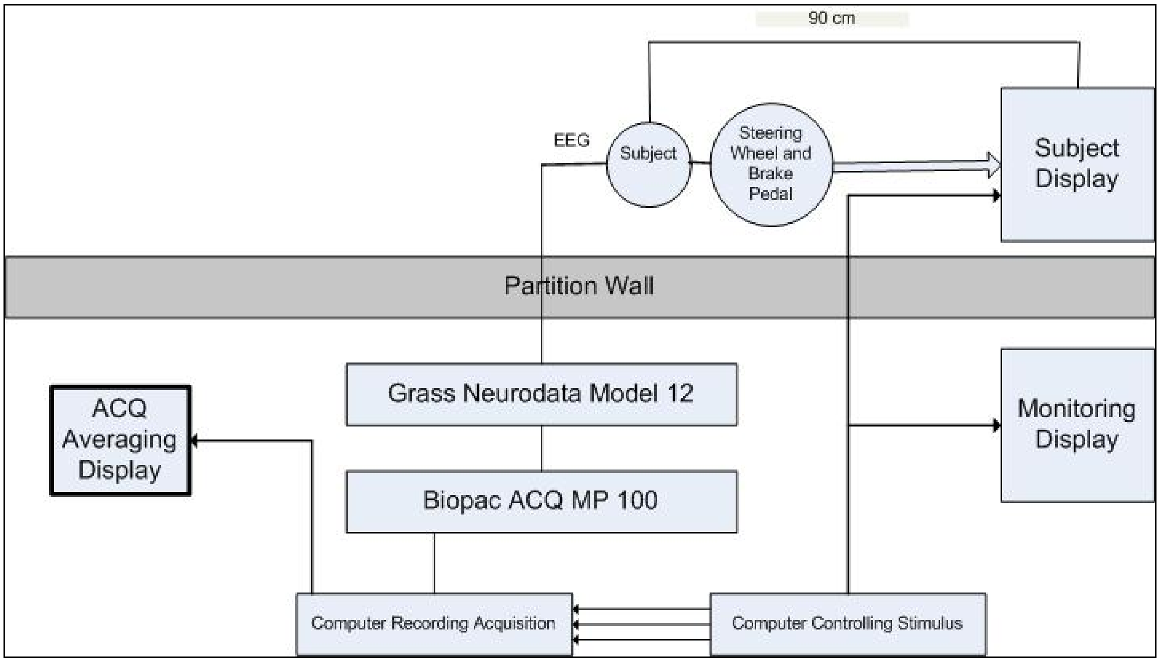

Figure 2.4 Schematic of the Multi-Stimuli VEP Presentation System (MSVPres) and acquisition system including system interconnections and synchronization lines.

Special precautions have been taken to minimize noise in the data during the experiments. The subjects were required neither to move their head or body nor to have eye blinking or teeth biting when performing the handgrips.

Figure 2.5 is an example of the signal recorded by Biopac, and viewed and saved using the Acknowledge software.

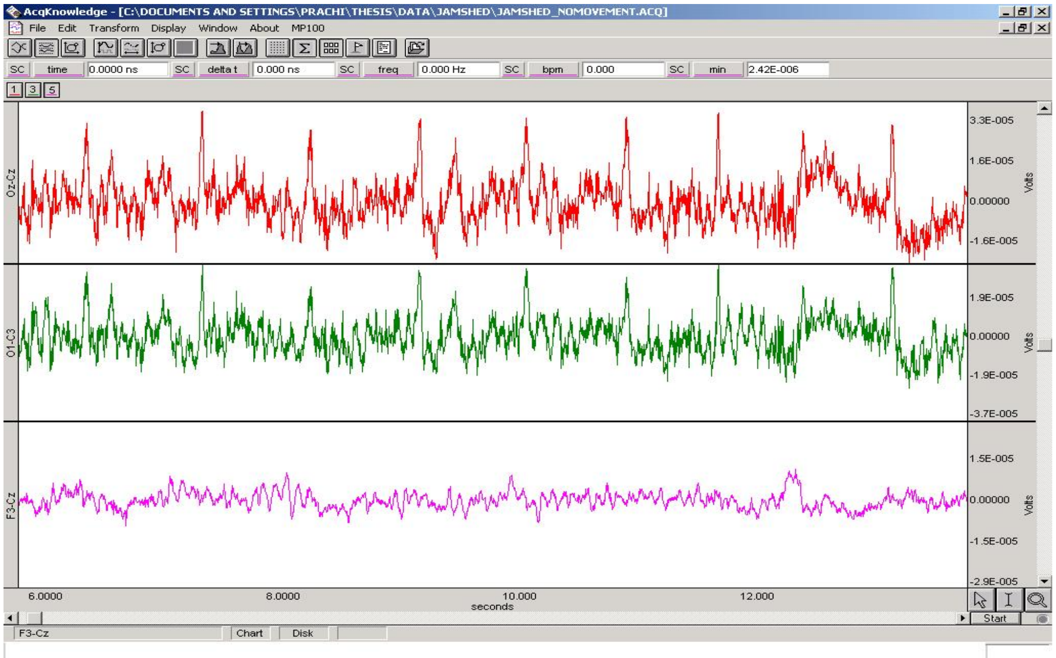

Fig 2.5 Example of signal recorded by Biopac

2.5 Analysis

The data were saved in the proprietary ACQ file format and later resaved as tab-delimited text files which can be easily imported into other programs such as Microsoft Excel. The main part of the analysis was accomplished using MATLAB 6.1 with a script file to automatically load the data from the text files, perform the analytical calculations and write the results to another text file. The script also automatically generated JPG files of the plots of the coefficients and their standard deviations. All statistics were saved to a file for use in Excel and for further analysis.

2.6 Wavelet Analysis

A signal can be expressed as the sum of a series of sines and cosines as per the Fourier theory [53]. Fourier Transform provides only frequency solution and no time resolution. In most biomedical applications, there is interest in the localized complex phenomena superposed on the periodic signals as well as the background noise [54]. Because of its drawbacks, Fourier analysis is not well suited for analysis of localized phenomena.

The short time Fourier Transform (STFT) [55] was designed for analysis when both time and frequency localization were required. The STFT enables the time localization of a particular sinusoidal frequency; however it is limited by the application of Heisenberg's uncertainty principle applied to signal processing [56]. This implies that it is impossible to know the exact frequency and time of occurrence of a particular signal frequency [57].

S. Mallat [58] proposed a new solution for the multiresolution representation of images and this was effectively applied to signal processing as well. This method is known as Wavelet Transform.

The Wavelet Analysis uses a fully scalable modulated window that is shifted along the signal to calculate the spectrum along every position [57]. This process is repeated multiple times with a shorter window in each cycle. The end result will be a collection of time-frequency representations of the signal with different resolutions.

Figure 2.6 below gives a high-level block diagram of the process. The Scale is defined as the inverse of frequency.

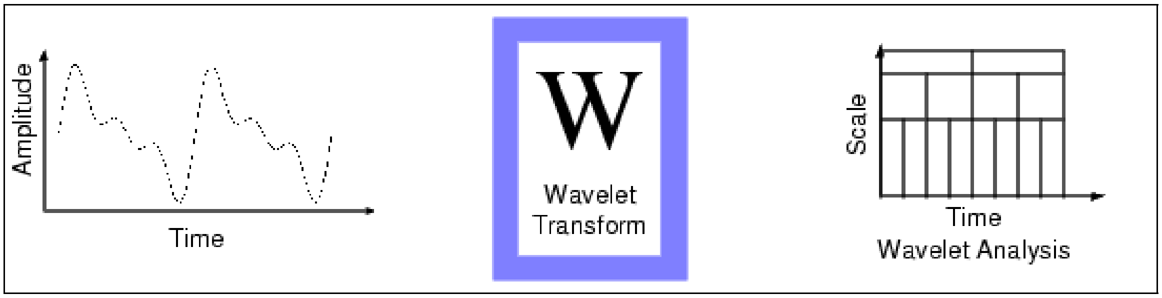

Fig. 2.6 Block Diagram for Wavelet Analysis [11]

The mathematical representation [57] of the Wavelet Transform is give as follows:

$$\gamma(s,\tau) = \int f(t)\psi^*_{s,\tau}(t)dt$$

where * denotes complex conjugation. This equation shows how a function $f(t)$ is decomposed into a set of basis functions $\psi_{s,\tau}(t)$, called the wavelets. The variables s and τ, scale and translation, are the new dimensions after the wavelet transform.

The wavelets are generated from a single basic wavelet ψ by scaling and translation:

$$\psi_{s,\tau}(t) = \frac{1}{\sqrt{s}}\psi\left(\frac{t-\tau}{s}\right)$$

where s is the scale factor, τ is the translation factor and the factor $s^{-1/2}$ is for energy normalization across the different scales.

The decomposition coefficients computed using the Continuous Wavelet Transform have a lot of redundant information and are large in number. To avoid this issue, the Discrete Wavelet Transform was developed, the algorithm of which makes it extremely fast to compute coefficients without losing the significant details of the signal. This DWT can be mathematically represented [57] as follows:

$$\psi_{j,k}(t) = \frac{1}{\sqrt{s_0^j}} \psi\left(\frac{t - k\tau_0 s_0^j}{s_0^j} \right)$$

where j and k are integers and $s_0 > 1$ is a fixed dilation step. The translation factor τ_0 depends on the dilation step.

Continuous Wavelet Transform is easier to read since its redundancy reinforces the traits and makes the information more visible [59]. This is especially helpful in EEG analysis since it is the subtle differences that need to be interpreted easily.

Santana Diaz et al [60] measured the lateral position, steering wheel angle and vehicle speed while the driver was in motion. These variables were then processed using the Haar, Symmlet and cubic B-Spline wavelets. The Haar wavelet analysis was determined to be the best for road bend detection, the Symmlet for noise filtering and the B-Spline wavelet to determine the ruptures in the signal. These values along with the EEG analysis and the self report provided by the driver were used to determine the alertness of the driver.

Quadratic Spline Wavelets were first used to study pattern-reversal visual evoked potentials (PRVEPs) collected from normal and demented subjects by Ademoglu, Micheli-Tzanakou, et al [56]. Quiroga and Schurrmann [61] used the quadratic B-Spline wavelet to analyze the VEP recordings from subjects in response to a checkerboard pattern used as stimulus. The statistical analysis to compare the coefficients was done using Analysis Of Variance (ANOVA). They concluded that even-related alpha oscillations were better determined using this method.

2.7 Fractal Analysis

"A fractal is a shape made of parts similar to the whole in some way" [62]. Fractal dimensions are the measure of the self-similarity of signals. Mathematically, the fractal dimension can be defined as follows [63]:

$$\boxed{\mathit{Fractal\ Dimension} = \frac{\log(\mathit{number\ of\ self-similar\ processes})}{\log(\mathit{magnification\ factor})}}$$

Fractal dimensions can be calculated using various methods.

Katz's Fractal Dimension (FD) [42] is derived directly from the waveform. The FD of a curve can be defined as:

$$D = \frac{Log(L)}{Log(d)},$$

where L is the total length of the curve or sum of distances between successive points, and d is the diameter estimated as the distance between the first point of the sequence and the point of the sequence that provides the farthest distance. Mathematically, d can be expressed as:

d= max (distance (1,i))

Considering the distance between each point of the sequence and the first, point i is the one that maximizes the distance with respect to the first point. The average distance between successive points a' is calculated and used as a normalizing factor. Katz's FD is calculated as:

$$D = \frac{Log(L/a')}{Log(d/a')}$$

Another approach used is calculating the Box dimension [66]. Suppose that there a number of boxes of equal length *r*. *N(*r) is the number of such boxes that covers the object whose FD is to be calculated. These boxes each have area r^n, and they are scaled by a factor of $1/ r^n$. If the object is a square of length *s*, *N(r)* can be determined as follows:

$$s^2 = N(r) * r^n$$
$$N(r) = \frac{s^2}{r^n}$$
$$N(r) = s^2 (\frac{1}{r})^n$$

Since s^2 is a constant, it can be denoted by C:

$$N(r) = C(\frac{1}{r})^n$$

Solving for *n* yields:

$$n = \frac{\ln N(r) - \ln C}{\ln(\frac{1}{r})}$$

n is the dimension of the object. Since *C* is a constant, it can be ignored. Taking the limit of this formula as *r* approaches 0, the formula for box dimension is:

$$D_B(S) = \lim_{r \to 0} \frac{\ln N(r)}{\ln(\frac{1}{r})}$$

Regularization dimension [66] is defined in the following way: One first computes smoother and smoother versions of the original signal, obtained through convolutions with a kernel. When the original signal is fractal, its graph has infinite length, while all regularized versions have finite length. When the smoothing parameter tends to 0, the smoothened version tends to the original signal, and its length will to tend to infinity. The regularization dimension measures the speed with which the convergence takes place.

2.8 EEG Analysis

EEG analysis was done using the wavelet function and the Wavelet Toolbox that are a part of MATLAB 6.1. The mother wavelets used were Daubechies wavelet of order 4 and the frequency B-spline wavelet.

INRIA [65] have developed a Matlab based Software that does Fractal Analysis. This toolbox is known as FracLab. Regularization dimensions of the EEG signals were calculated using the functions provided by this toolbox.

CHAPTER 3

RESULTS OF FRACTAL ANALYSIS

The frequency content of signals from C3-O1 and Cz-Oz were similar. Hence, only the results from Cz-Oz are reported here. The EEG signals for each subject were filtered by an FIR filter using the Kaiser-Bessel window [49]. An FIR filter was used since it handles low frequency features much more efficiently. The signals were filtered in four different ways as follows:

1) Containing all frequencies
2) Containing only alpha frequency (8-13 Hz)
3) Containing only delta frequency (0.5-4 Hz)
4) Excluding alpha frequency

The sampling frequency of the recorded EEG is 312.5Hz. In order to reduce redundancy and for better processing time, each signal was divided into windows of 512 points (1.6384 seconds). There was an overlap of 10% between adjacent windows in order to avoid edge effect. Regularization dimension [66] was calculated for each of these windows and the values plotted as shown in the following figures.

Figures 3.1 to 3.4 below represent the average of the regularization dimensions of all subjects for the different sets of data. Figure 3.1 has the EEG signal containing all frequencies. It is observed that the plots for the two different periods are different and on an average, the amplitude of the fractal dimensions in the final period increase by 0.35% as compared to the initial period.

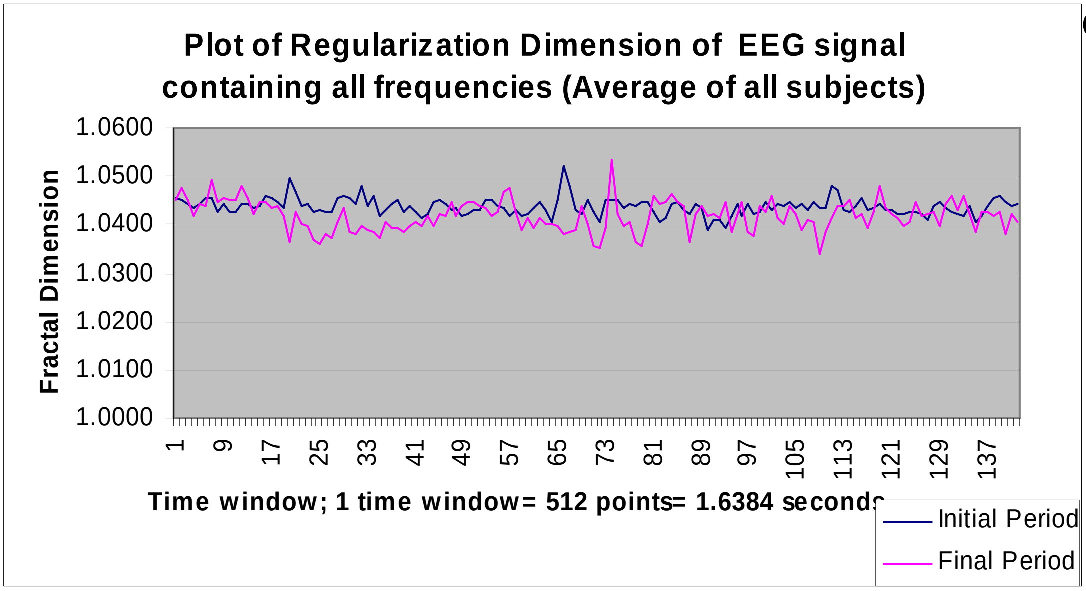

Figure 3.1

Figure 3.2 below shows the difference in the alpha frequency amplitudes in the initial and final periods. There is an average increase of 0.28% in the amplitude of the dimensions when between the two periods. Thus the major increase in amplitude is due to the alpha frequencies.

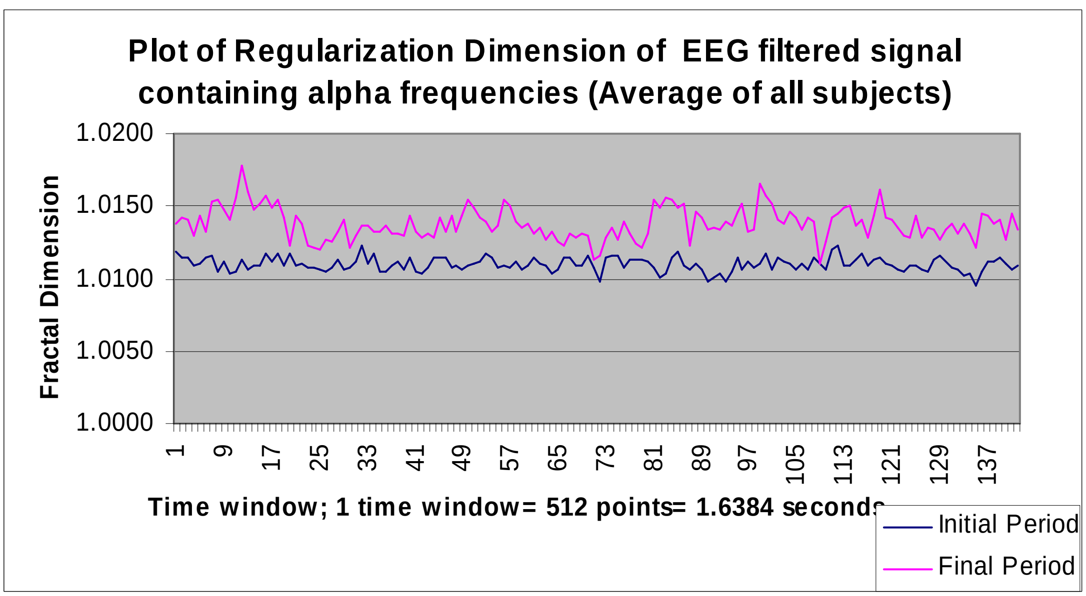

Figure 3.2

Figure 3.3 below plots the dimensions of the signal containing only delta frequencies. There is some differentiation between the two plots and the average increase in amplitude is 0.07% in the final period as compared to the initial period. Thus delta frequencies are present in the state of drowsiness.

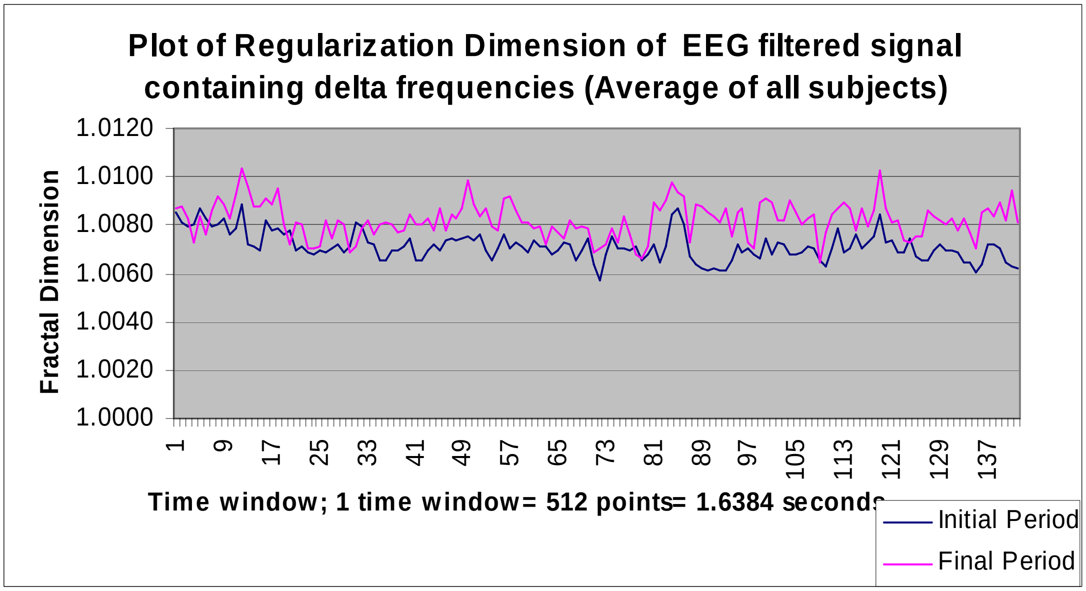

Fig 3.3

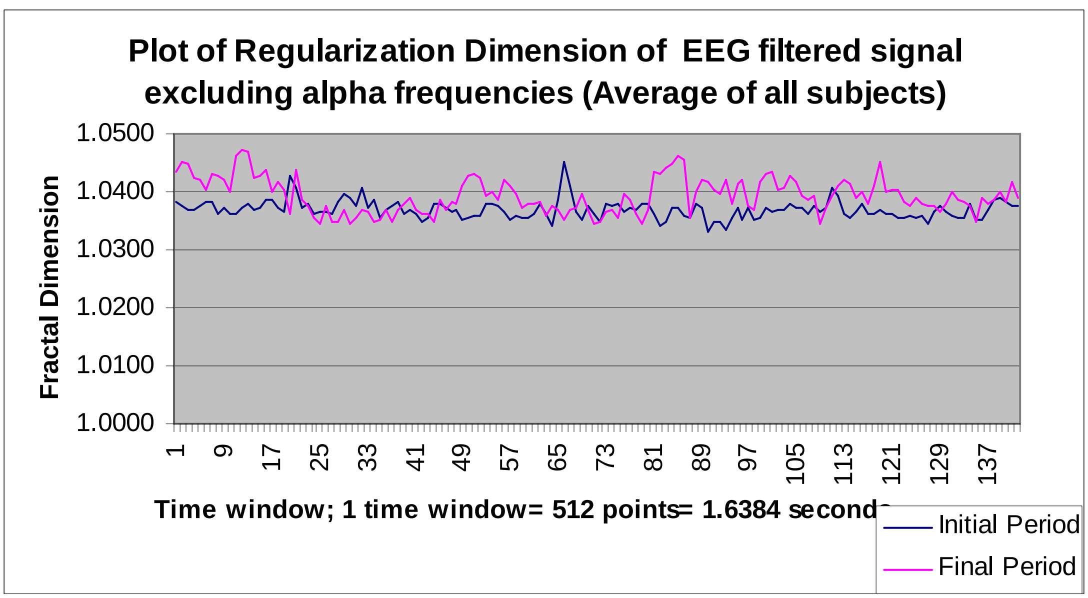

Fig 3.4

Figure 3.4 above has the all frequencies excluding alpha, and it is observed that there is no clear demarcation between the awake and drowsy periods. In fact, the average amplitude increase is about 0.07%, same as the amplitude change in delta frequencies. This confirms that alpha frequencies get affected the most with the change in alertness**.**

Figures 3.5-3.12 below represent the analysis of 2 subjects. The graphs for the remaining subjects will be found in Appendix B.

Subject 1

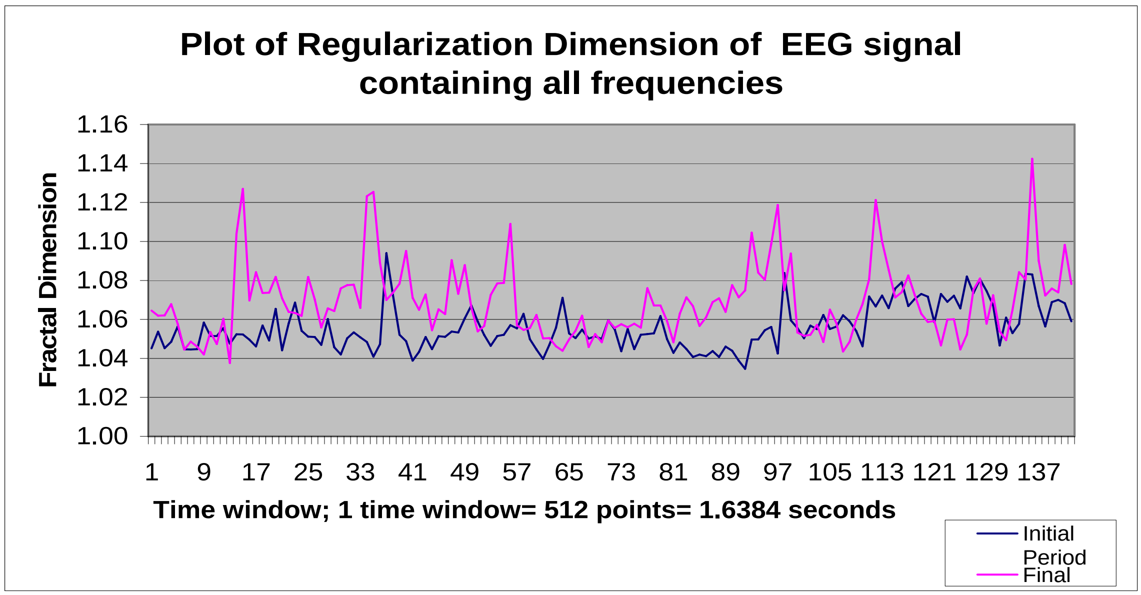

Fig 3.5

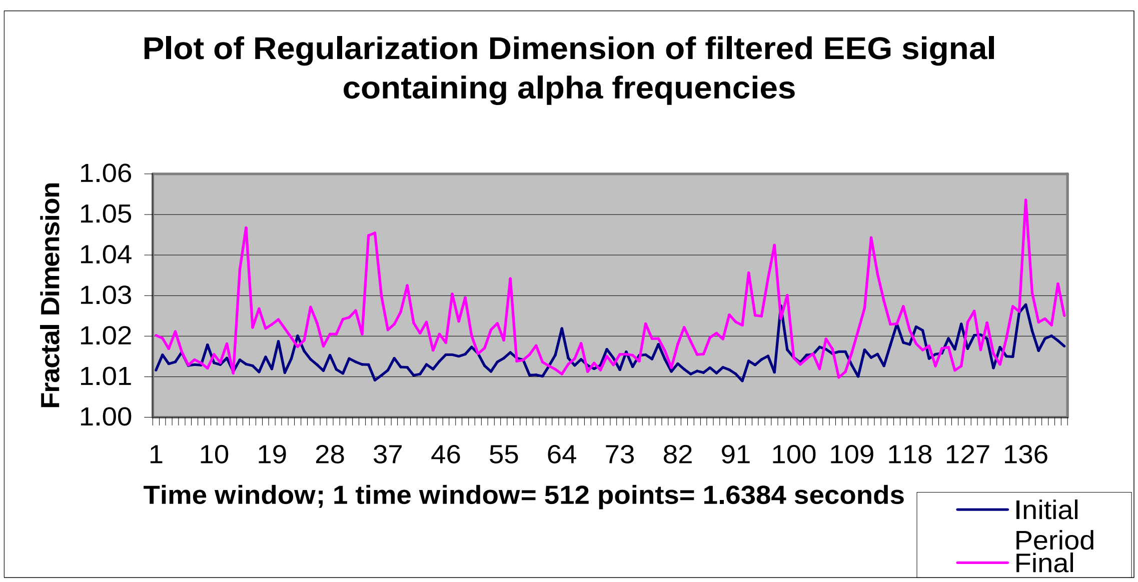

Fig 3.6

Subject 1

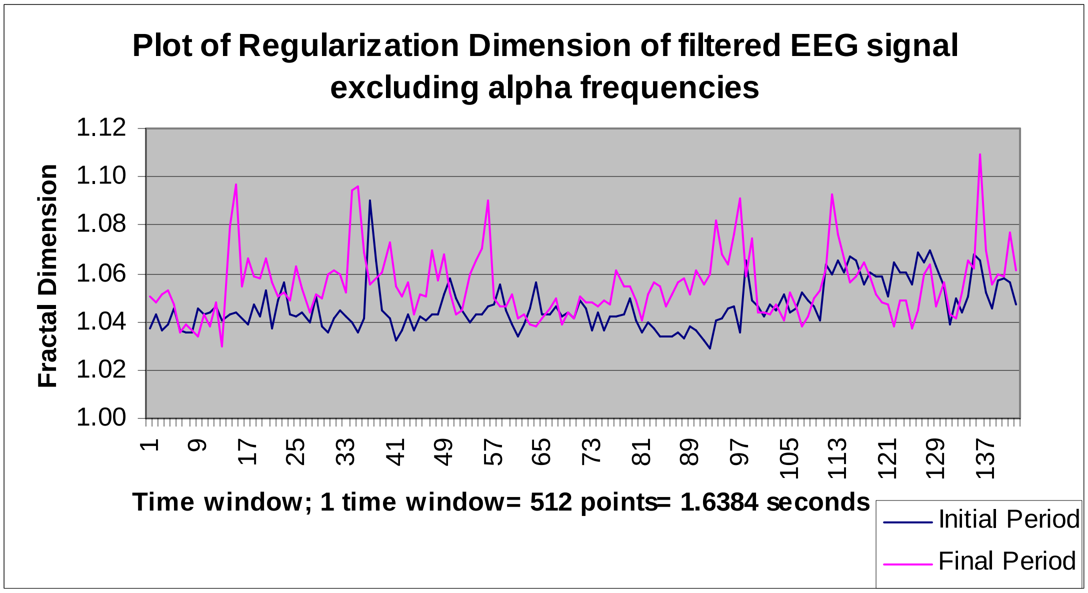

Fig 3.7

Subject 1

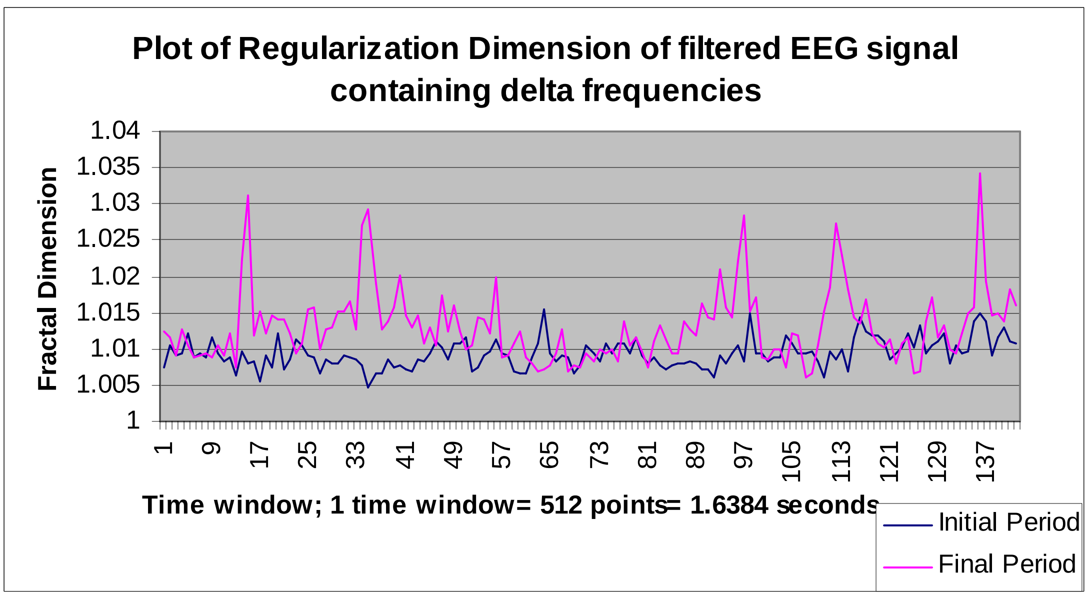

Fig 3.8

Subject 2

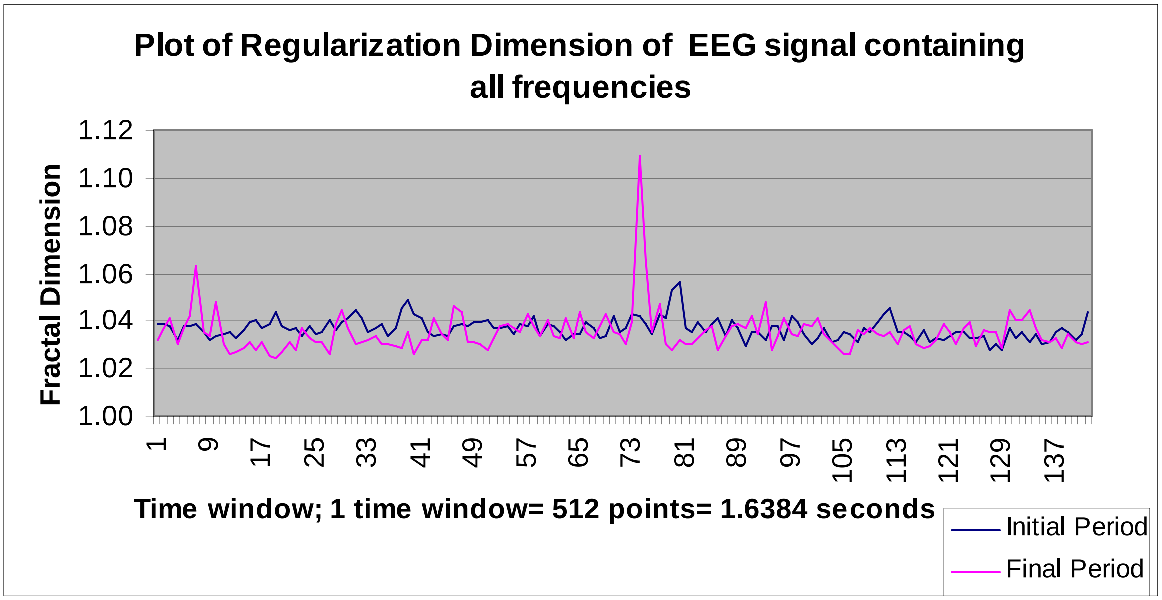

Fig 3.9

Subject 2

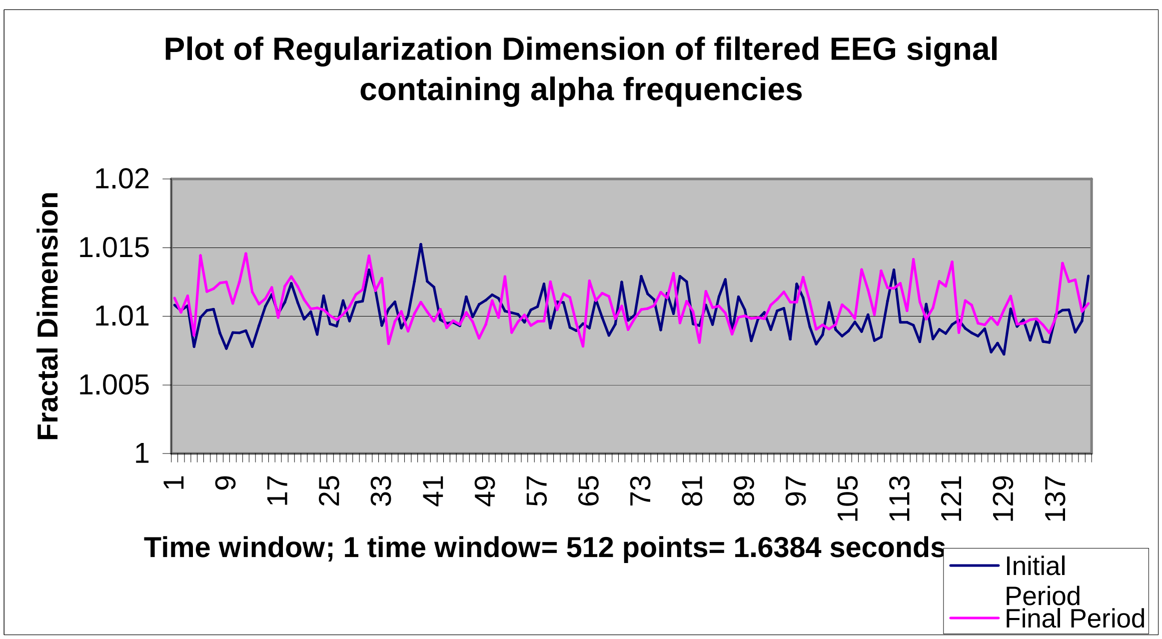

Fig 3.10

Subject 2

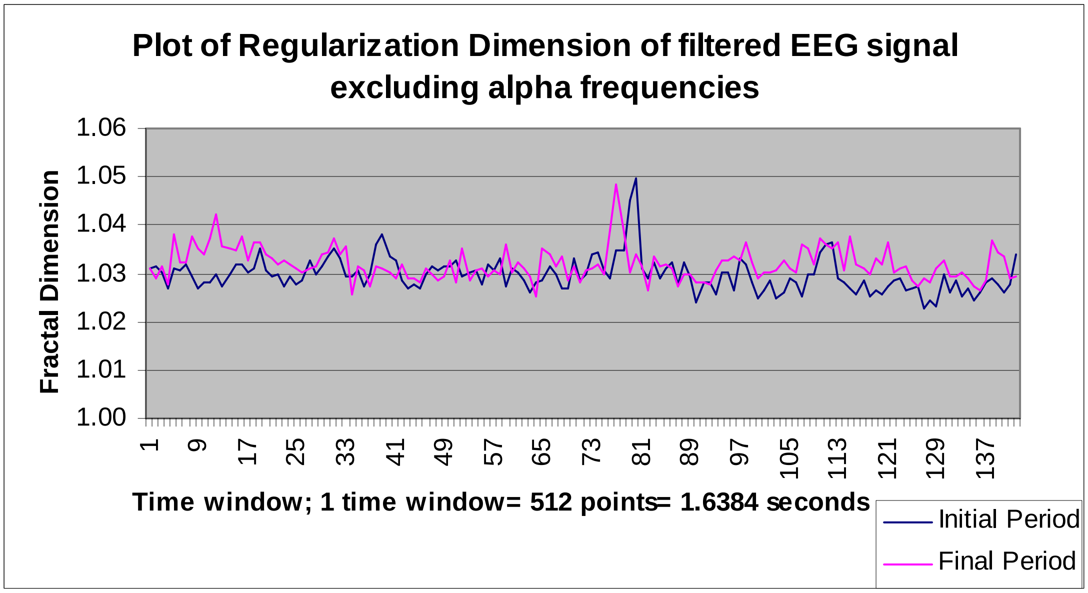

Fig 3.11

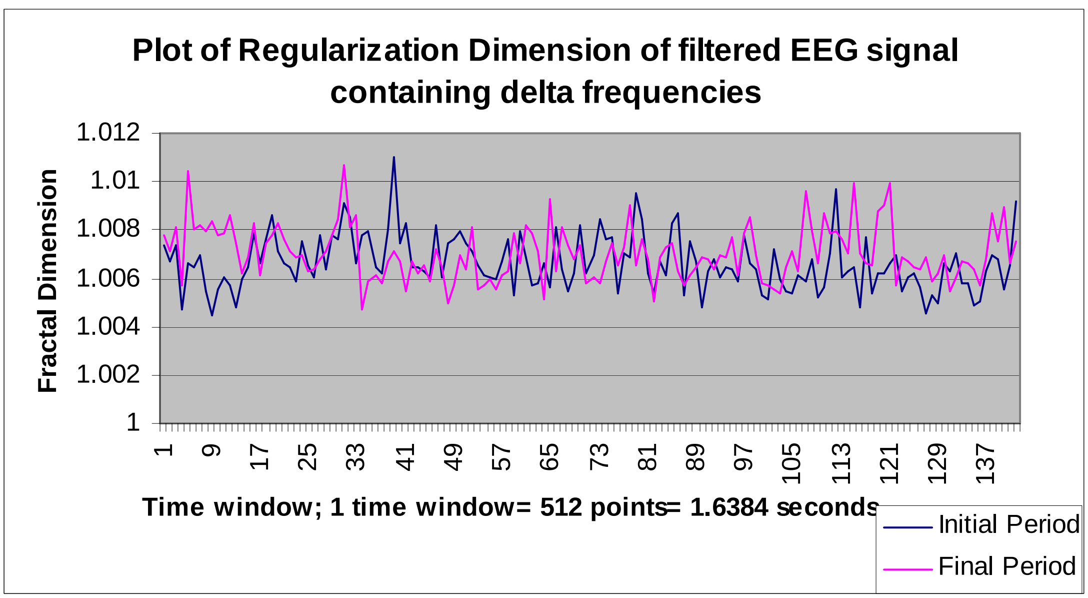

Fig 3.12

Further statistical analysis is done on the results. The standard error of the mean is often used as the most appropriate measure of error/variance in a set of data [67]. It is defined as the standard deviation divided by the square root of the number of samples. Table 3.1 below provides a summary of the standard errors for the different sets of data extracted from the EEG signals of each subject. “Initial” denotes the signal during the first 232.7295 seconds and “final” represents the signal in the last 232.7295 seconds.

From table 3.1, it is observed that the standard errors of the mean for the initial and final periods do not overlap. This indicates that the difference in the two sets of data for each subject for a particular frequency is statistically significant.

To further confirm this hypothesis, a two-sided t-test [67] is used to analyze the two sets of data for each subject. The null hypothesis is "means are equal". The alternative hypothesis is “means are not equal”. The significance level of a statistical hypothesis test is a fixed probability of wrongly rejecting the null hypothesis, if it is in fact true. The significance level chosen for this study is 5% or 0.05 [67]. The t-test calculated the variables P, CI and t statistic. P is the *probability* of observing the given result by chance given that the null hypothesis is true. Small values of P cast doubt on the validity of the null hypothesis. CI is the *confidence interval* that gives an estimated range of values, which is likely to include an unknown parameter, the estimated range being calculated from a given set of sample data. *Confidence limits* are the lower and upper boundaries of a confidence interval, that is, the values that define the range of a confidence interval. The *t statistic* is a measure of how extreme a statistical estimate is. This statistic is computed by subtracting the hypothesized value, which is the standard deviation of the sample, from the statistical estimate and then dividing by the estimated standard error.

Subjects	All Frequencies		Only Alpha		Excluding Alpha		Only Delta	
	Initial	**Final**	**Initial**	**Final**	**Initial**	**Final**	**Initial**	**Final**
Subject 1	0.00093941	0.00157182	0.00029182	0.00066737	0.00083704	0.00114934	0.00016349	0.00041643
Subject 2 Trial1	0.00036511	0.00073509	0.00011922	0.00011811	0.00030116	0.00028255	0.00009483	0.0001031
Subject 2 Trial2	0.00038953	0.00101203	0.00013409	0.00038245	0.00032549	0.00074796	0.00009472	0.00022572
Subject 3	0.00045521	0.00119385	0.00017452	0.00046505	0.00036041	0.000868	0.00012656	0.00029612
Subject 4	0.00027993	0.00040184	0.00009202	0.00010353	0.00024777	0.00038692	0.00007421	0.00008038
Subject 5	0.00051193	0.00082434	0.00015836	0.0001926	0.00044192	0.00086011	0.00011972	0.00014842
Subject 6	0.00082969	0.00073509	0.00021201	0.00026178	0.00075857	0.00098917	0.00016155	0.00016537
Subject 7	0.00046348	0.00181481	0.00015306	0.00063943	0.00036218	0.00137922	0.00012579	0.00039788
Subject 8	0.00056762	0.00054231	0.00013638	0.00014518	0.00054487	0.00090503	0.00039788	0.0001138
Subject 9 Trial1	0.00036689	0.00061167	0.00012952	0.00061167	0.00061167	0.00045025	0.00061167	0.00015255
Subject 9 Trial2	0.00096498	0.00071651	0.00011449	0.00026928	0.00098046	0.0005406	0.00008701	0.00016498
Subject 10	0.00036895	0.00019301	0.00009828	0.00009799	0.0003377	0.00023273	0.000082	0.0000823

Table 3.1
Comparison of Standard Error of Fractal dimensions

It is observed that the null hypothesis is rejected in 76.9% of the subjects in the EEG data containing all frequencies [Table 3.2], 92.3% of the subjects in the EEG data containing only the alpha frequencies [Table 3.3], 92.3% of the subjects in the EEG data excluding the alpha frequencies [Table 3.4], and 84.6% of the subjects in the EEG data containing only the delta frequencies [Table 3.5].

The probability value is assumed reasonable when the t-statistic is close to zero. It is not large enough when the t-statistic is a large positive (>1) and is too large when the t-statistic is a large negative (<-1). It is observed that where the null hypothesis is true, the t-statistic is close to zero. This indicates that the calculated probability of the two sets of data being similar is correct. In the majority of cases where the null hypothesis has been rejected, the t-statistic is a large negative (<-1). This shows that the calculated probability has been exaggerated and the actual probability of the two sets of data being similar is much lower.

The regularization fractal dimension is able to distinguish between the different states of alertness in EEG data.

	Reject Null Hypothesis	Probability	Confidence Interval (Lower Boundary)	Confidence Interval (Upper Boundary)	Tstat	df
Subject 1	1	0.00000000	-0.01684706	-0.00963816	-7.23186600	282
Subject 2 Trial1	0	0.07777824	-0.00016271	0.00306851	1.77017600	282
Subject 2 Trial2	1	0.00000000	0.00784626	0.01211539	9.20392900	282
Subject 3	1	0.00000000	0.00584979	0.01087983	6.54682200	282
Subject 4	1	0.00000000	-0.00552593	-0.00359794	-9.31518100	282
Subject 5	1	0.00000000	-0.00946507	-0.00564492	-7.78572300	282
Subject 6	0	0.66365600	-0.00266451	0.00169940	-0.43532990	282
Subject 7	0	0.23067970	-0.00593687	0.00143702	-1.20120500	282
Subject 8	1	0.00000000	0.01366556	0.01675614	19.37582000	282
Subject 9 Trial1	1	0.00000000	-0.01393415	-0.01112615	-17.56731000	282
Subject 9 Trial2	1	0.00000000	-0.01207523	-0.00734354	-8.07833500	282
Subject 10	1	0.00000000	0.02208001	0.02371923	54.99664000	282

Table 3.2
Ttest results for EEG data containing all frequencies

	Reject Null Hypothesis	Probability	Confidence Interval (Lower Boundary)	Confidence Interval (Upper Boundary)	Tstat	df
Subject 1	1	0.00000000	-0.00776216	-0.00489463	-8.68825400	282
Subject 2 Trial1	1	0.00003599	-0.00103502	-0.00037434	-4.19898100	282
Subject 2 Trial2	0	0.65996900	-0.00097625	0.00061926	-0.44042190	282
Subject 3	1	0.00575584	-0.00235991	-0.00040444	-2.78264200	282
Subject 4	1	0.00000009	-0.00103173	-0.00048641	-5.47999000	282
Subject 5	1	0.00925005	-0.00114428	-0.00016265	-2.62072500	282
Subject 6	1	0.00000000	-0.00439056	-0.00306437	-11.06510000	282
Subject 7	1	0.00005424	-0.00398950	-0.00140105	-4.09931000	282
Subject 8	1	0.00000000	0.00106839	0.00185257	7.33203000	282
Subject 9 Trial1	1	0.00000000	-0.01970828	-0.01842816	-58.64165000	282
Subject 9 Trial2	1	0.00000000	-0.00440648	-0.00325454	-13.09093000	282
Subject 10	1	0.00002131	0.00032686	0.00087322	4.32359500	282

Table 3.3
Ttest results for EEG data containing alpha frequencies

	Reject Null Hypothesis	Probability	Confidence Interval (Lower Boundary)	Confidence Interval (Upper Boundary)	Tstat	Df
Subject 1	1	0.00000001	-0.01130626	-0.00570875	-5.98347500	282
Subject 2 Trial1	1	0.00000013	-0.00305025	-0.00142454	-5.41807200	282
Subject 2 Trial2	1	0.00000000	0.01029106	0.01350238	14.58443000	282
Subject 3	1	0.00000000	0.00948423	0.01318425	12.05963000	282
Subject 4	1	0.00000000	-0.00532120	-0.00351242	-9.61321500	282
Subject 5	1	0.00000000	-0.01004952	-0.00624265	-8.42414900	282
Subject 6	1	0.00000000	-0.02584545	-0.02093800	-18.76517000	282
Subject 7	0	0.70739460	-0.00227113	0.00334272	0.37573750	282
Subject 8	1	0.01804643	-0.00459210	-0.00043328	-2.37856000	282
Subject 9 Trial1	1	0.00000000	-0.01052172	-0.00839300	-17.49024000	282
Subject 9 Trial2	1	0.00000000	-0.00923939	-0.00483164	-6.28382900	282
Subject 10	1	0.00000000	0.00621683	0.00783144	17.12656000	282

Table 3.4
Ttest results for EEG data excluding alpha frequencies

	Reject Null Hypothesis	Probability	Confidence Interval (Lower Boundary)	Confidence Interval (Upper Boundary)	Tstat	df
Subject 1	1	0.00000000	-0.00461337	-0.00285213	-8.34365100	282
Subject 2 Trial1	1	0.00000000	-0.00199507	-0.00144359	-12.27366000	282
Subject 2 Trial2	1	0.00000000	-0.00200650	-0.00104280	-6.22839300	282
Subject 3	1	0.04688367	-0.00127672	-0.00000892	-1.99610800	282
Subject 4	1	0.00099023	-0.00057944	-0.00014876	-3.32820400	282
Subject 5	0	0.13211460	-0.00066332	0.00008738	-1.51019000	282
Subject 6	1	0.00000000	-0.00231949	-0.00140937	-8.06478300	282
Subject 7	1	0.00041284	-0.00231297	-0.00067016	-3.57437600	282
Subject 8	0	0.42384930	-0.00048315	0.00114606	0.80092510	282
Subject 9 Trial1	1	0.00000000	-0.00282941	-0.00213177	-13.99802000	282
Subject 9 Trial2	1	0.00000000	-0.00254980	-0.00181549	-11.70167000	282
Subject 10	1	0.00058795	0.00017522	0.00063261	3.47656000	282

Table 3.5
Ttest results for EEG data containing delta frequencies

CHAPTER 4

RESULTS OF WAVELET TRANSFORM

The frequency content of signals from C3-O1 and Cz-Oz were similar. Hence, only the results from Cz-Oz are reported here. Fig.4.1 shows the color-coded wavelet coefficients of two signals from the same subject.

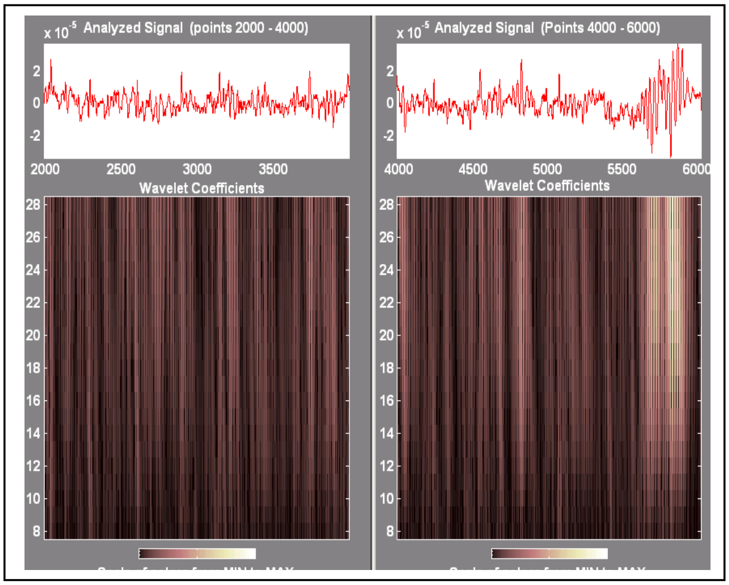

Fig. 4.1.
Wavelet Coefficients from Scales 8 to 28.

The first signal (top left) is taken from the latter part of the cycle while driving and the second signal (top right) is taken from the corresponding part of the cycle during observation with no movement. Scales 8 to 28 depict the maximum variations in the signal amplitude. These scales represent frequencies from 6.975 Hz to 13.95 Hz. The lighter the color, the higher is the absolute magnitude of the wavelet coefficient and this represents higher amplitude of that particular frequency of the signal. As seen, the wavelet coefficients are of higher magnitude in the last 500 points of the second signal.

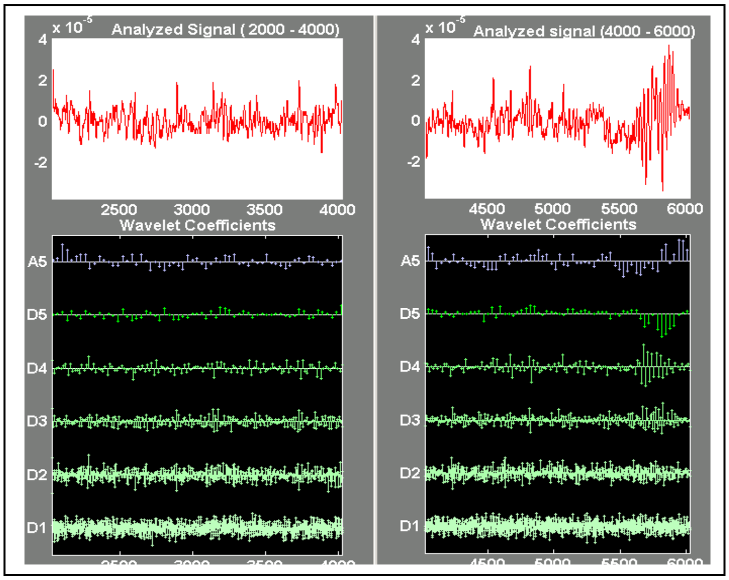

Fig.4.2
Wavelet Coefficients at various levels of detail

Fig.4.2 shows the details of the wavelet coefficients at different powers of 2. The first signal (top left) is taken from the latter part of the cycle while driving and the second signal (top right) is taken from the corresponding part of the cycle during observation with no movement. Presence of alpha waves is very evident at levels 4 and 5. Similar results have been observed for all subjects. They were also observed in both recordings of the subjects who did the experiment twice. In general, there were a large number of alpha waves in the latter parts of the driving cycle during observation with no- movement. The same inferences are made when observing the wavelet coefficients of the average EEG signal of all subjects (Fig 4.3 and Fig 4.4).

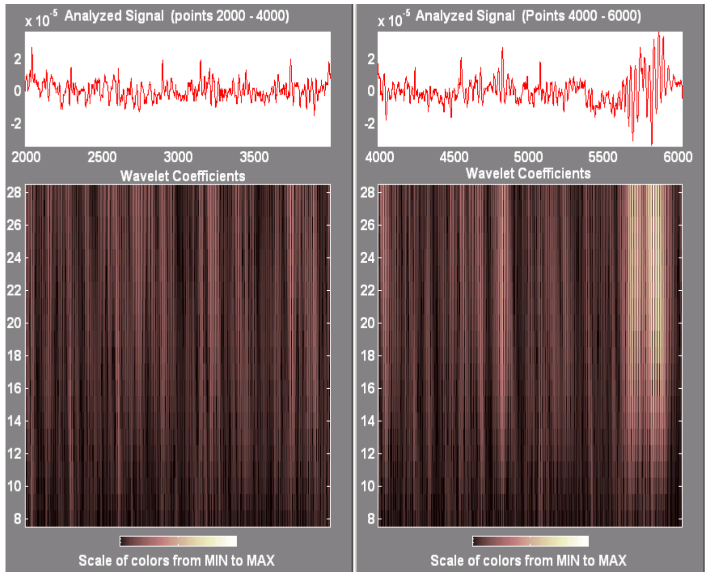

Fig. 4.3.
Wavelet Coefficients from Scales 8 to 28 for the averaged EEG signal

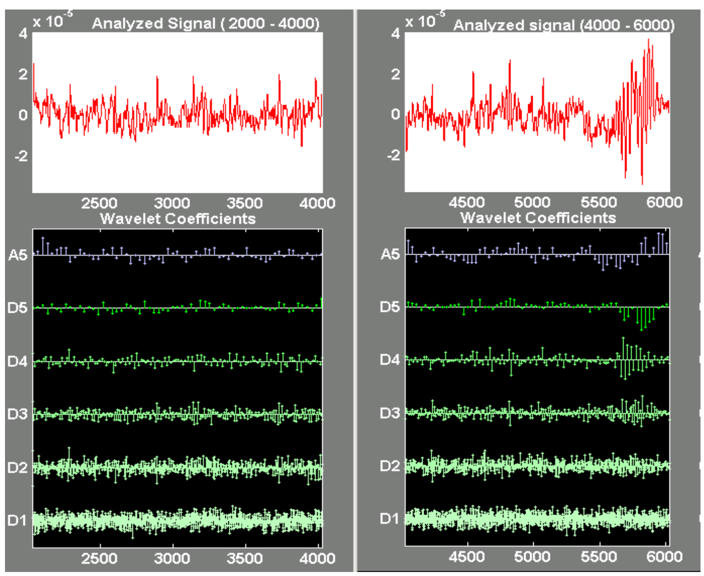

Fig.4.4
Wavelet Coefficients at various levels of detail for the averaged EEG signal

To ensure that the signals did not contain very high amount of 60hz signal, Fourier Transform was done using the ACQ software. It was observed that an insignificant amount of this frequency was present in the recorded data. Fig 4.5 is the plot for one set of data.

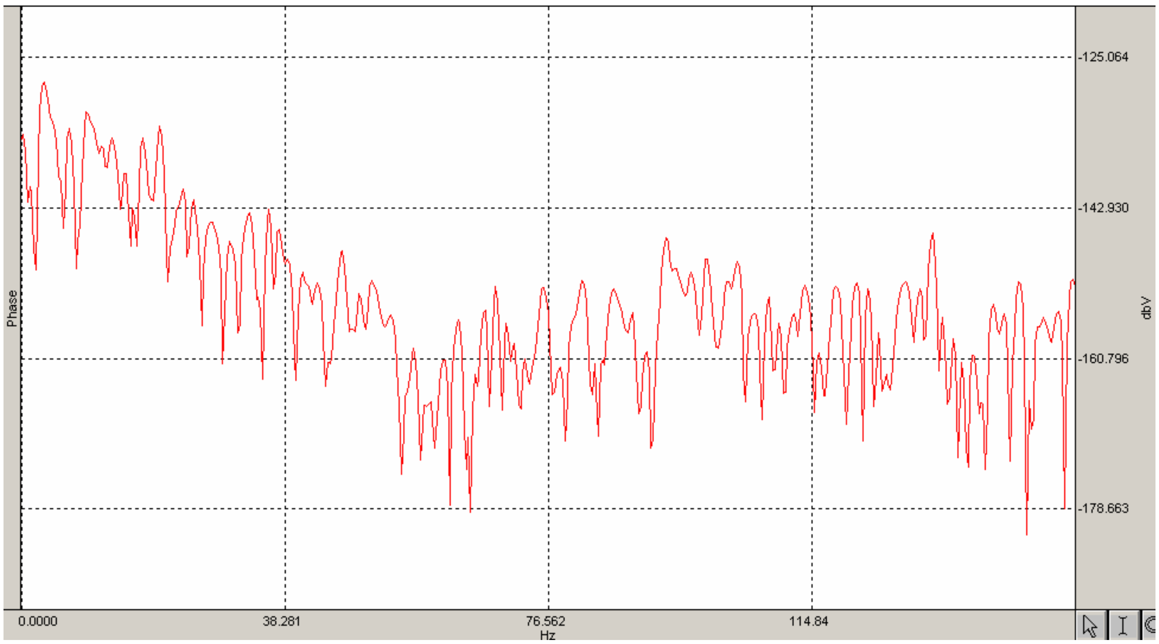

Figure 4.5
Plot of Fourier Transform

Figures 4.6 and 4.7 below plot the Fourier transform of the averaged EEG signal in the initial and final periods. Micheli-Tzanakou and Pavlopoulos [69] have used the phase characteristics of the power spectrum as a criterion for distinguishing between normal and abnormal Visual Evoked Potentials (VEP). They showed that the phase spectrum of a VEP has a certain periodicity in the 0- to 40-Hz region and were able to determine the range of the period that characterizes normal and abnormal populations. Thus an experimental method for objectively examining any kind of VEP waveforms was established.

Similarly, in this study the two plots were compared for their periodicity wherein; the peaks above 50 degrees in the 0-80Hz range were counted. It is observed that the periodicity in both periods is similar (97 for initial period and 99 for final period). When analyzed for only the alpha frequencies the periodicity was the same for both periods (6 for initial period and 6 for final period). This reinforces our observations that Fourier Transform is not a suitable analysis technique for the problem in this study.

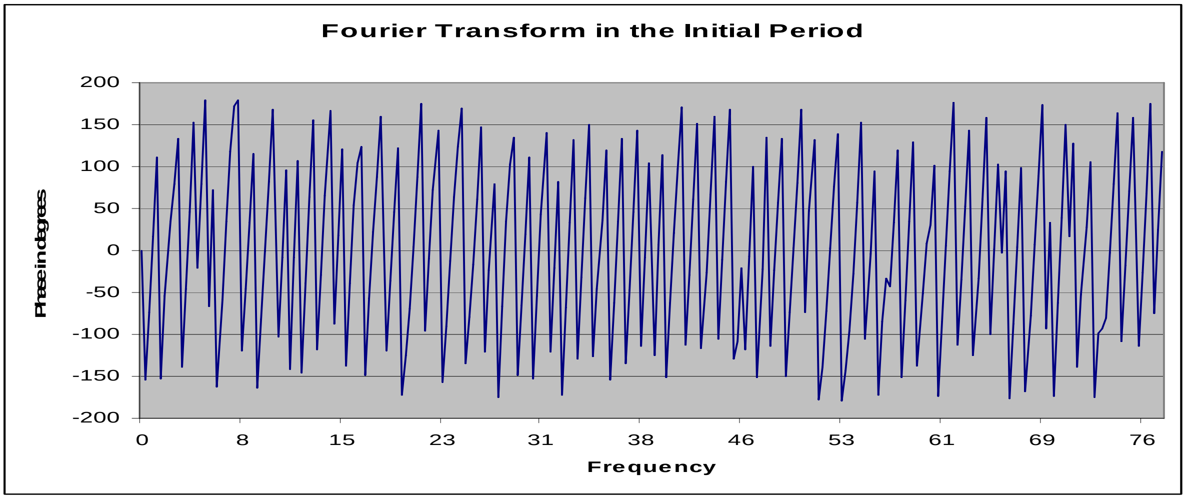

Figure 4.6

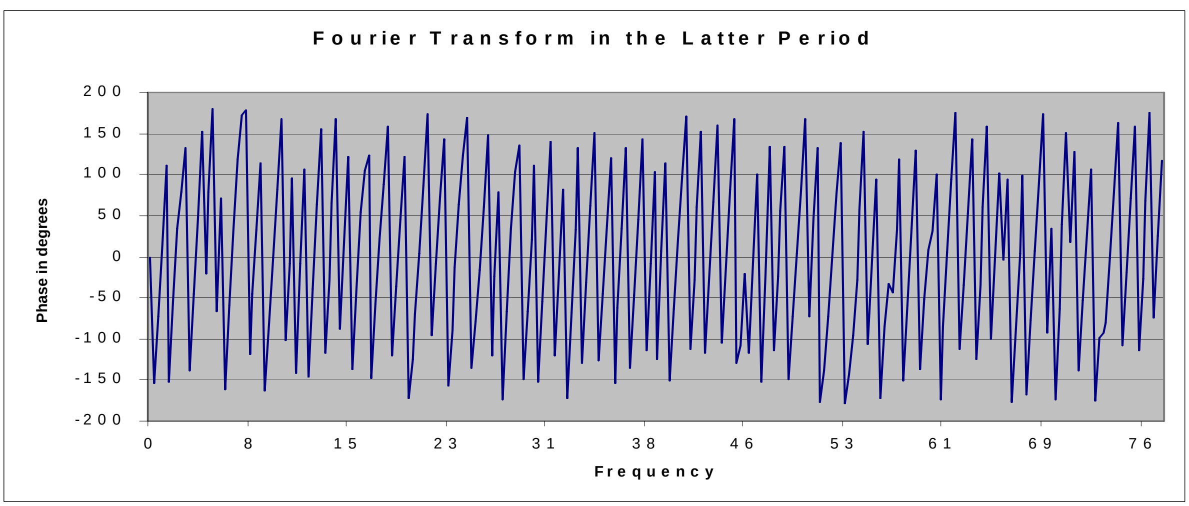

Figure 4.7

Figure 4.8 below, provides the comparison of standard deviations of the wavelet coefficients using different wavelets. Each signal was divided into windows of 1024 points (3.2768 seconds). There was an overlap of 10% between adjacent windows in order to avoid edge effects. The wavelet coefficients were calculated using Matlab and standard deviation of the coefficients obtained using different wavelets were plotted. Daubechies and Symlet wavelets did not filter the signal for noise effectively before analysis and it will be observed that this caused a shift in the amplitude of the wavelet coefficients. This increases the chances of error. B-spline wavelets provide the best indication and hence, they have been used for the analysis of all subjects.

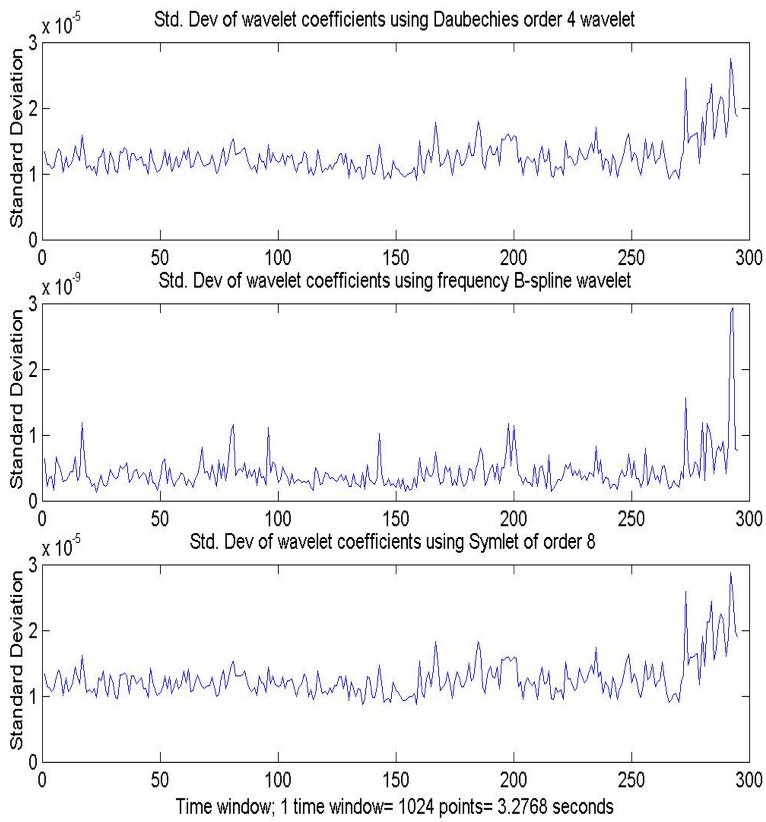

Fig 4.8
Comparison of Coefficients using Different Wavelets

Figures 4.9 to 4.12 provide the plots for the wavelet coefficients of three subjects. Subject 2 was requested to come on different days at different times. This was to avoid selection bias while analyzing the signals. Trial 1 was conducted at the start of the day whereas Trial 2 was conducted at the end of the day. It is observed that the difference in amplitudes of the wavelet coefficients is more pronounced in Trial 2. The plots for the remaining subjects will be found in Appendix C. The time windows are of 1.6384 seconds.

Subject 1

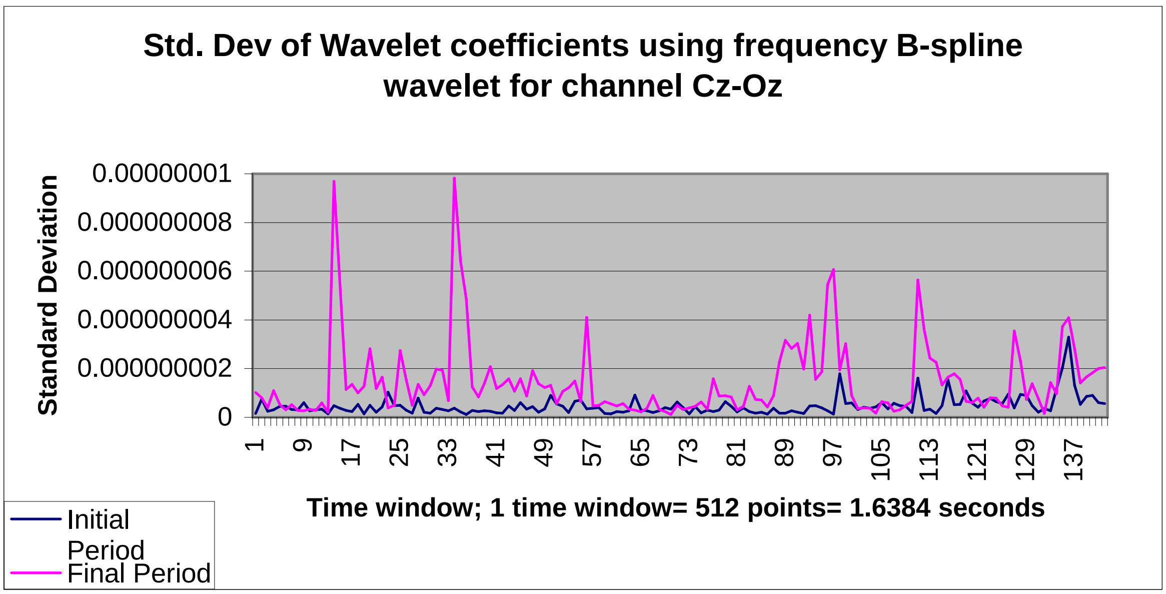

Fig 4.9

Subject 2-Trial 1

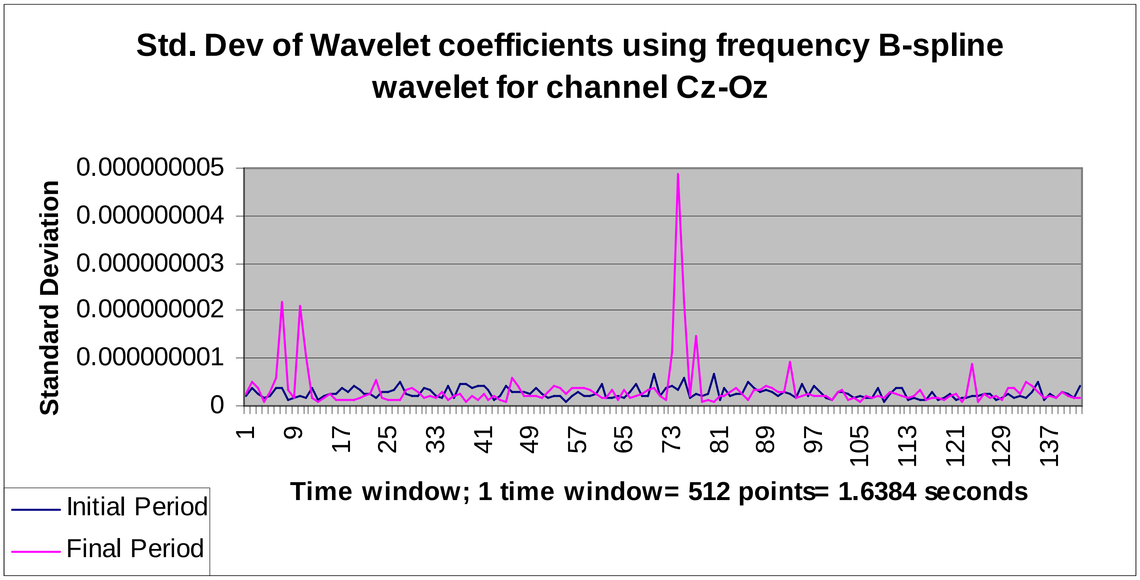

Fig 4.10

Subject 2- Trial 2

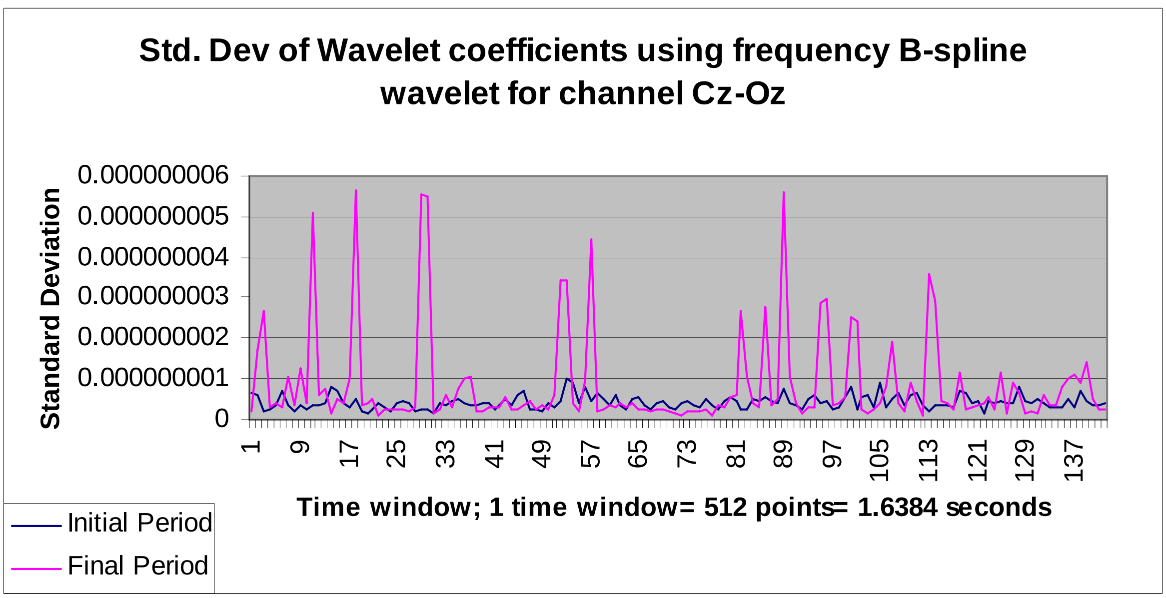

Fig 4.11

Subject 3

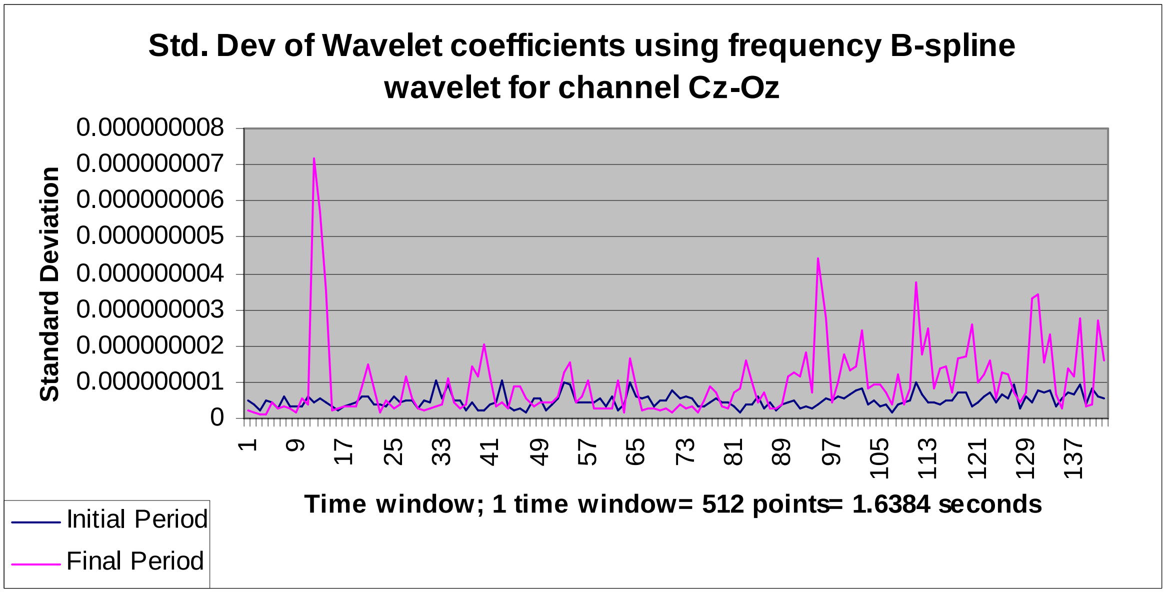

Fig 4.12

Fig. 4.13 gives the average of the standard deviation when calculated across all subjects. It is observed that the standard deviation is on an average 95.59% higher in the final period indicating the increased presence of alpha waves during the latter driving stages.

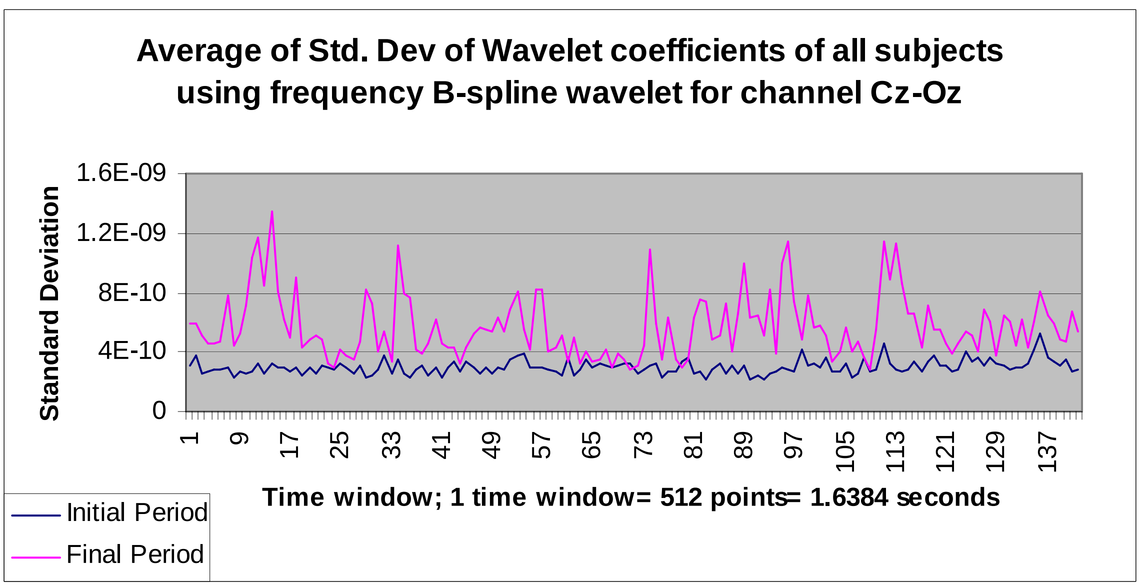

Fig. 4.13

Table 4.1 below provides a summary of the standard errors for the two sets of data extracted from the EEG signals (Cz-Oz) of each subject. “Initial” denotes the signal during the first 232.7295 seconds and “final” represents the signal in the last 232.7295 seconds.

Subjects	**All Frequencies**	
	Initial	**Final**
Subject 1	0.0000000000335500	0.0000000001356864
Subject 2 Trial1	0.0000000000095956	0.0000000000425839
Subject 2 Trial2	0.000000000139065	0.0000000001008122
Subject 3	0.0000000000160894	0.0000000000879784
Subject 4	0.0000000000061353	0.0000000000089000
Subject 5	0.000000000188965	0.0000000000234886
Subject 6	0.0000000000087998	0.0000000000425839
Subject 7	0.0000000000076737	0.0000000000672184
Subject 8	0.0000000000088896	0.0000000000100078
Subject 9 Trial1	0.0000000000108688	0.0000000000294674
Subject 9 Trial2	0.0000000000069589	0.0000000000409784
Subject 10	0.0000000000047087	0.0000000000011612
Average	0.0000000000040517	0.0000000000179009

Table 4.1

Standard Error for data extracted from EEG Signal

A two-sided t-test is used to analyze the two sets of data for each subject (Table 4.2). The null hypothesis is "means are equal". The alternative hypothesis is “means are not equal”. The significance level chosen is 5% or 0.05 [67]. It is observed that the null hypothesis is rejected in 76.9% of the subjects in the EEG data.

The probability value is assumed reasonable when the t-statistic is close to zero. It is not large enough when the t-statistic is large positive (greater than 1) and is too large when the t-statistic is large negative (less than –1). It is observed that where the null hypothesis is true, the t-statistic is close to zero. This indicates that the calculated probability of the two sets of data being similar is correct. In the majority of cases where the null hypothesis has been rejected, the t-statistic is a large negative. This shows that the calculated probability has been exaggerated and the actual probability of the two sets of data being similar is much lower.

Wavelet transform is a visually effective tool to observe the change in frequency of a non-stationary signal like EEG.

Various states of EEG signal correspond to different representation of information in each scale. The features of the waveform in each scale using the wavelet transform can reflect the states of the EEG signal. So, a new analysis tool for signal feature acquisition, automatic discrimination, false wave elimination and automatic analysis is provided. Continuous Wavelet Analysis is often easier to interpret, since its redundancy tends to reinforce the traits and makes all the information more visible. This is especially true of very subtle information. Thus, the analysis gains in “readability” and in ease of interpretation. Thus we can use wavelet transform to distinguish between the different states of alertness in EEG data.

	Reject Null Hypothesis	Probability	Confidence Interval (Lower Boundary)	Confidence Interval (Upper Boundary)	tstat	df
Subject 1	1	3E-12	-1.2933E-09	-7.4304E-10	-7.284494	282
Subject 2 Trial1	0	0.1184036	-1.543E-10	1.755E-11	-1.566284	282
Subject 2 Trial2	1	4.31588E-05	-6.2317E-10	-2.2253E-10	-4.155063	282
Subject 3	1	7.5813E-08	-6.6999E-10	-3.1789E-10	-5.522718	282
Subject 4	1	0.007515835	-5.038E-11	-7.83E-12	-2.692514	282
Subject 5	0	0.2256957	-9.594E-11	2.274E-11	-1.214178	282
Subject 6	1	0.000220556	-2.4834E-10	-7.716E-11	-3.742761	282
Subject 7	1	3.791E-09	-5.4485E-10	-2.785E-10	-6.084934	282
Subject 8	0	0.1626453	-7.61E-12	4.509E-11	1.39989	282
Subject 9 Trial1	1	0	-4.2643E-10	-3.0278E-10	-11.60874	282
Subject 9 Trial2	1	0	-4.7637E-10	-3.1274E-10	-9.492511	282
Subject 10	1	0	9.185E-11	1.1095E-10	20.90805	282

Table 4.2

Ttest results for EEG data after Wavelet Transform

Chapter 5

Discussion And Further Work

The EEG signal can be viewed as one generated by a self-organized, chaotic, nonlinear, dynamical system governed by deterministic evolution equations and perturbed by noisy perturbations [5]. It has been observed that there is an increase of slow alpha activity on the EEG when cerebrum activity goes down because of less tension or because of a tendency to drowsiness [32].

Experimentally, it has been found that for a driver on the highway, it is easy to become drowsy in about 40 minutes [28]. In the current study, EEG signals were recorded while subjects were driving for 40 minutes and then while they were observing their driving course for the same amount of time in the same seating position without actually driving. Fractal analysis and Wavelet Transform were used to analyze the signals. Two of the subjects were requested to come on different days and at different times of the day. This was done in order to show that at different times of the day the signals obtained where different. Trial 1 was conducted at the start of the day whereas Trial 2 was conducted at the end of the day. It is observed that the difference in amplitudes of the fractal dimensions and wavelet coefficients is more pronounced in Trial 2, i.e. the latter part of the day, since during that part of the day, the subjects were more tired.

Wavelet transform is a visually effective tool to observe the change in frequency of a non-stationary signal like EEG. It is observed that the standard deviation is on an average 95.59% higher in the later driving stages indicating the increased presence of alpha waves. Continuous Wavelet Analysis is also easier to interpret, since its redundancy tends to reinforce the significant characteristics of the signal and makes all the information more visible. This is especially true of very subtle information. The analysis gains in “readability” and in ease of interpretation. Thus we can use wavelet transform to distinguish between the different states of alertness in EEG data.

The regularization fractal dimension is able to distinguish between the different states of alertness in EEG data. When the entire EEG signal is analyzed, the average increase in amplitude of the dimension is 0.35% and it is in the latter driving period. Amplitude of alpha frequencies increases by 0.28% and that of the delta frequencies increase by 0.07%. Thus the major increase in amplitude is due to the alpha frequencies.

Previous studies have determined that there is an anterior-posterior gradient in the EEG, proving that alpha rhythm is less represented in the frontal region [64].Accardo et al recorded the EEG signals from four normal subjects and two subjects with generalized epilepsy. All recordings were carried out on wakeful subjects with open or closed eyes. The signals were analyzed using Higuchi’s algorithm. They observed that the fractal dimension with the eyes closed was larger than the value of the fractal dimension with the eyes open. Also, the presence of alpha frequencies was greater in the signal recorded with closed eyes. It is thus possible to conjecture that a bioelectrical activity characterized by the increased presence of rhythmic waves at an unwanted time (such as the alpha rhythm on the onset of drowsiness) represents a situation with high chaotic behavior producing higher values of the fractal dimension. The reduced value of the fractal dimension during regular activity, when alpha is not present, indicated that the brain network acts as a less chaotic system.

Two-sided t-test was done on the results obtained by both methods. One set was the result obtained for the EEG signal recorded in the initial period and the second set was the signal recorded in the latter period. The null hypothesis was "means are equal".

The alternative hypothesis was “means are not equal”. It is observed that the null hypothesis is rejected in 76.9% of the subjects in the results of the EEG data obtained by both techniques.

While driving, an individual tends to get drowsier as time passes and this is very clearly depicted from the increasing amplitude of the alpha frequencies. The increase in amplitude is observed using wavelet transform and fractal analysis. The time required to analyze the signal was 7 seconds for wavelet analysis and 10 seconds for fractal analysis. This is an important factor while considering instant feedback to alert the driver in order to avoid possible mishaps. In the future, this analysis can be used to monitor driver alertness and physical condition and to provide instantaneous response for the driver’s awareness and accident prevention.

The Fractal results show that alpha and to some extent delta waves are the ones contributing towards drowsiness. However, in the current study these frequencies had to be separated for accurate analysis. Since analysis of the signal needs to be instant and accurate, a real-time filtering technique such as Fourier transform [35] will need to be incorporated. Combining fractal dimension changes to spectral parameters could increase the sensitivity of real time detection of the onset of drowsiness. Alternatively, there could be techniques such as Hjorth parameters [68], Artificial Neural Networks [45], Higuchi’s algorithm [43] that would provide results in real-time without the need for filtering.

The possible feedback mechanisms that could be installed as a result of the detection could be an audio alarm or an electric buzzer. The reaction provided by the system needs to be instantaneous to avoid the possibility of accidents.

As described in the methods section, a cap with electrode placements as per the 10-20 electrode system was used to record the EEG signals. Based on this, a cap is required to be designed taking into consideration its cosmetic appearance in order to appease to users for regular use. Also the cap will need to be able to be insensitive to the diverse resistances provided by different users to the electrodes. The drawback of this system could be the reluctance on the part of the users to regularly and correctly wear the cap to capture the signals as per the 10-20 electrode system.

As for the needed instrumentation, the analysis carried out in this study was done using a desktop with the Pentium 4 microprocessor. This is a standard processor available in most standard computers. However the analysis was done post-recording. . The time required to analyze the signal was 7 seconds for wavelet analysis and 10 seconds for fractal analysis. Real-time processing and analysis will require more advanced hardware to decrease the time required for feedback.

In the current study, there are no assumptions made regarding the noise generated by the surroundings and the electrical components of the car while driving. The recordings were carried out in a closed room where all external noise was filtered out. In future studies, this will be an important factor for practical applications of the techniques considered in this study.

Other applications of drowsiness detection can be for workers in factories and for air traffic controllers where it is extremely essential to be vigilant at all times. Here too, an important consideration will be the constant hum generated by the machines along with the environmental noise. Hence filters will be required to be used to nullify the effect of the unwanted frequencies.

To summarize, in the current study, EEG recordings were done while subjects were driving in a simulated environment. The recorded signals were analyzed using Fractal analysis and Wavelet Transform. There is an increased presence of alpha frequencies with the onset of drowsiness. While the techniques used were successful in detecting the presence of these alpha waves, further studies need to be done to study the effect of external noises while driving and to improve the techniques in order to decrease the time required to provide analysis.

APPENDIX A

SUBJECT CONSENT FORM

APPENDIX B

FRACTAL ANALYSIS: REMAINING SUBJECTS

Subject 2: Trial 2

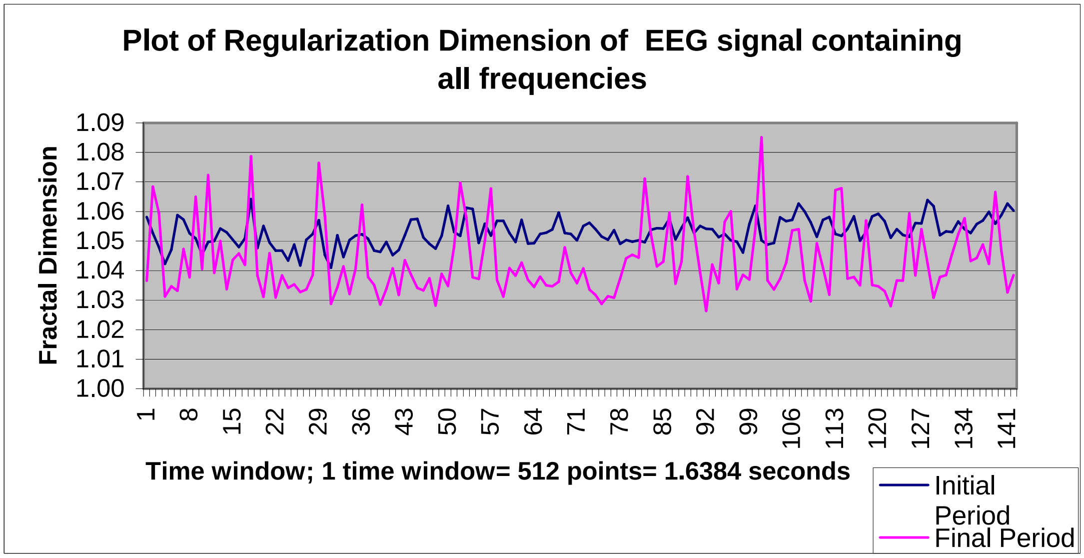

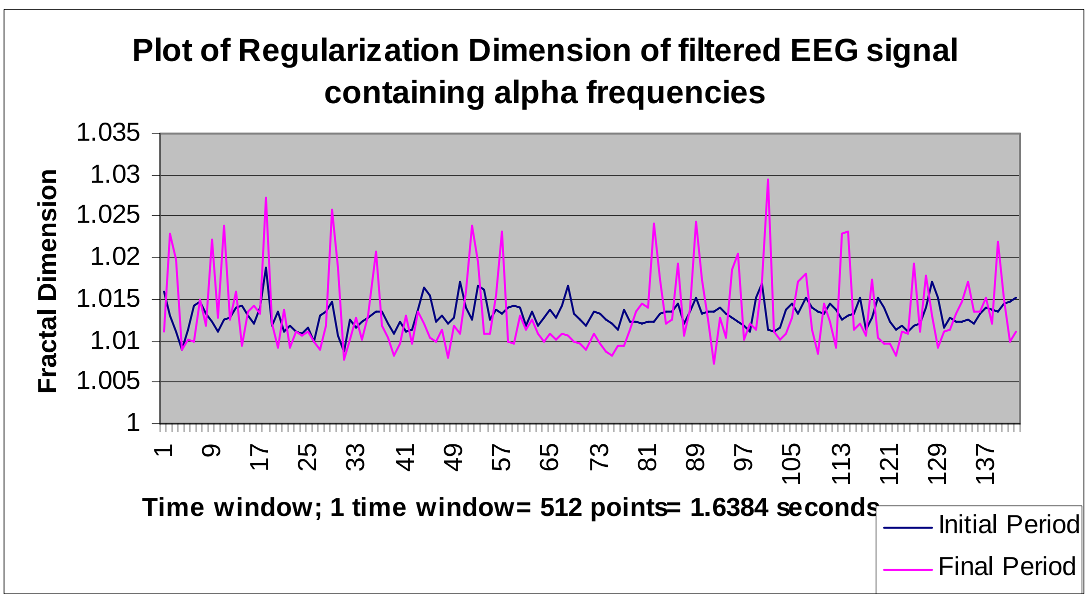

Subject 2: Trial 2

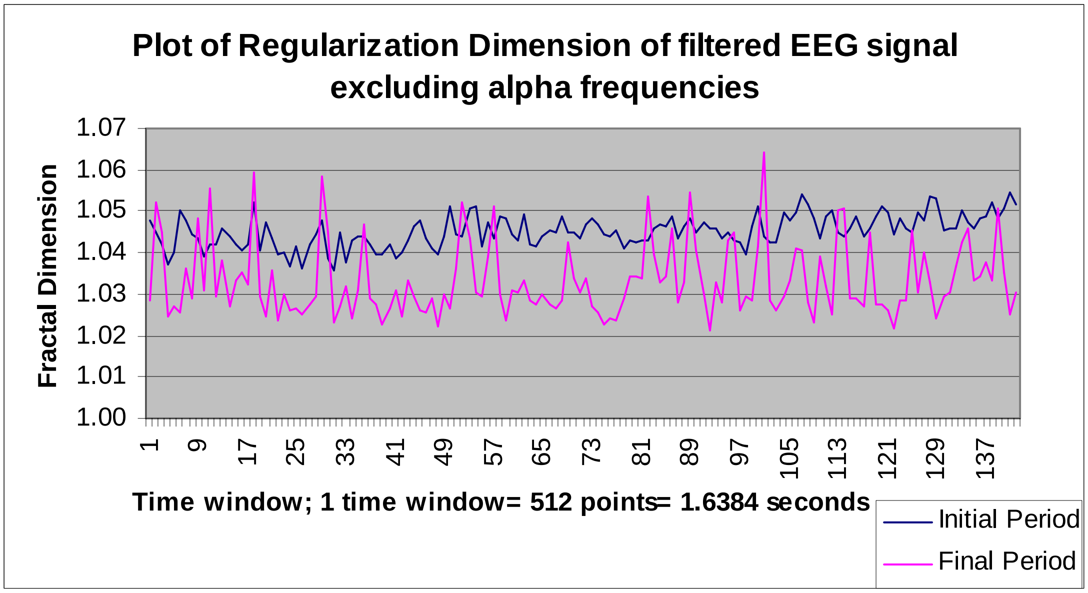

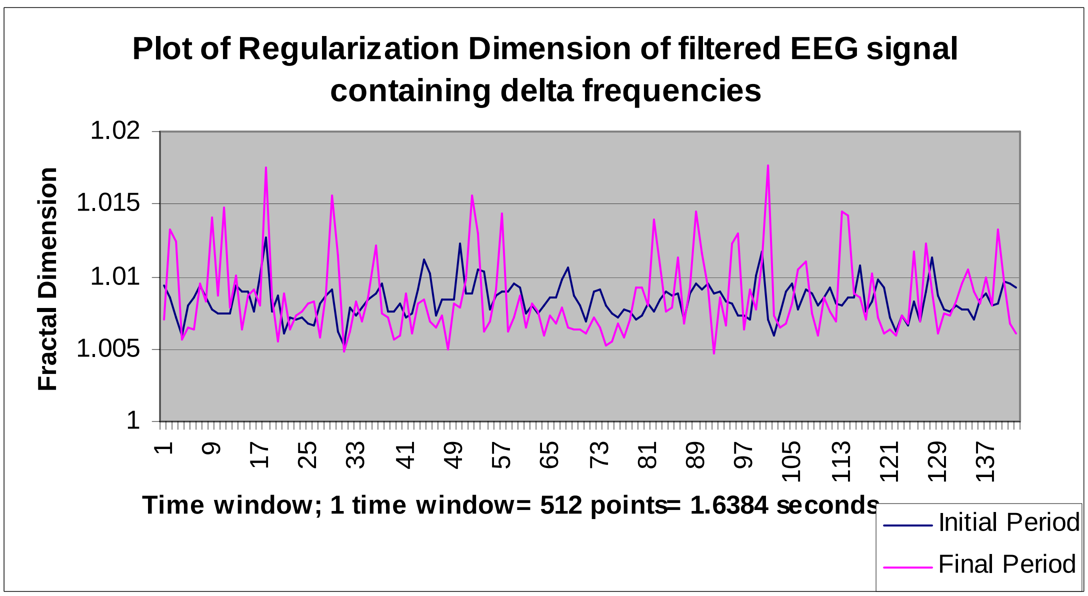

Subject 3

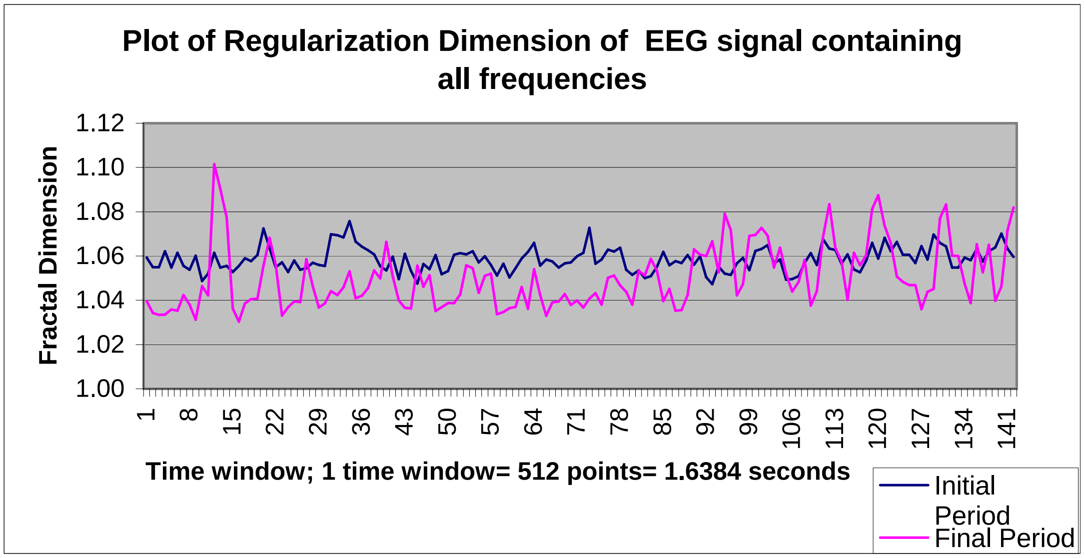
Plot of Regularization Dimension of EEG signal containing all frequencies
Fractal Dimension
1.12
1.10
1.08
1.06
1.04
1.02
1.00
1
8
15
22
29
36
43
50
57
64
71
78
85
92
99
106
113
120
127
134
141
Time window; 1 time window= 512 points= 1.6384 seconds
Initial Period
Final Period

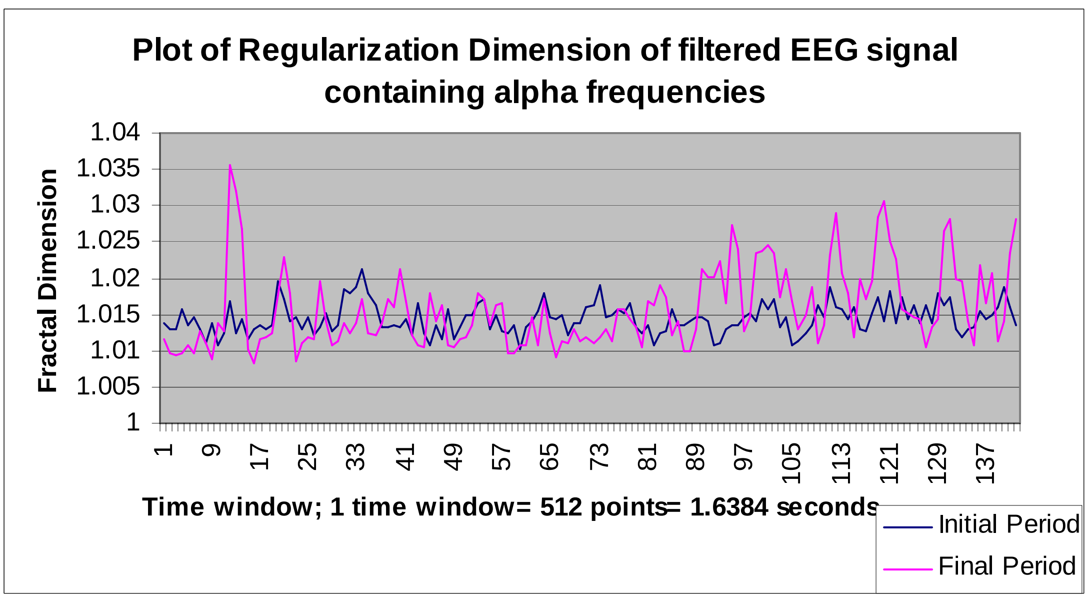
Plot of Regularization Dimension of filtered EEG signal containing alpha frequencies
Fractal Dimension
1.04
1.035
1.03
1.025
1.02
1.015
1.01
1.005
1
1
9
17
25
33
41
49
57
65
73
81
89
97
105
113
121
129
137
Time window; 1 time window= 512 points= 1.6384 seconds
Initial Period
Final Period

Subject 3

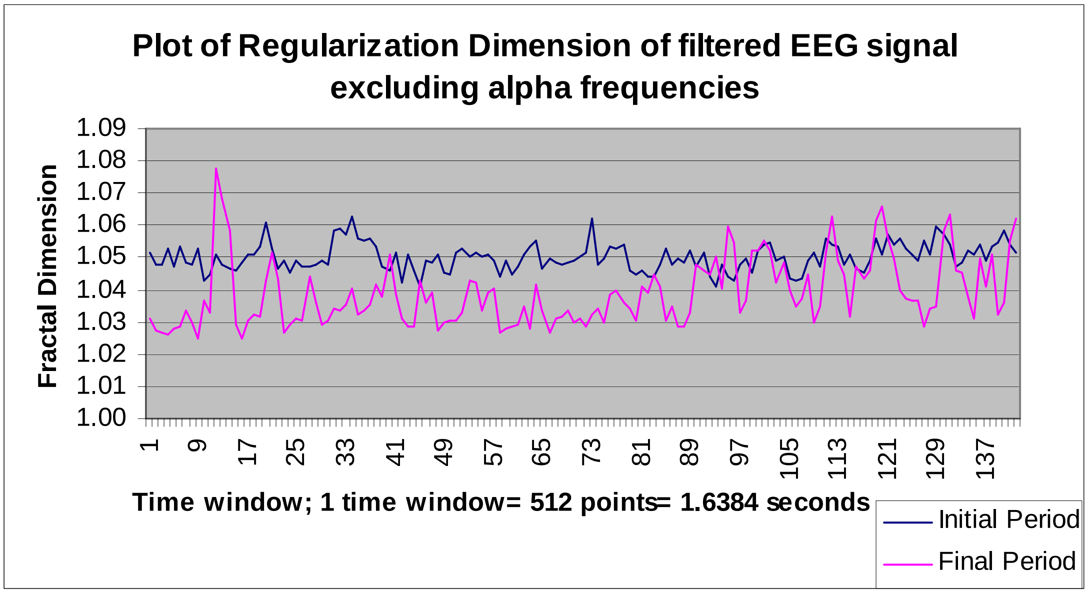
Plot of Regularization Dimension of filtered EEG signal excluding alpha frequencies
Fractal Dimension
1.09
1.08
1.07
1.06
1.05
1.04
1.03
1.02
1.01
1.00
1 9 17 25 33 41 49 57 65 73 81 89 97 105 113 121 129 137
Time window; 1 time window= 512 points= 1.6384 seconds
Initial Period
Final Period

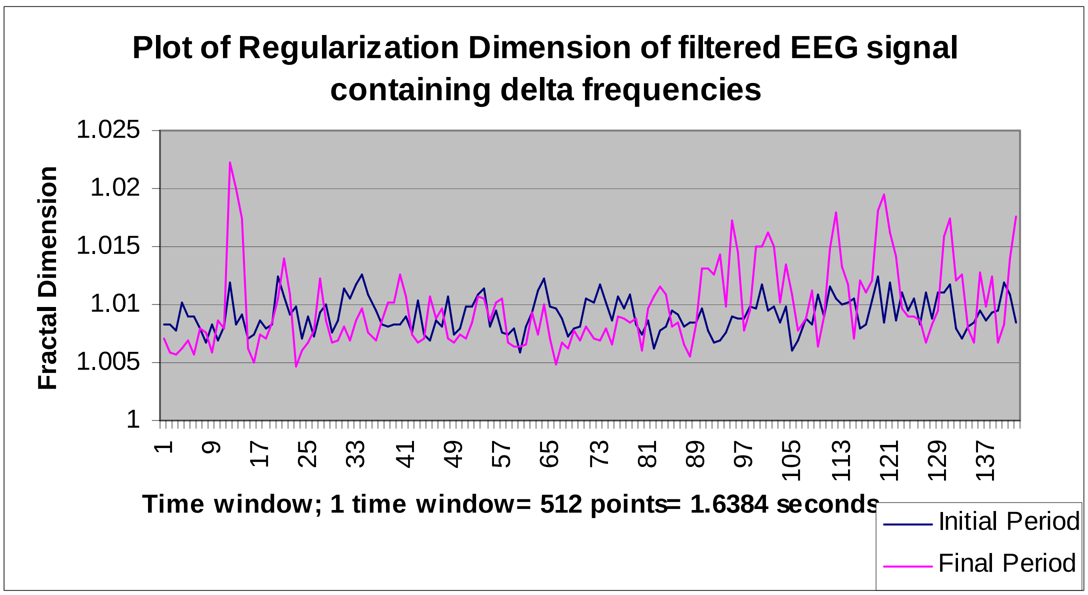
Plot of Regularization Dimension of filtered EEG signal containing delta frequencies
Fractal Dimension
1.025
1.02
1.015
1.01
1.005
1
1 9 17 25 33 41 49 57 65 73 81 89 97 105 113 121 129 137
Time window; 1 time window= 512 points= 1.6384 seconds
Initial Period
Final Period

Subject 4

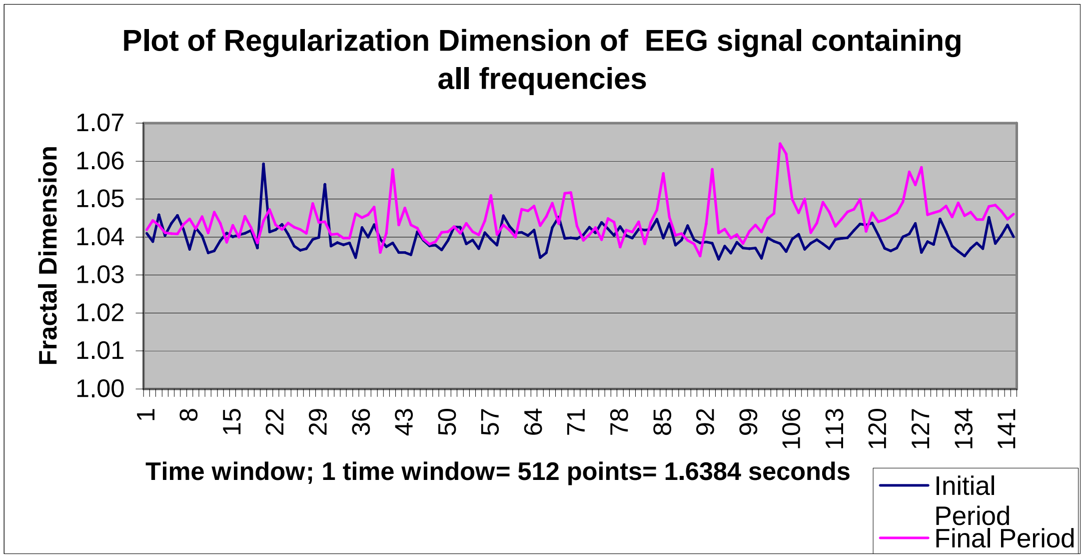
Plot of Regularization Dimension of EEG signal containing all frequencies
Fractal Dimension
1.07
1.06
1.05
1.04
1.03
1.02
1.01
1.00
1
8
15
22
29
36
43
50
57
64
71
78
85
92
99
106
113
120
127
134
141
Time window; 1 time window= 512 points= 1.6384 seconds
Initial Period
Final Period

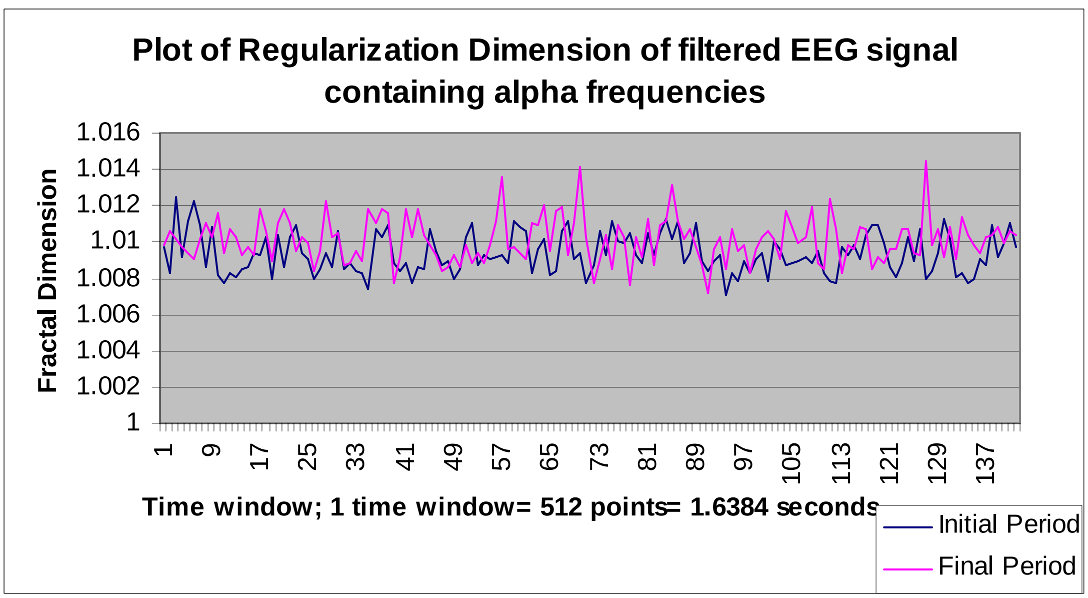
Plot of Regularization Dimension of filtered EEG signal containing alpha frequencies
Fractal Dimension
1.016
1.014
1.012
1.01
1.008
1.006
1.004
1.002
1
1
9
17
25
33
41
49
57
65
73
81
89
97
105
113
121
129
137
Time window; 1 time window= 512 points= 1.6384 seconds
Initial Period
Final Period

Subject 4

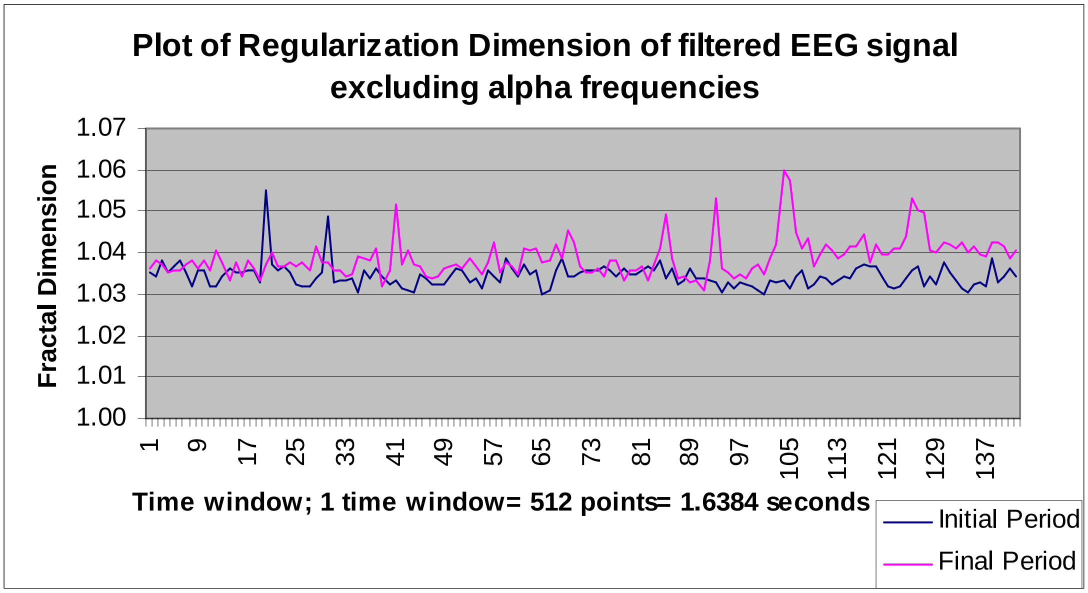
Plot of Regularization Dimension of filtered EEG signal excluding alpha frequencies
Fractal Dimension
1.07
1.06
1.05
1.04
1.03
1.02
1.01
1.00
1
9
17
25
33
41
49
57
65
73
81
89
97
105
113
121
129
137
Time window; 1 time window= 512 points= 1.6384 seconds
Initial Period
Final Period

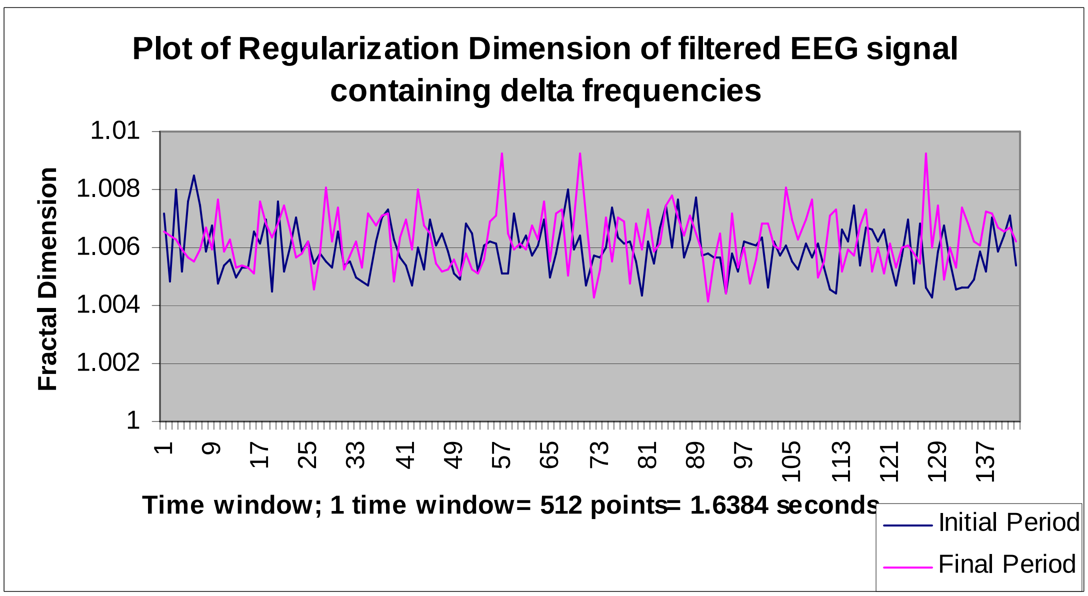
Plot of Regularization Dimension of filtered EEG signal containing delta frequencies
Fractal Dimension
1.01
1.008
1.006
1.004
1.002
1
1
9
17
25
33
41
49
57
65
73
81
89
97
105
113
121
129
137
Time window; 1 time window= 512 points= 1.6384 seconds
Initial Period
Final Period

Subject 5

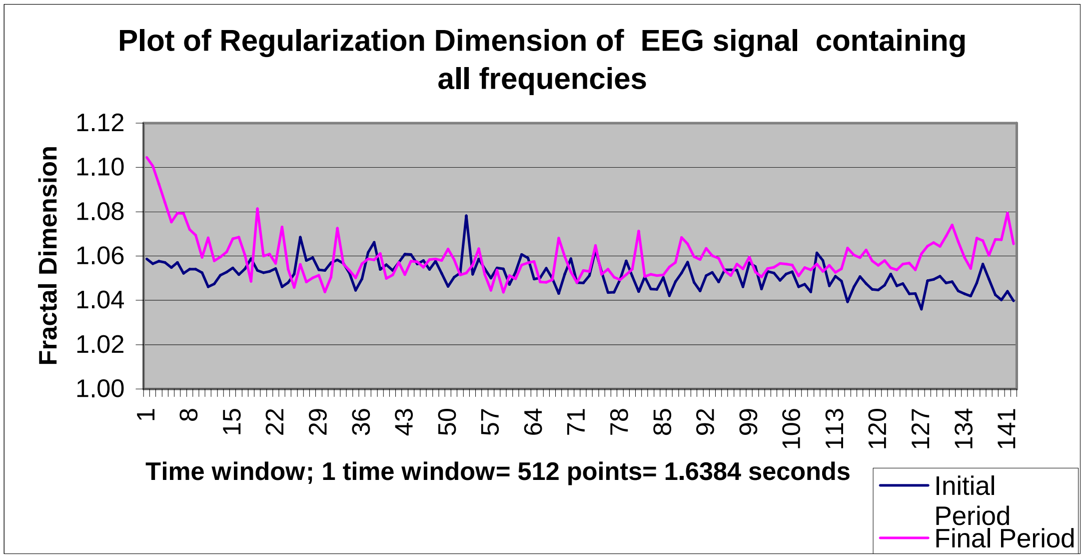

Plot of Regularization Dimension of EEG signal containing all frequencies
Fractal Dimension
1.12
1.10
1.08
1.06
1.04
1.02
1.00
1
8
15
22
29
36
43
50
57
64
71
78
85
92
99
106
113
120
127
134
141
Time window; 1 time window= 512 points= 1.6384 seconds
Initial Period
Final Period

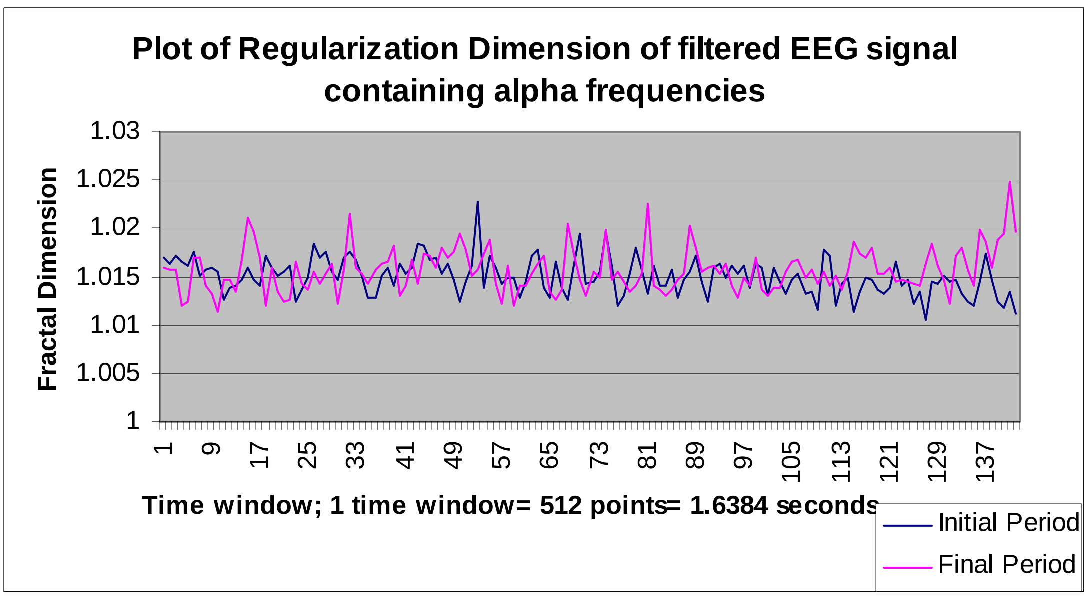

Plot of Regularization Dimension of filtered EEG signal containing alpha frequencies
Fractal Dimension
1.03
1.025
1.02
1.015
1.01
1.005
1
1
9
17
25
33
41
49
57
65
73
81
89
97
105
113
121
129
137
Time window; 1 time window= 512 points= 1.6384 seconds
Initial Period
Final Period

Subject 5

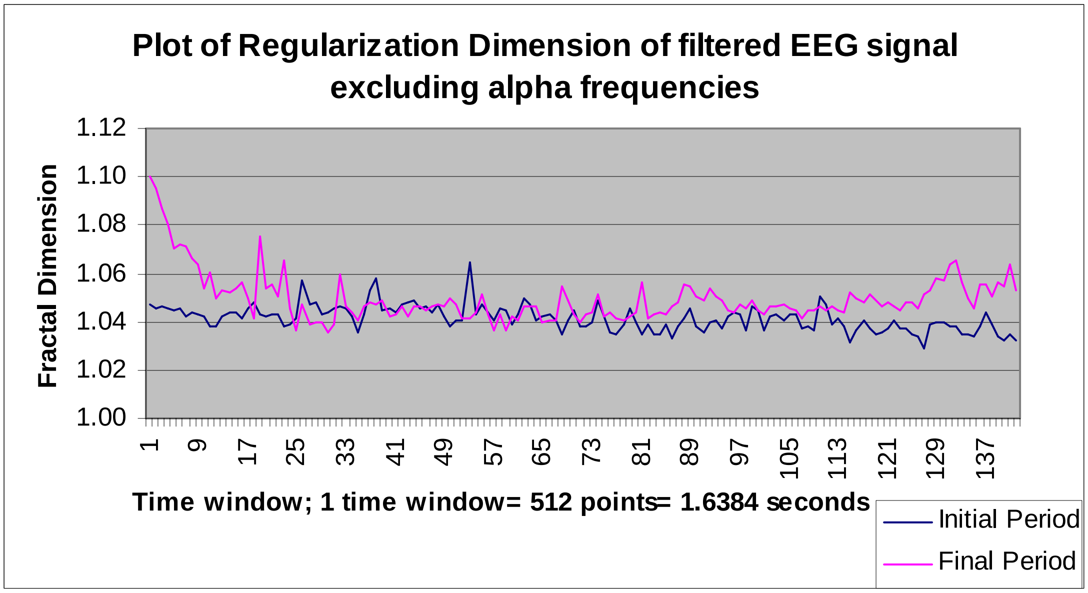
Plot of Regularization Dimension of filtered EEG signal excluding alpha frequencies
Fractal Dimension
1.12
1.10
1.08
1.06
1.04
1.02
1.00
1
9
17
25
33
41
49
57
65
73
81
89
97
105
113
121
129
137
Time window; 1 time window= 512 points= 1.6384 seconds
Initial Period
Final Period

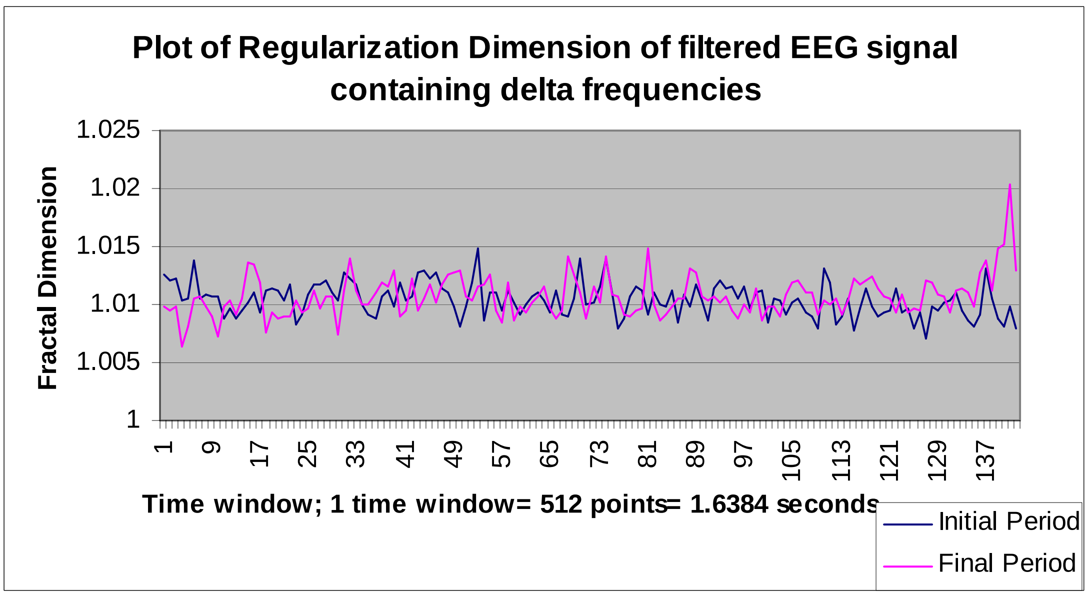
Plot of Regularization Dimension of filtered EEG signal containing delta frequencies
Fractal Dimension
1.025
1.02
1.015
1.01
1.005
1
1
9
17
25
33
41
49
57
65
73
81
89
97
105
113
121
129
137
Time window; 1 time window= 512 points= 1.6384 seconds
Initial Period
Final Period

Subject 6

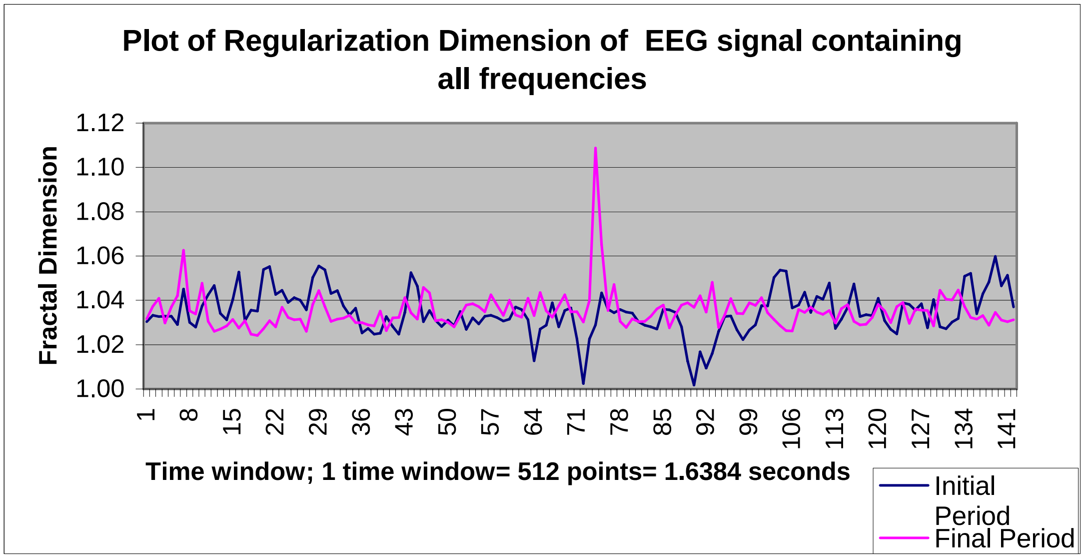
Plot of Regularization Dimension of EEG signal containing all frequencies
Fractal Dimension
1.12
1.10
1.08
1.06
1.04
1.02
1.00
1
8
15
22
29
36
43
50
57
64
71
78
85
92
99
106
113
120
127
134
141
Time window; 1 time window= 512 points= 1.6384 seconds
Initial Period
Final Period

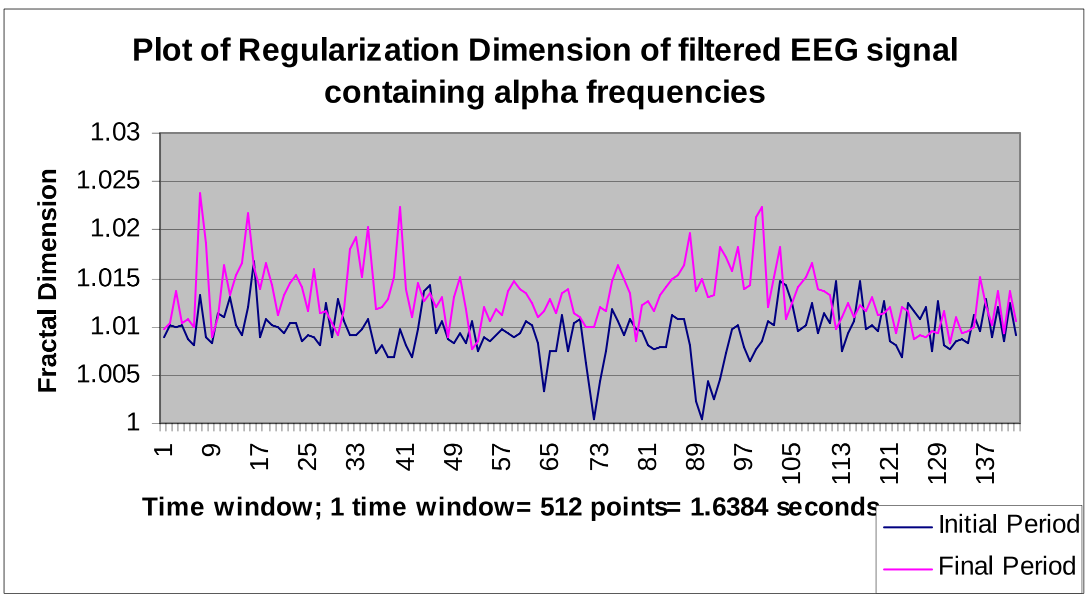
Plot of Regularization Dimension of filtered EEG signal containing alpha frequencies
Fractal Dimension
1.03
1.025
1.02
1.015
1.01
1.005
1
1
9
17
25
33
41
49
57
65
73
81
89
97
105
113
121
129
137
Time window; 1 time window= 512 points= 1.6384 seconds
Initial Period
Final Period

Subject 6

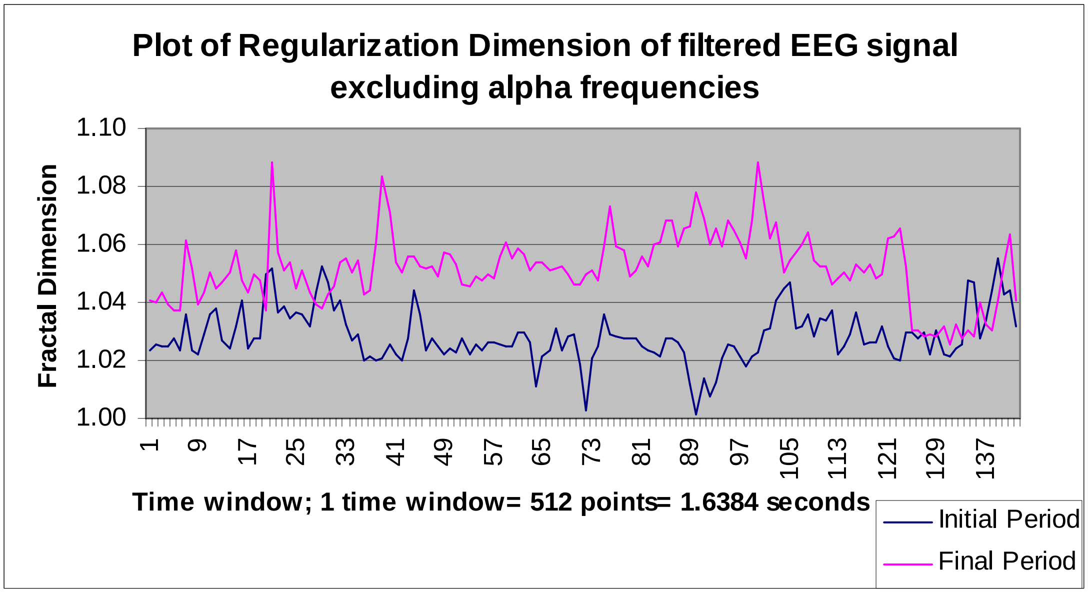
Plot of Regularization Dimension of filtered EEG signal excluding alpha frequencies
Fractal Dimension
1.10
1.08
1.06
1.04
1.02
1.00
1
9
17
25
33
41
49
57
65
73
81
89
97
105
113
121
129
137
Time window; 1 time window= 512 points= 1.6384 seconds
Initial Period
Final Period

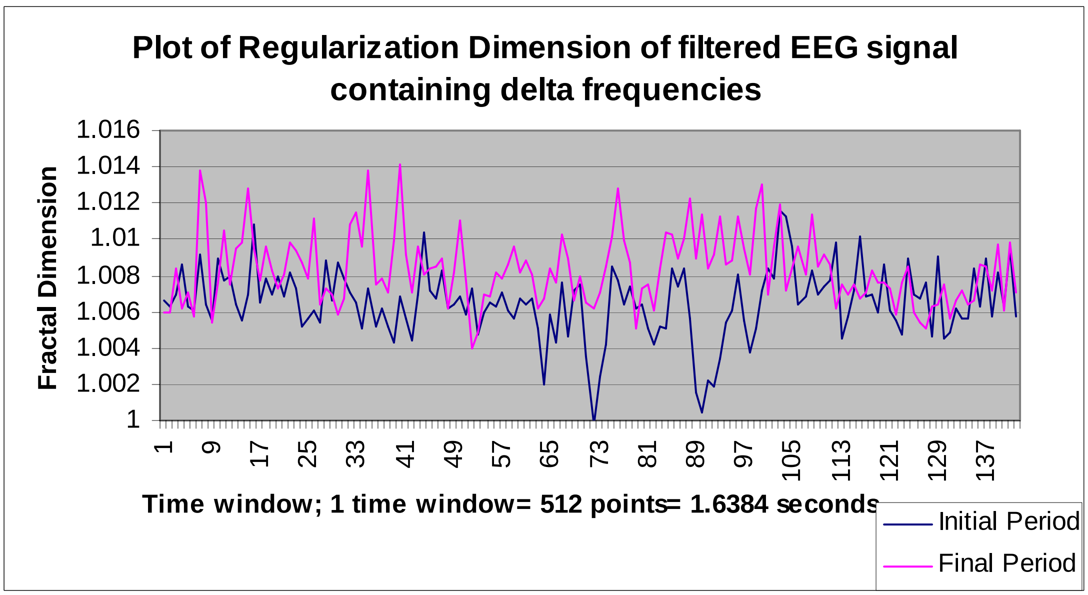
Plot of Regularization Dimension of filtered EEG signal containing delta frequencies
Fractal Dimension
1.016
1.014
1.012
1.01
1.008
1.006
1.004
1.002
1
1
9
17
25
33
41
49
57
65
73
81
89
97
105
113
121
129
137
Time window; 1 time window= 512 points= 1.6384 seconds
Initial Period
Final Period

Subject 7

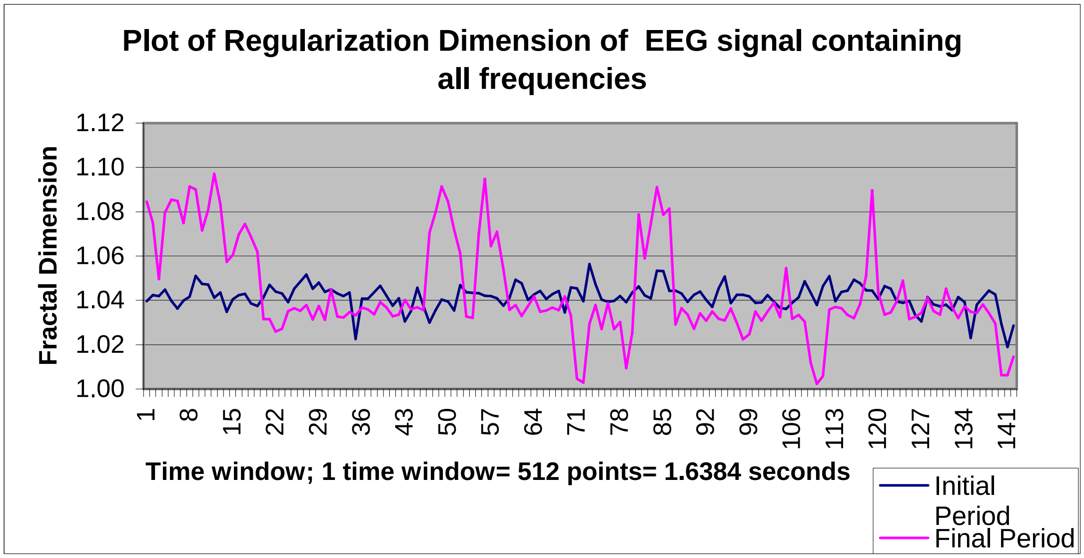

Plot of Regularization Dimension of EEG signal containing all frequencies
Fractal Dimension
1.12
1.10
1.08
1.06
1.04
1.02
1.00
1
8
15
22
29
36
43
50
57
64
71
78
85
92
99
106
113
120
127
134
141
Time window; 1 time window= 512 points= 1.6384 seconds
Initial Period
Final Period

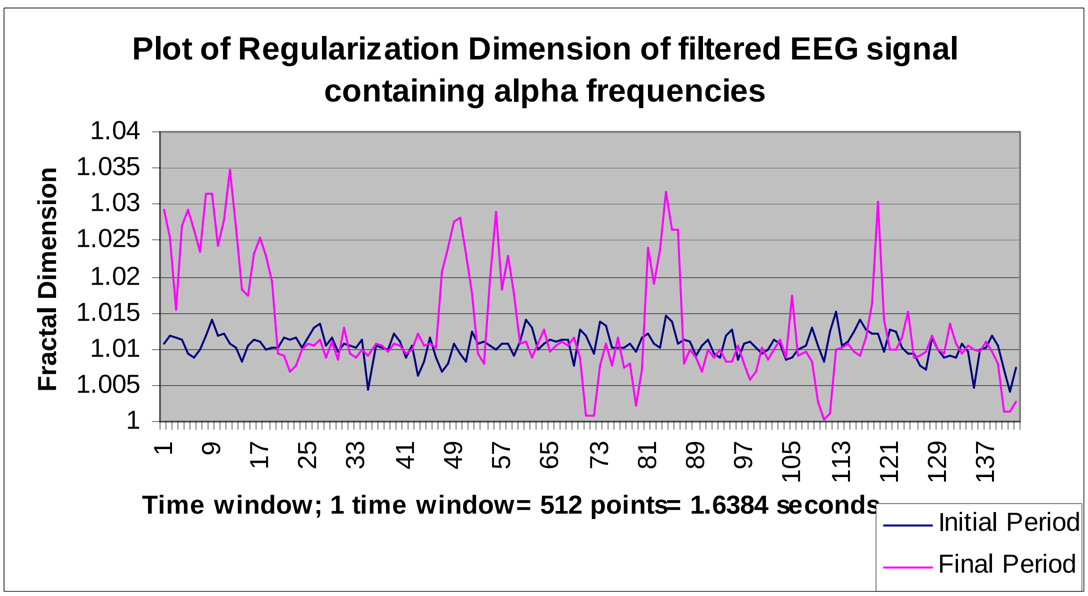

Plot of Regularization Dimension of filtered EEG signal containing alpha frequencies
Fractal Dimension
1.04
1.035
1.03
1.025
1.02
1.015
1.01
1.005
1
1
9
17
25
33
41
49
57
65
73
81
89
97
105
113
121
129
137
Time window; 1 time window= 512 points= 1.6384 seconds
Initial Period
Final Period

Subject 7

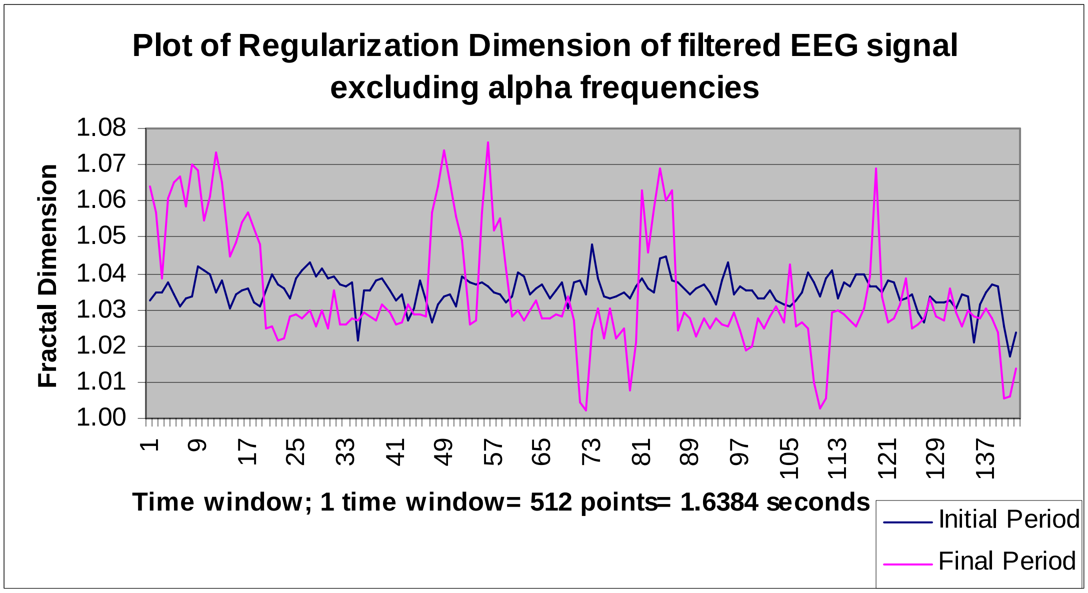
Plot of Regularization Dimension of filtered EEG signal excluding alpha frequencies
Fractal Dimension
1.08
1.07
1.06
1.05
1.04
1.03
1.02
1.01
1.00
1
9
17
25
33
41
49
57
65
73
81
89
97
105
113
121
129
137
Time window; 1 time window= 512 points= 1.6384 seconds
Initial Period
Final Period

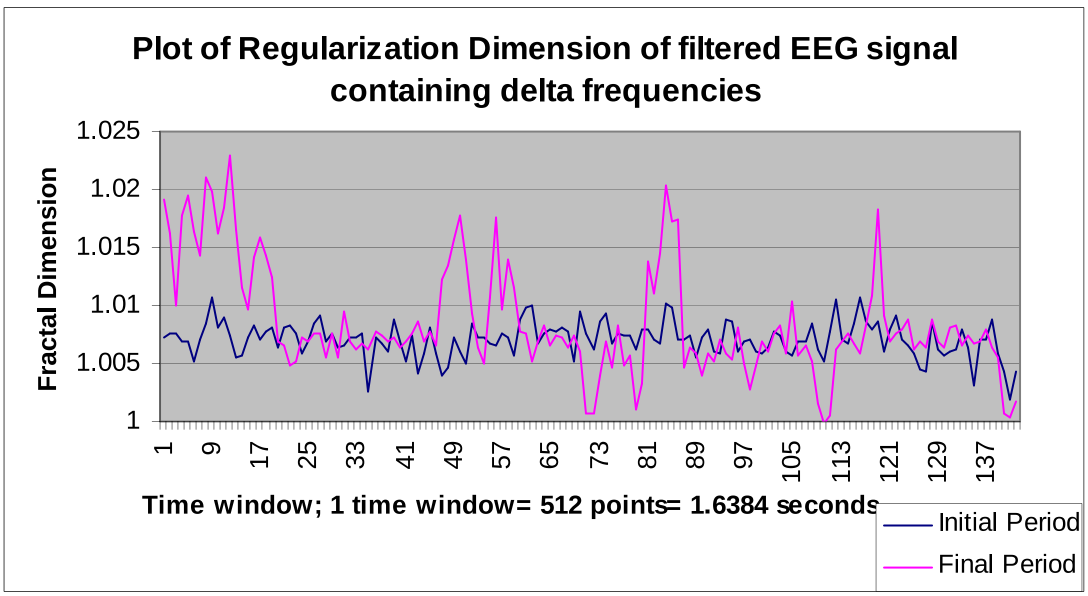
Plot of Regularization Dimension of filtered EEG signal containing delta frequencies
Fractal Dimension
1.025
1.02
1.015
1.01
1.005
1
1
9
17
25
33
41
49
57
65
73
81
89
97
105
113
121
129
137
Time window; 1 time window= 512 points= 1.6384 seconds
Initial Period
Final Period

Subject 8

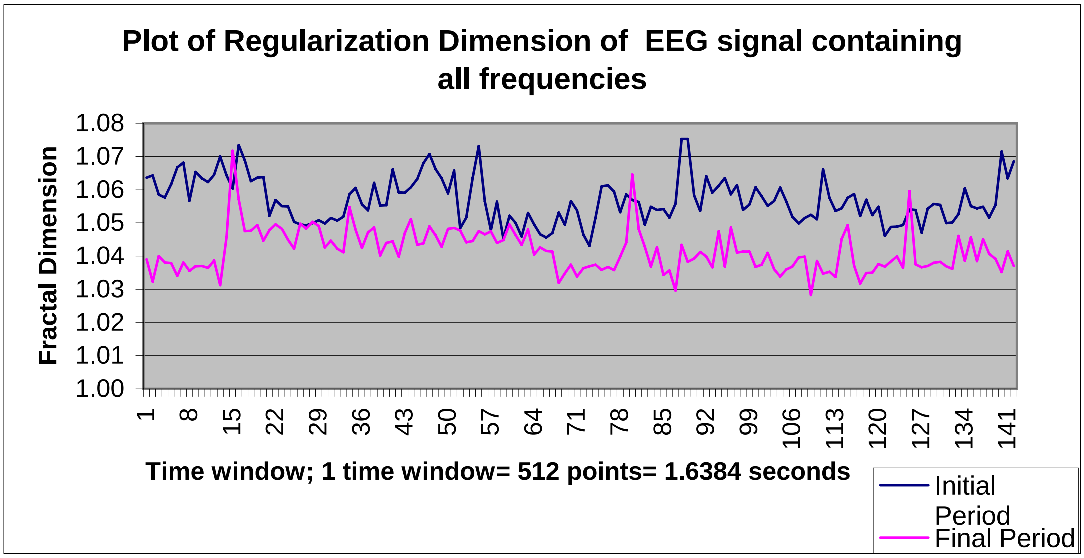
Plot of Regularization Dimension of EEG signal containing all frequencies
Fractal Dimension
1.08
1.07
1.06
1.05
1.04
1.03
1.02
1.01
1.00
1
8
15
22
29
36
43
50
57
64
71
78
85
92
99
106
113
120
127
134
141
Time window; 1 time window= 512 points= 1.6384 seconds
Initial Period
Final Period

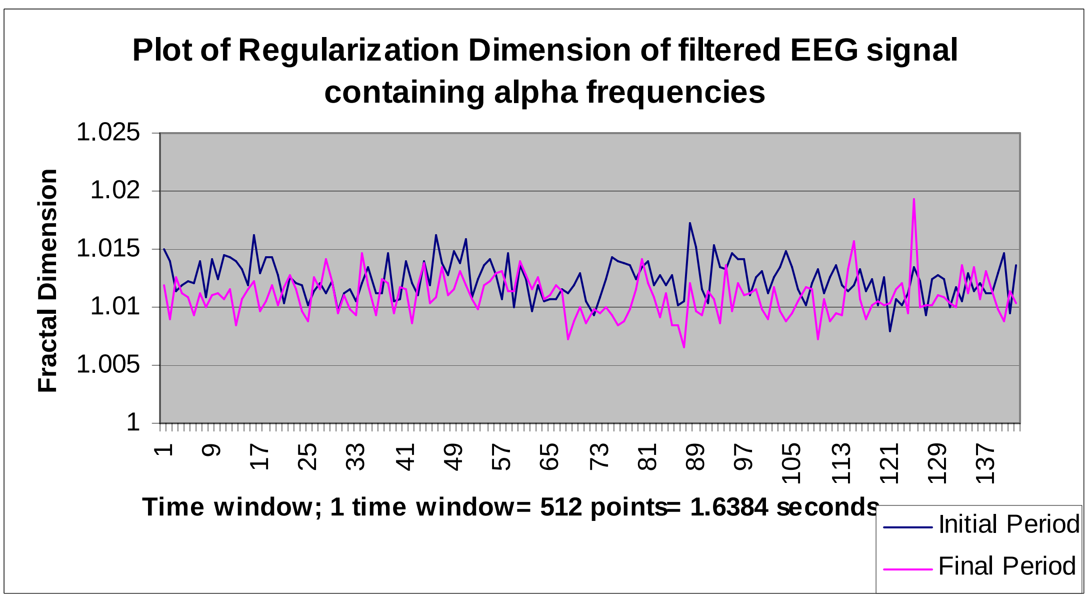
Plot of Regularization Dimension of filtered EEG signal containing alpha frequencies
Fractal Dimension
1.025
1.02
1.015
1.01
1.005
1
1
9
17
25
33
41
49
57
65
73
81
89
97
105
113
121
129
137
Time window; 1 time window= 512 points= 1.6384 seconds
Initial Period
Final Period

Subject 8

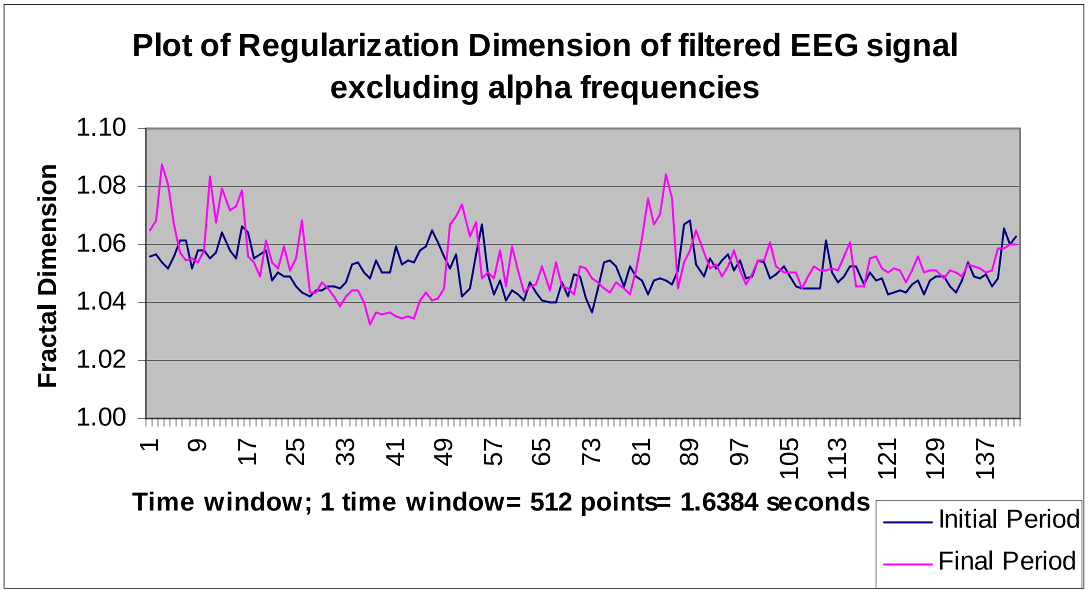
Plot of Regularization Dimension of filtered EEG signal excluding alpha frequencies
Fractal Dimension
1.10
1.08
1.06
1.04
1.02
1.00
1
9
17
25
33
41
49
57
65
73
81
89
97
105
113
121
129
137
Time window; 1 time window= 512 points= 1.6384 seconds
Initial Period
Final Period

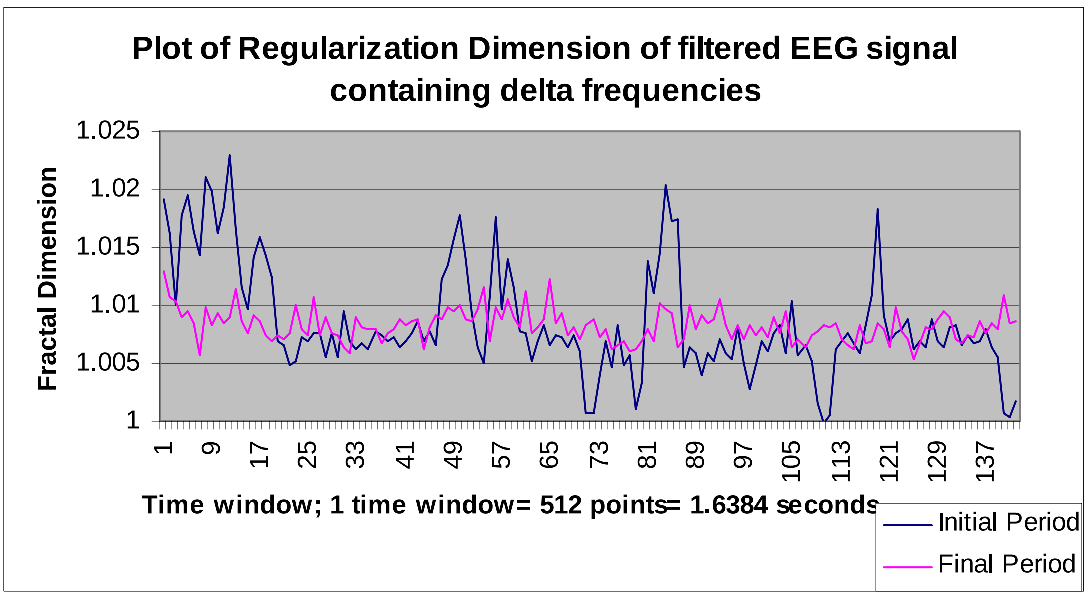
Plot of Regularization Dimension of filtered EEG signal containing delta frequencies
Fractal Dimension
1.025
1.02
1.015
1.01
1.005
1
1
9
17
25
33
41
49
57
65
73
81
89
97
105
113
121
129
137
Time window; 1 time window= 512 points= 1.6384 seconds
Initial Period
Final Period

Subject 9: Trial 1

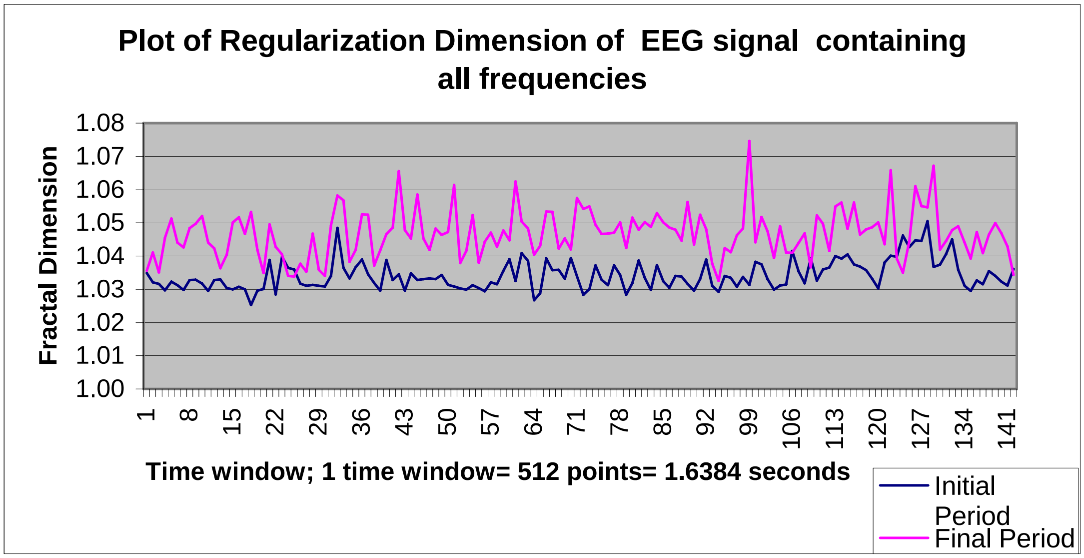

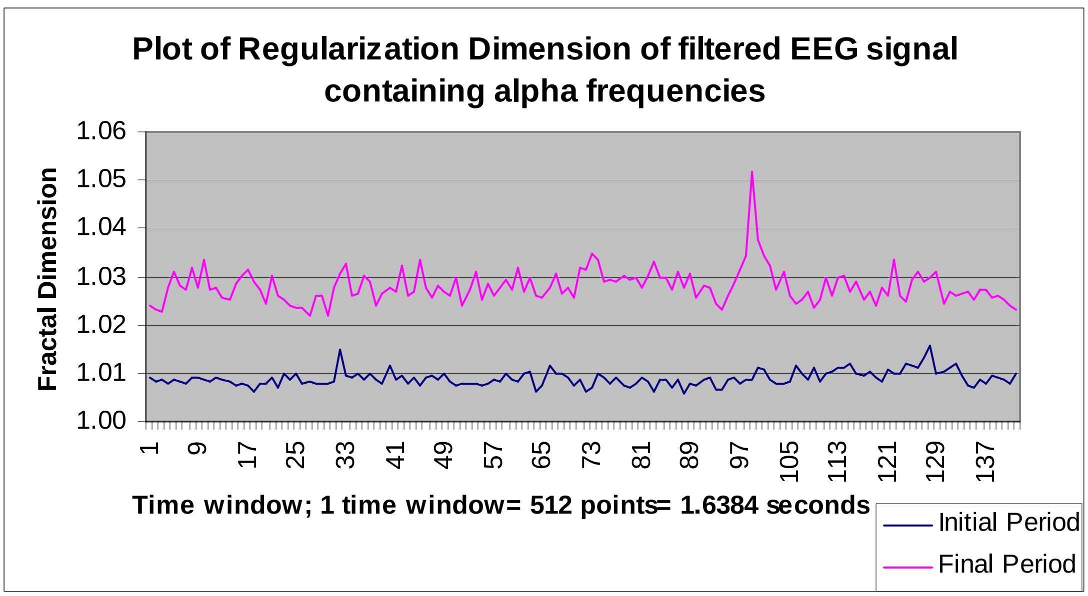

Subject 9: Trial 1

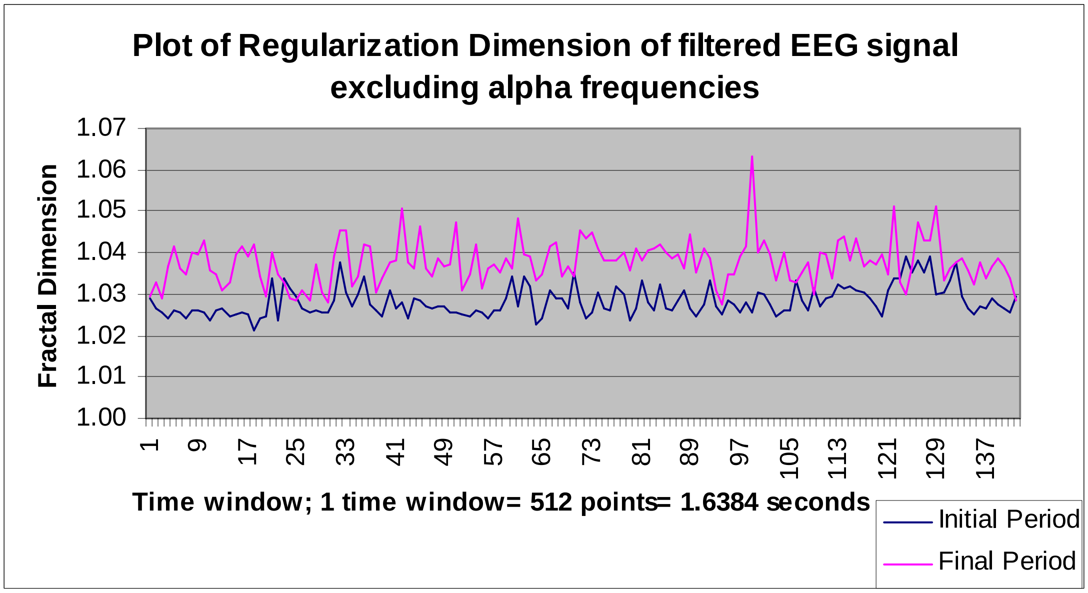

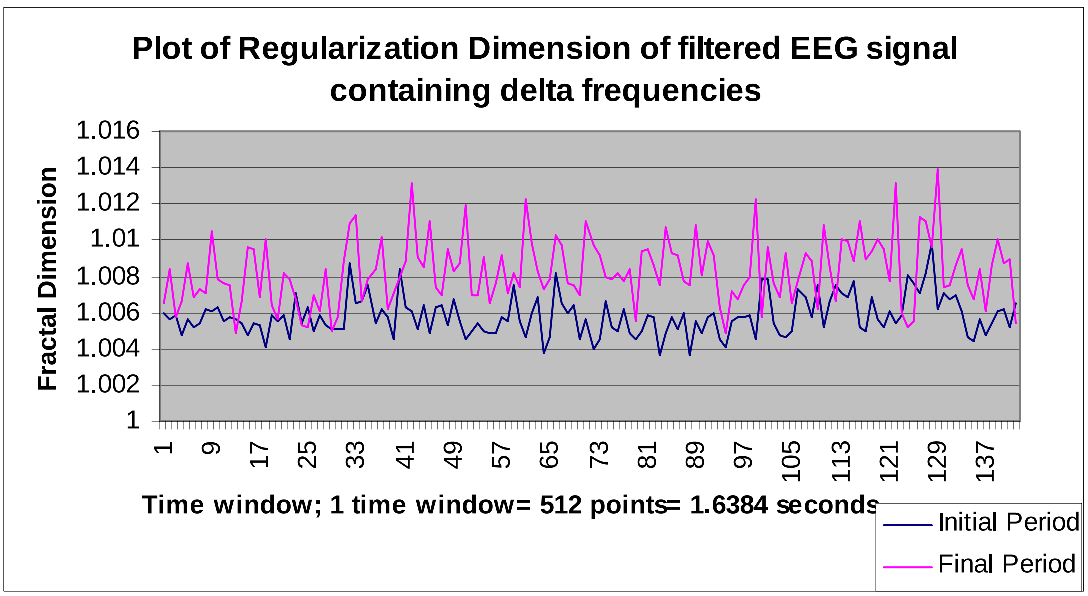

Subject 9: Trial 2

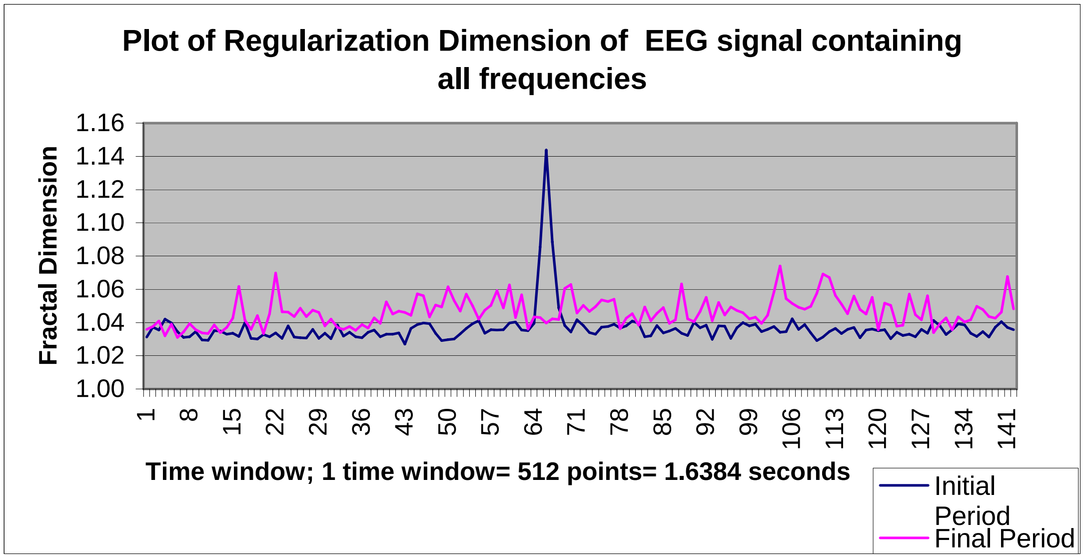

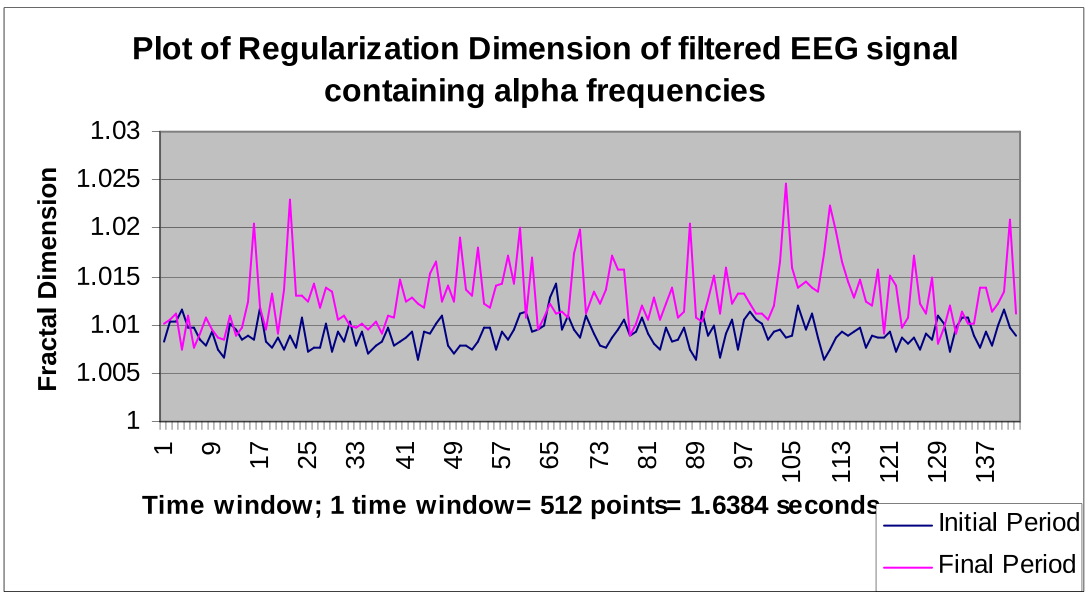

Subject 9: Trial 2

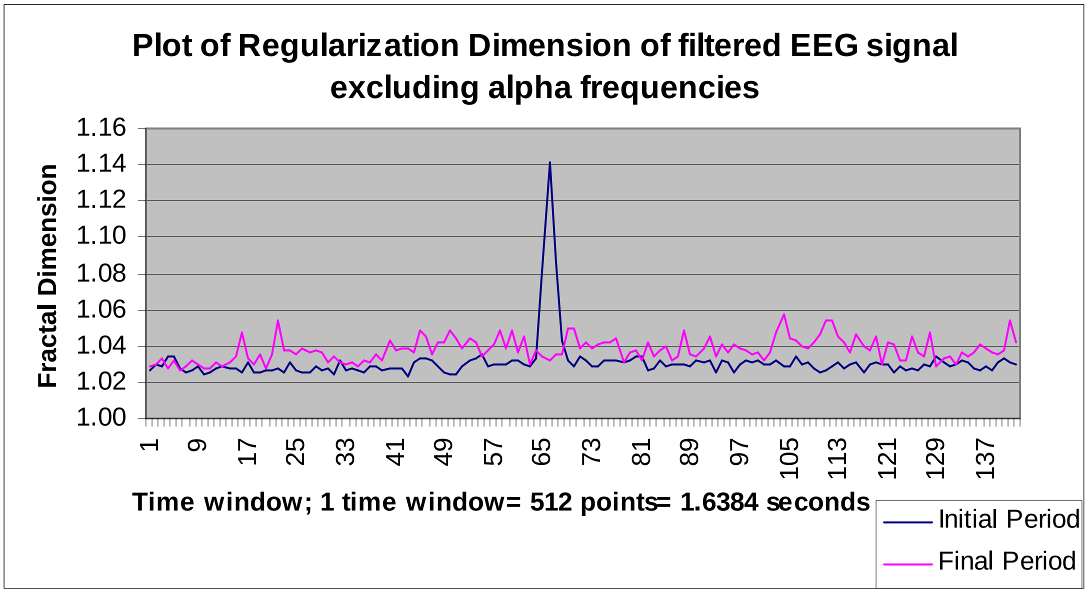

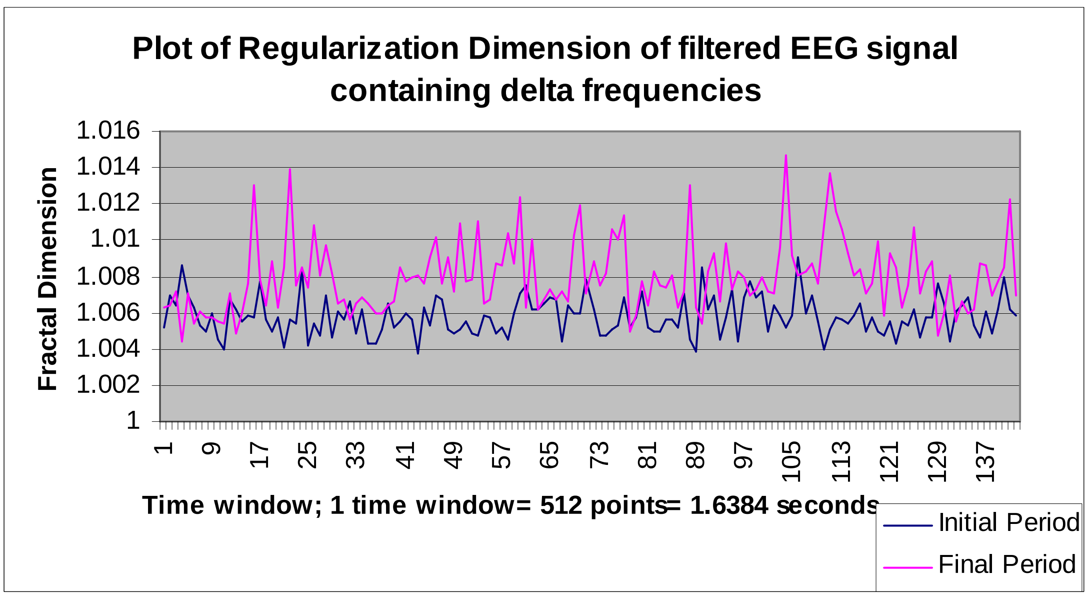

Subject 10

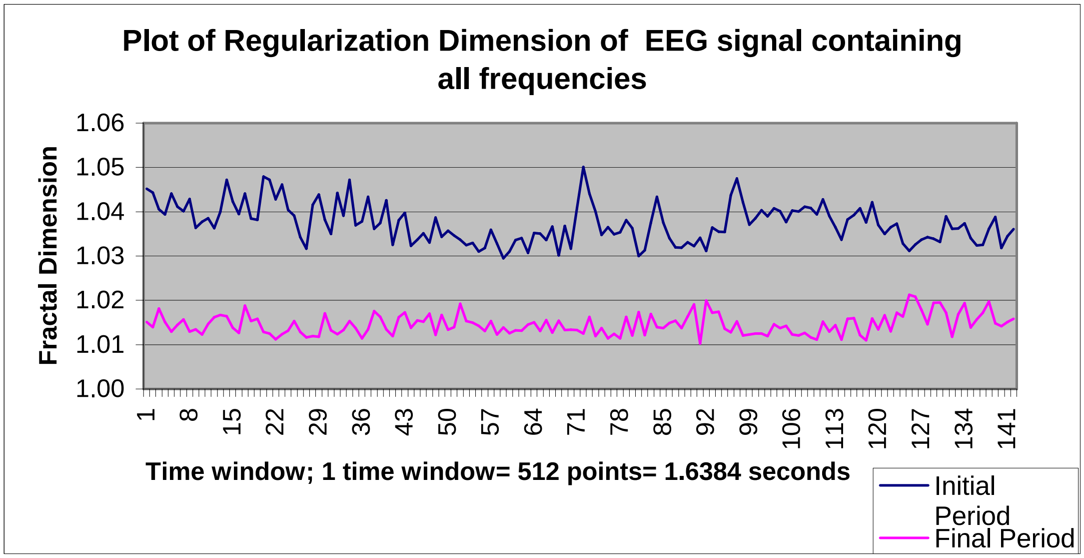

Plot of Regularization Dimension of EEG signal containing all frequencies
Fractal Dimension
1.06
1.05
1.04
1.03
1.02
1.01
1.00
1
8
15
22
29
36
43
50
57
64
71
78
85
92
99
106
113
120
127
134
141
Time window; 1 time window= 512 points= 1.6384 seconds
Initial Period
Final Period

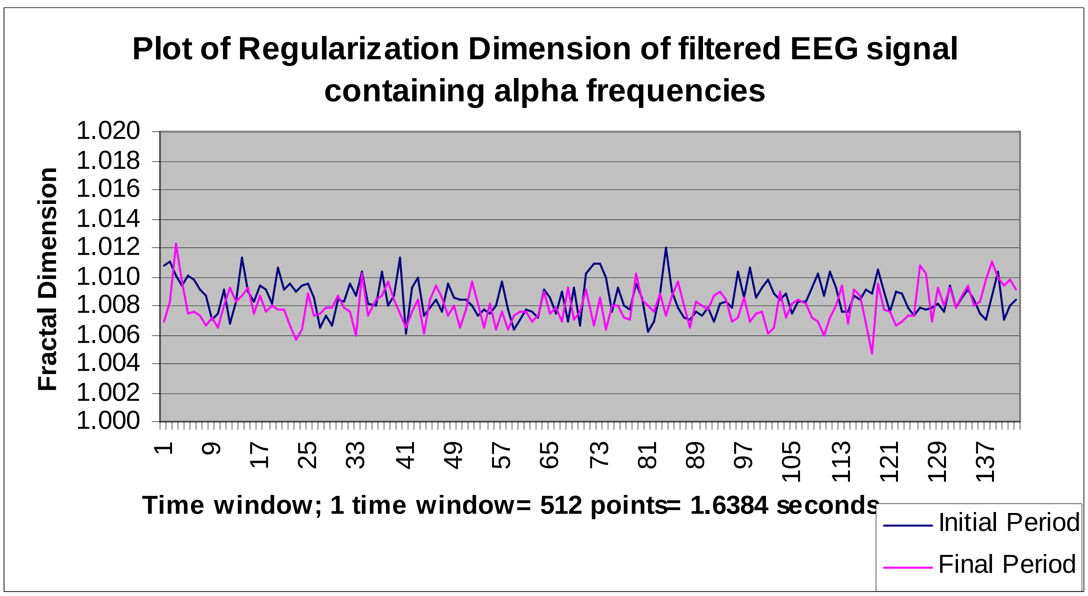

Plot of Regularization Dimension of filtered EEG signal containing alpha frequencies
Fractal Dimension
1.020
1.018
1.016
1.014
1.012
1.010
1.008
1.006
1.004
1.002
1.000
1
9
17
25
33
41
49
57
65
73
81
89
97
105
113
121
129
137
Time window; 1 time window= 512 points= 1.6384 seconds
Initial Period
Final Period

Subject 10

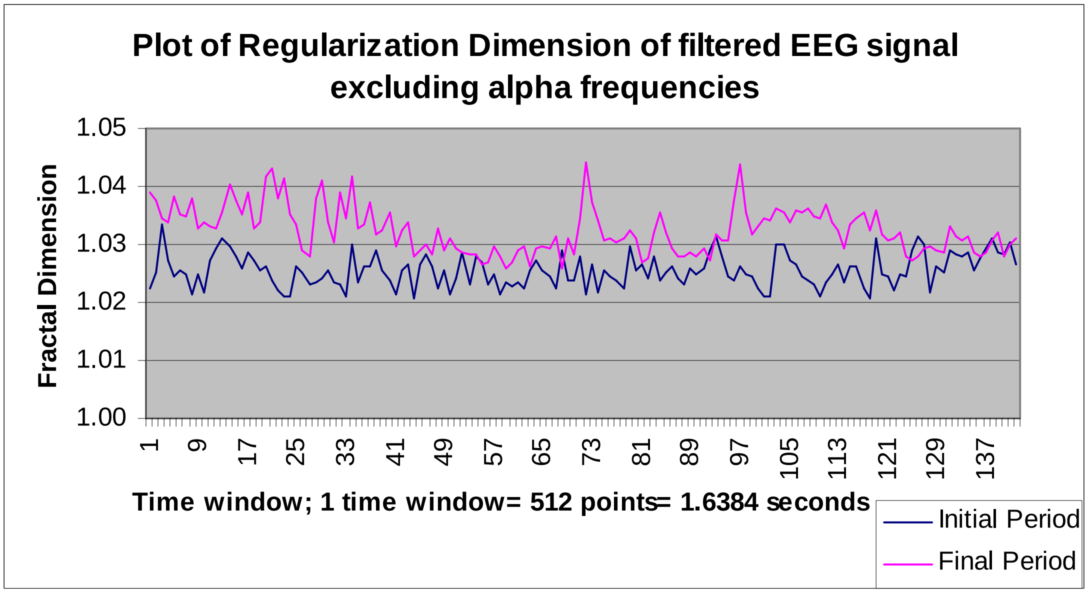
Plot of Regularization Dimension of filtered EEG signal excluding alpha frequencies
Fractal Dimension
1.05
1.04
1.03
1.02
1.01
1.00
1
9
17
25
33
41
49
57
65
73
81
89
97
105
113
121
129
137
Time window; 1 time window= 512 points= 1.6384 seconds
Initial Period
Final Period

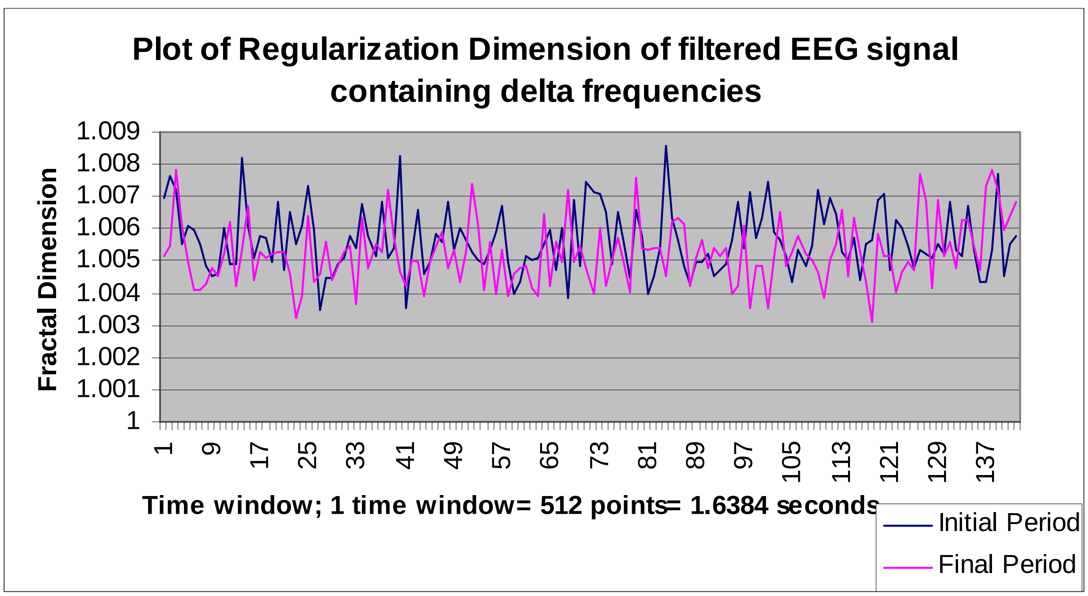
Plot of Regularization Dimension of filtered EEG signal containing delta frequencies
Fractal Dimension
1.009
1.008
1.007
1.006
1.005
1.004
1.003
1.002
1.001
1
1
9
17
25
33
41
49
57
65
73
81
89
97
105
113
121
129
137
Time window; 1 time window= 512 points= 1.6384 seconds
Initial Period
Final Period

APPENDIX C

WAVELET TRANSFORM: REMAINING SUBJECTS

Subject 4

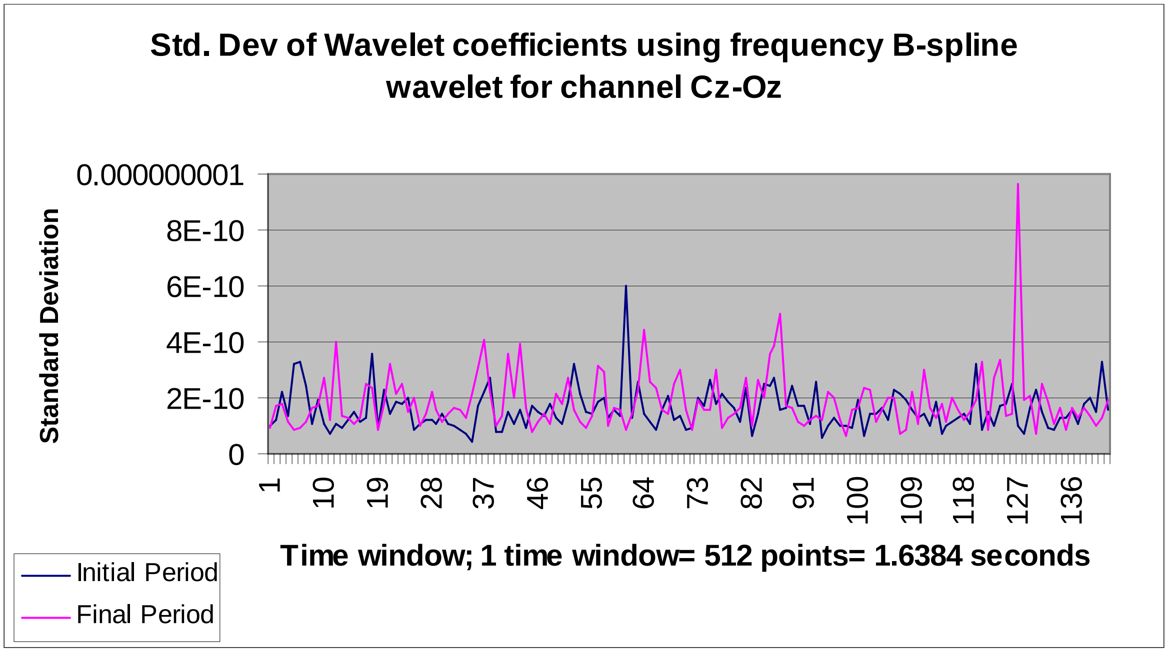

Subject 5

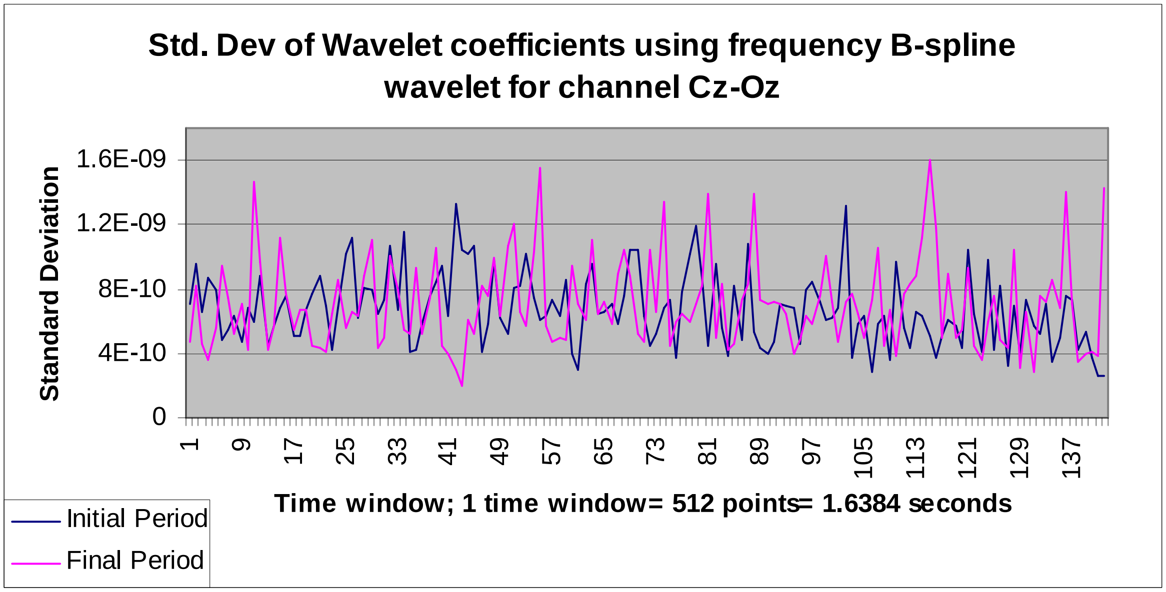

Subject 6

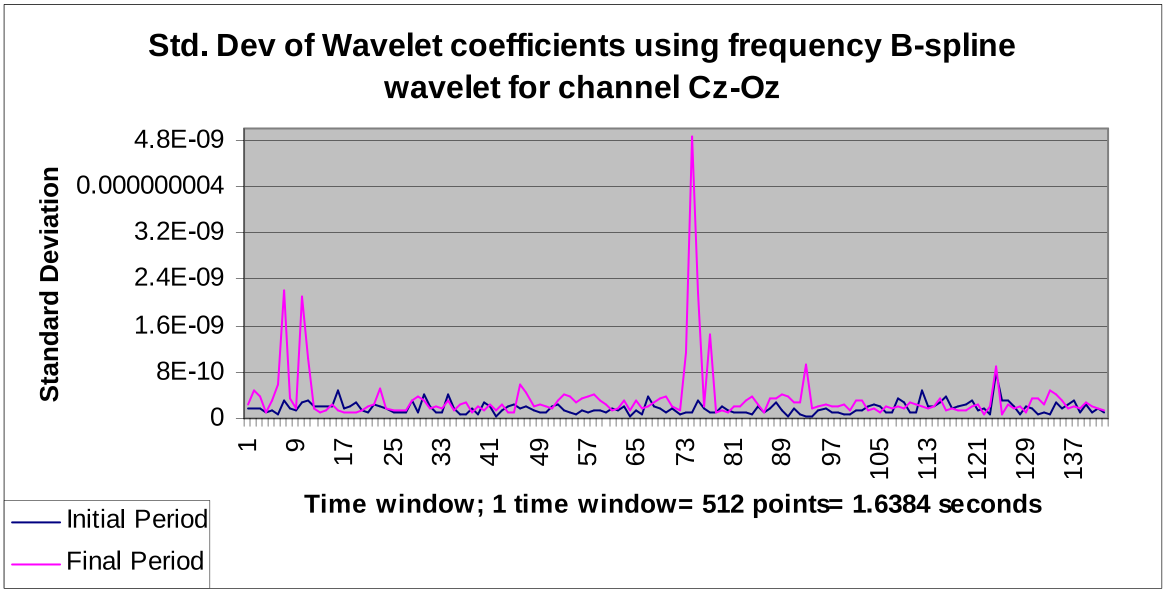

Subject 7

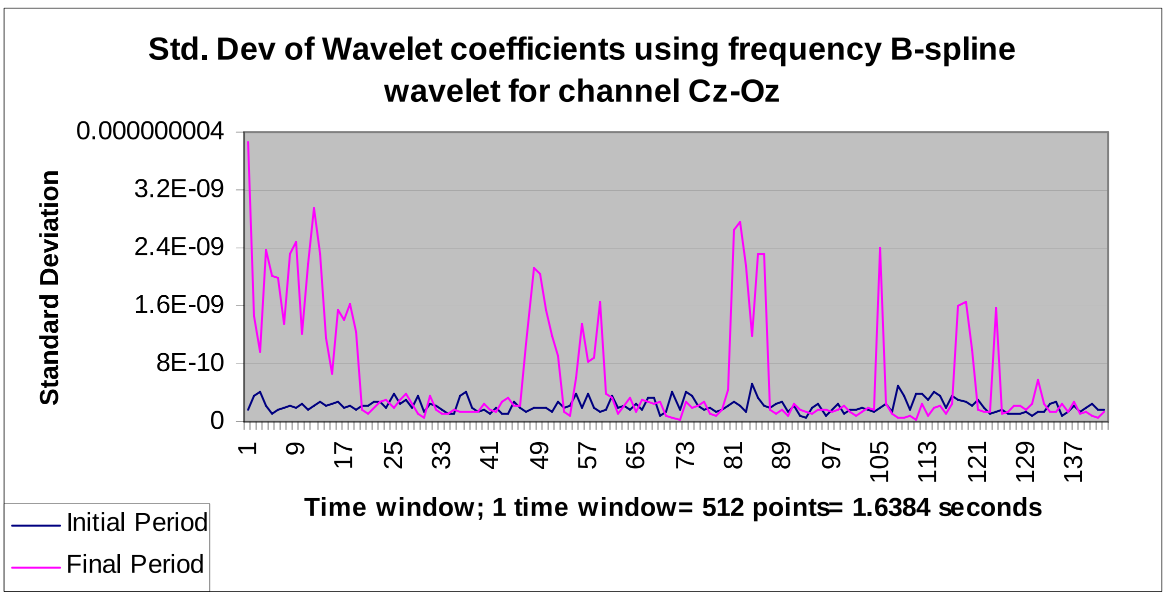

Subject 8

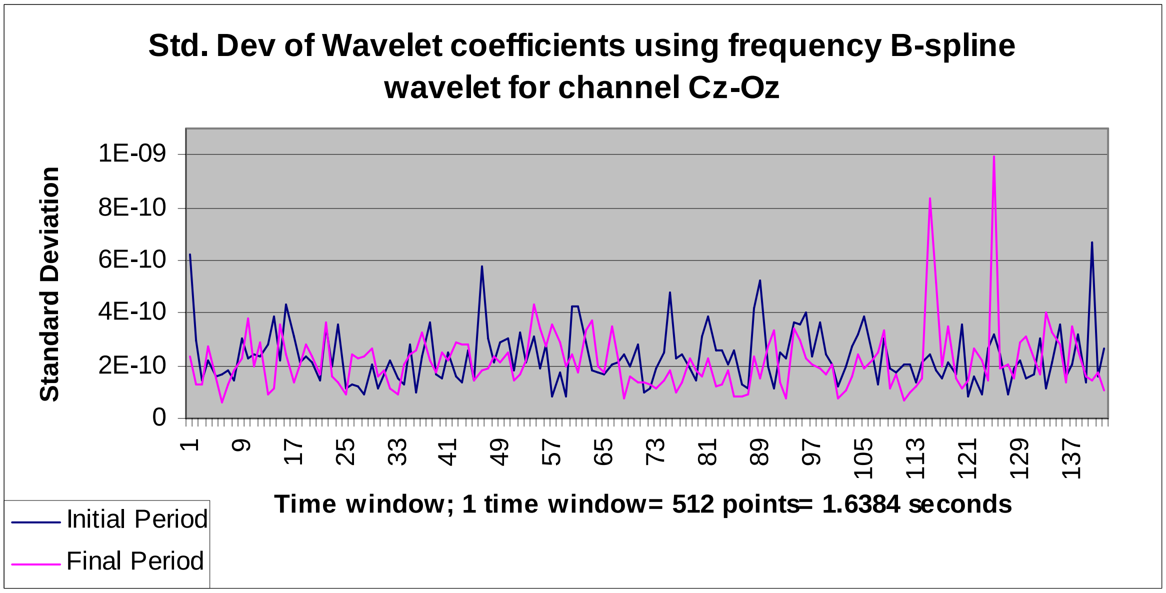

Subject 9- Trial 1

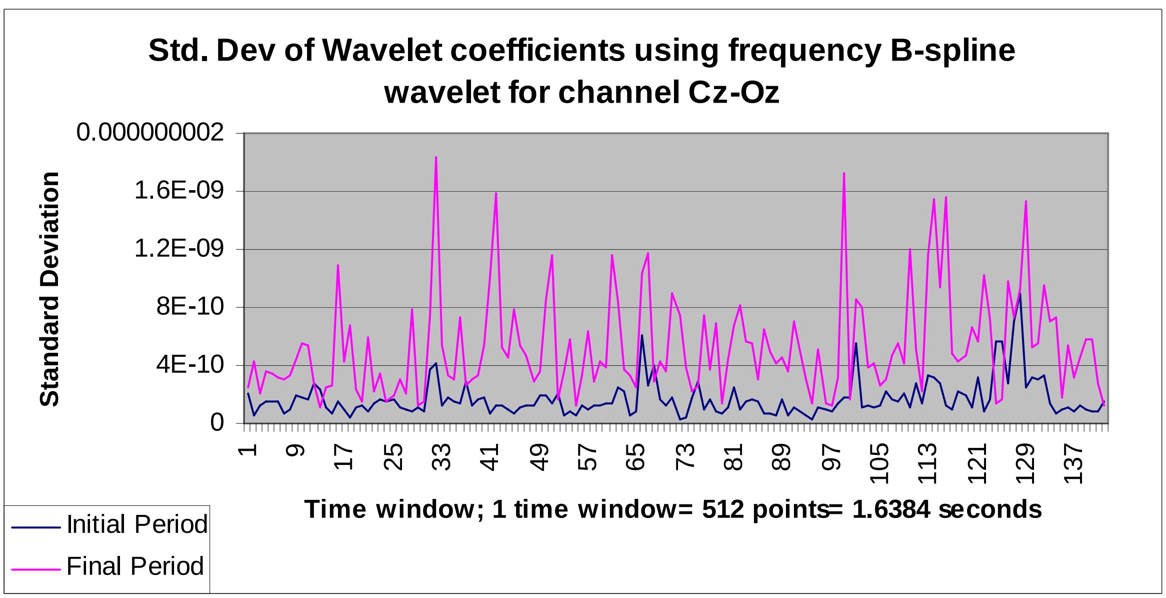

Subject 9- Trial 2

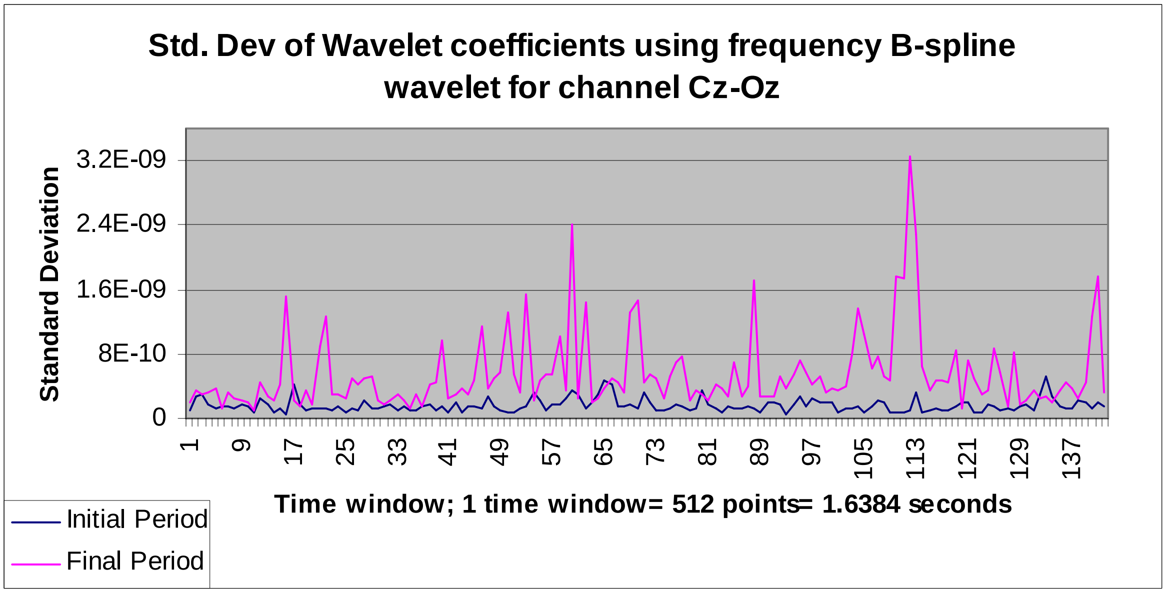

Subject 10

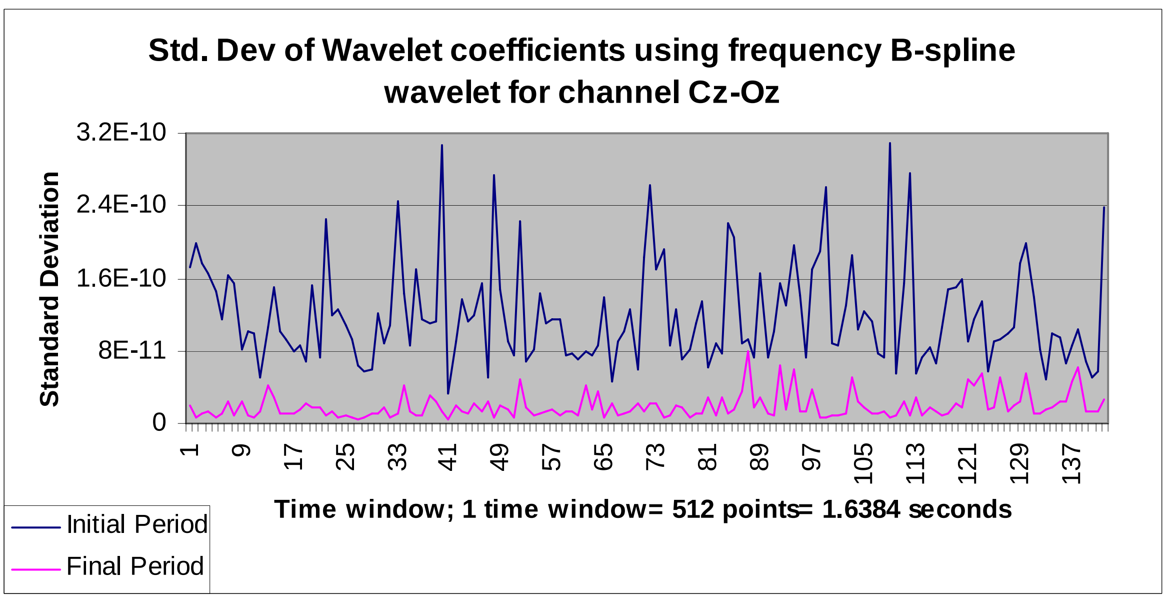

REFERENCES

1) http://www.sleepfoundation.org

2) http://www.aaafoundation.org

3) http://www.nhtsa.dot.gov/

4) http://neurocog.psy.tufts.edu/courses/images/eeg_tracing.htm

5) Shen Minfen, Shen Fenglin. The analysis of dynamic EEG signals by using wavelet packets decomposition .*Time-Frequency and Time-Scale Analysis, 1998. Proceedings of the IEEE-SP International Symposium on* , 6-9 Oct. 1998 Page(s): 85 -88

6) S. Makeig and T-P. Jung. Changes in alertness are a principal component of variance in the EEG spectrum. *NeuroReport,* 7:213-216, 1995.

7) Terán-Santos, J., Jimenez-Gomez, A., Cordero-Guevara, J. The Association between Sleep Apnea and the Risk of Traffic Accidents. *N Engl J Med* 1999; 340:847-851, Mar 18, 1999

8) Levendowski, D.J., Berka C., Olmstead, R.E., Konstantinovic, Z.R., Davis G., Lumicao, M.N., Westbrook, P. Electroencephalographic indices predict future vulnerability to fatigue induced by sleep deprivation. *Sleep Conference,* June 2001.

9) Funada, M.F., Ninomija, S.P., Suzuki, S., Idogawa, K., Yazu, Y., Ide, H. On an image processing of eye blinking to monitor awakening levels of human beings. *Engineering in Medicine and Biology Society, 1996. Bridging Disciplines for Biom'edicine. Proceedings of the 18th Annual International Conference of the IEEE* Volume 3, 31 Oct.-3 Nov. 1996 Page(s):966 - 967 vol.3

10) Suzuki, S.; Funada, M.F.; Yazu, Y.; Ninomija, S.P. A study about relation between appearance of grouped alpha-waves and shift to asleep condition. *Engineering in Medicine and Biology Society, 1993. Proceedings of the 15th Annual International Conference of the IEEE.* Oct 28-31, 1993 Page(s):1400 - 1401

11) Álvarez, R., Pozo, F., Hernando, M.E., Gómez, E., Jiménez, A., Carpizo, R. Real-time Monitoring of Human Alertness. *Sleep Review,* July/August 2003.

12) Schier MA. Changes in EEG alpha power during simulated driving: a demonstration. *International Journal of Psychophysiology* 37(2): 155-162,2000

13) Tietze, H. Stages of wakefulness during long duration driving reflected in alpha related events in the EEG. *3rd International Conference on Psychophysiology in Ergonomics,* San Diego, 2000.

14) Jansen, B.H.; Dawant, B.M. Knowledge-based approach to sleep EEG analysis-a feasibility study. *Biomedical Engineering, IEEE Transactions on,* Volume 36, Issue 5, May 1989 Page(s):510 - 518

15) Gonzalez-Mendoza, M.; Santana-Diaz, A.; Hernandez-Gress, N.; Titli. A. Driver vigilance monitoring, a new approach. *Intelligent Vehicle Symposium*, 2002. IEEE, Volume: 2, 17-21 June 2002 Page(s): 358 -363 vol.2.

16) Verwey, W. B., Zaidel, D. M. Preventing drowsiness accidents by an alertness maintenance device**.** *Accident Analysis and Prevention*, v 31, n 3, May, 1999, p 199-211.

17) Santana-Diaz, A.; Hernandez-Gress, N.; Esteve, D.; Jammes, B. Discriminating sensors for driver's impairment detection. *Microtechnologies in Medicine and Biology, 1st Annual International, Conference*, 12-14 Oct. 2000 Page(s): 578 –583.

18) Jung, T-P., Makeig, S., Stensmo, M., & Sejnowski, T.J. Estimating alertness from the EEG power spectrum. *IEEE Transactions on Biomedical Engineering*, 44:60-69 (1997)

19) Haris, M.B., Asim, R., Bhatti, M.I. Integrated sleep stage diagnosis system, analysis and classification with neural networks. *8th International Conference on Neural Information Processing*.110:2001

20) Ahaoll Kirk, B.P., LaCourse, J.R. Vigilance monitoring from the EEG power spectrum with a neural network *Proceedings of the 19th Annual International Conference of the IEEE* , Volume: 3 , 30 Oct.-2 Nov 1997 Page(s): 1218 -1219 vol.3

21) Khalifa, K., Bedoui, M. Raytchev, R. Dogui, M. A portable device for alertness detection. *Microtechnologies in Medicine and Biology*, 12-14 Oct. 2000 Page(s): 584 –586

22) Dixon, T.L., Livezey, G.T. Wavelet-based feature extraction for EEG classification. *Proceedings of the 18th Annual International Conference of the IEEE* , Volume: 3 , 31 Oct.-3 Nov. 1996 Page(s): 1003 -1004 vol.3

23) Yamaguchi, C. Wavelet analysis of normal and epileptic EEG *EMBS/BMES Conference, 2002. Proceedings of the Second Joint*. Volume: 1, 2002 Page(s): 96 -97

24) Johns, Murray W. A new method for measuring daytime sleepiness: the Epworth Sleepiness Scale. *Sleep* 1991 (14):540-5

25) Santana-Diaz, A. Driver hypovigilance diagnosis using wavelets and statistical analysis.

26) Subasi, A. Automatic recognition of alertness level from EEG by using neural network and wavelet coefficients. *Expert Systems with Applications*, v 28, n 4, May, 2005, p 701-711

27) Benke, G., Bozek-Kuzmicki, M., Colella, D., Jacyna, G. M., Benedetto, J. J. Wavelet-based analysis of electroencephalogram (EEG) signals for detection and localization of epileptic seizures. *Proceedings of SPIE - The International Society for Optical Engineering*, v 2491/1, 1995, p 760-769

28) Idogawa, K., Ninomija, S.P., Yano, F A time variation of professional driver's EEG in monotonous work *Proceedings of the Annual International Conference of the IEEE Engineering* .9-12 Nov. 1989 : 719 -720 vol.2

29) Yong, L.; Shenxgun, Z. Apply wavelet transform to analyse EEG signal *Engineering in Medicine and Biology Society, 1996. Bridging Disciplines for Biomedicine. Proceedings of the 18th Annual International Conference of the IEEE* Volume 3, 31 Oct.-3 Nov. 1996 Page(s):1007 - 1008 vol.3

30) Schier MA & Gorman M. Two-channel data logger for quantitative EEG recording while driving. *Proceedings of the 2nd Conference of the Victorian Chapter of the IEEE Engineering in Medicine and Biology Society*, pp 36-39, 2001.

31) Ayoob, E. M., Grace, R., Steinfeld, A. A User-Centered Drowsy-Driver Detection and Warning System. *AIGA*, 2003.

32) http://www.sleepfoundation.org

33) Camp, D. van. User's Guide for the Xerion Neural Network Simulator. *Dept. Comp Science, Univ. of Toronto.*1993

34) Welch, P.D. The Use of Fast Fourier Transform for the Estimation of Power Spectra: A Method Based on Time Averaging Over Short, Modified Periodograms. *IEEE Trans. Audio Electroacoustics*, Vol. AU-15 (June 1967), pp. 70-73.

35) Oppenheim, A. V., Schafer, R. W. *Discrete-Time Signal Processing*. Prentice-Hall, 1989

36) Celka, P., Mesbah, M., Keir, M.; Booshash, B., Colditz, P. Time-varying dimension analysis of EEG using adaptive principal component analysis and model selection. *Engineering in Medicine and Biology Society, 2000. Proceedings of the 22nd Annual International Conference of the IEEE.* Volume 2, 23-28 July 2000 Page(s):1404 - 1407 vol.2

37) http://fonsg3.let.uva.nl/praat/manual/Principal_component_analysis.html

38) Ciszewski, J., Klonowski, W., Stepien, R., Jernajczyk, W., Karlinski, A., Niedzielska, K. Application of Chaos Theory for EEG-signal Analysis in Patients with Seasonal Affective Disorder. *Med. Biol. Eng. Comput.*, vol. 37, Supplement 1, pp. 359-360, 1999.

39) Pereda E, Gamundi A, Nicolau MC, Rial R, Gonzalez J. Interhemispheric differences in awake and sleep human EEG: a comparison between non-linear and spectral measures. *Neuroscience Letter* 1999 Mar 19;263(1):37-40

40) Bullmore, E.T., Brammer, M.J., Bourlon, P., Alarcon, G., Polkey, C.E., Elwes, R., Binnie, C.D. Fractal analysis of electroencephalographic signals intracerebrally recorded during 35 epileptic seizures: evaluation of a new method for synoptic visualisation of ictal events. *Electroencephalography and Clinical Neurophysiology*, v 91, n 5, Nov. 1994, p 337-45

41) Yang, Q., Yao, B., Brown, R.W., Yue, G.H. Linear correlation between fractal dimension of EEG signal and handgrip force. *Biological Cybernetics*, v 93, n 2, Aug. 2005, p 131-40

42) Katz, M.J. Fractals and the analysis of waveforms. *Comp Biol Med* ,18:145–156

43) Higuchi, T. Approach to an irregular time series on the basis of the fractal theory. *Physica D* 31:277–283

44) Sevcik, C. A procedure to estimate the fractal dimension of waveforms. *Complexity Int'l*. http://www.complexity.org.au/ci/vol05/sevcik/sevcik.html

45) Kohonen, T. Self -Organizing Maps: Optimization Approach. *Artificial Neural Networks*, Kohonen, T. Makisara, K. Simula,O., Kangas, J. Eds. New York: Elsevier Science, 1991, pp. 183-186

46) S. Mallat, (1989). A Theory for Multiresolution Signal Decomposition: the Wavelet Representation. *IEEE Transactions on Pattern Analysis and Machine Intelligence*, 11:674--693.

47) Mandelbrot, B. B. *Fractals: Form, Chance, & Dimension.* San Francisco, CA: W. H. Freeman, 1977.

48) Baker, G. L. and Gollub, J. B. *Chaotic Dynamics: An Introduction, 2nd ed.* Cambridge, England: Cambridge University Press, 1996.

49) Uyeda, E., Wojnicki, P.J., Micheli-Tzanakou, E. A Visual Evoked Potential Study of Spatial Noise. *IEEE 29th Annual, Proceedings of Bioengineering Conference*, 2003; 260 – 261.

50) Schier MA. Changes in EEG alpha power during simulated driving: a demonstration. *International Journal of Psychophysiology* 37(2): 155-162, 2000.

51) Ahaoll Kirk, B.P.; LaCourse, J.R. Vigilance monitoring from the EEG power spectrum with a neural network. *Proceedings of the 19th Annual International Conference of the IEEE* , Volume: 3 , 30 Oct.-2 Nov. 1997 Page(s): 1218 -1219 vol.3

52) Ray, W. J., Cole, H.W. EEG alpha activity reflects attentional demands, and beta activity reflects emotional and cognitive processes. *Science* 228,750-852

53) Oppenheim, A. V., Schafer, R. W. *Discrete-Time Signal Processing*. Prentice-Hall, 1989

54) Yamaguchi, C. Wavelet analysis of normal and epileptic EEG *EMBS/BMES Conference, 2002. Proceedings of the Second Joint*,Volume:1 , 2002 Page(s): 96 -97 vol.1

55) Bertrand, O. , Bohorquez, J., Pernier, J. Time-frequency digital filtering based on an invertible wavelet transform: an application to evoked potentials *IEEE Transactions on Biomedical Engineering* v 41, n 1, Jan. 1994, p 77-88

56) Ademoglu, A., Micheli-Tzanakou, E., Istefanopoulos, Y. Analysis of pattern reversal visual evoked potentials (PRVEPs) by spline wavelets. *Biomedical Engineering, IEEE Transactions on* Volume 44, Issue 9, Sept. 1997 Page(s):881 – 890

57) Valens, C. A Really Friendly Guide to Wavelets. http://perso.wanadoo.fr/polyvalens/clemens/wavelets/wavelets.html

58) Mallat, S.G. **A** theory for multiresolution signal decomposition: the wavelet representation. *Pattern Analysis and Machine Intelligence, IEEE Transactions on* Volume 11, Issue 7, July 1989 Page(s):674 – 693

59) Wavelet Toolbox documentation. http://www.mathworks.com/access/helpdesk/help/toolbox/wavelet/

60) Santana Diaz, A., Jammes, B., Esteve, D., Gonzalez Mendoza, M. Driver hypovigilance diagnosis using wavelets and statistical analysis. *IEEE 5th International Conference on Intelligent Transportation Systems (Cat. No.02TH8613)*, 2002, p 162-7

61) Quian Quiroga, R., Schurmann, M. Functions and sources of event-related EEG alpha oscillations studied with the wavelet transform. *Clinical Neurophysiology*, v 110, n 4, April 1999, p 643-54

62) Feder J. *Fractals*. New York: Plenum Press, 1988

63) http://math.bu.edu/DYSYS/chaos-game/node6.html

64) Accardo, A., Affinito, M., Carrozzi, M. Bouquet, F. Use of the fractal dimension for the analysis of electroencephalographic time series. *Biological Cybernetics*, 77,339-350,1997

65) http://fc.units.it/ppb/NeuroBiol/Neuroscienze%20per%20tutti/1020.html

66) Lev'y, J. L., Roueff,F. A regularization approach to fractional dimension estimation, in *proceedings of Fractals 98*, Malta, 1998.

67) http://www.graphpad.com/articles/errorbars.htm

68) Hjorth, B. EEG analysis based on time domain properties. *Electroencephalography and Clinical Neurophysiology*, 29:306-3 10,1970.

69) Micheli-Tzanakou, E., Pavlopoulos, S. Phase information in Visual Evoked Potentials. *Journal of Medical Systems*, Volume 21, Number 4/August 1997